

I. Genotype Imputation

Because we propose to conduct multi-SNP analyses, missing genotype needs to be imputed in order to preserve the most information. Before imputing missing genotypes using IMPUTE2¹, the genotype data need to be in the same build as the reference panel. We chose the latest reference data, 1000 Genomes haplotypes Phase 3 integrated variant set release² in NCBI build 37 (hg19) coordinates. The eQTL genotype data was in the same build as reference data while the GWAS data are in hg18. We lifted the build of three GWAS datasets (550K, 610Q, 660W) from hg18 to hg19 using UCSC liftOver tool³, and then merged all three with eQTL SNP data using PLINK⁴. The final merged file contained 511,126 SNPs. To increase the computation efficiency, the combined genotype data was pre-phased into haplotypes using an accurate phasing method, SHAPEIT⁵. The estimated haplotypes were fed into IMPUTE2 program with seed 424242 and effective population size 20,000. We performed the imputation on one chunk of chromosome at a time, while the chunks were pre-defined based on hg19 cytoband positions provided by UCSC genome browser. The imputed genotype data contained non-missing genotypes of 509,100 SNPs for 372 samples in eQTL study and 4349 samples in GWAS study. SNPs with overall minor allele frequency less than 5% were excluded, resulting 482,217 SNPs. Hardy-Weinberg Equilibrium was evaluated for the 482,217 SNPs showing no inflation of disequilibrium (sFigure 9). By querying Ensemble release 75 database with use of R/Bioconductor package biomaRt⁶, we were able to determine chromosome and base-pair positions for 481,664 SNPs, which were the genetic loci that we used for further analyses.

II. Justification of using minimum p-value as the test statistic in iGWAS omnibus tests

We considered the following three models (and hypotheses): 1) the genetic effect of the gene on the glioma risk is not through its own transcription, 2) the effect is through both genetics and transcription of the gene but not their interaction, 3) effect is through both plus their interaction. The minimum p-value approach is to seek any possible evidence about the association of a gene with glioma risk given that we have three potential models. Alternatively, one may select the maximum p-value in the three models as the test statistic. The difference of the minimum p-value and the maximum p-value approaches is that the former considers the gene as a susceptibility one for glioma if any of the three has a significant effect, and the latter does so only if all three have significant effects. We think that the minimum p-value aligns better with our scientific interests. More intuitively, when one has three candidate models, the usual practice is to fit all three and see which gives us the most significant results, i.e., the smallest p-value. To take into account the fact that three models have been considered to obtain the result, the proposed perturbation procedure accounts for the multiplicity and the correlation of the three models. However, if one is interested in identifying genes with all three have significant effects, our proposed procedure can readily accommodate the maximum p-value.

III. Sensitivity analysis by adjusting for population stratification in eQTL analyses

We conducted additional analyses adjusting for the principal components (PCs) in the eQTL modeling. Specifically, we adjusted for four PCs to account for population stratification in univariate eQTL modeling, which was then used to build multivariate eQTL models for every transcript expression, again adjusting for the four PCs. The built multivariate eQTL models for all transcripts were utilized to predict transcript expression for GWAS subjects as described in Methods. The eQTL association of the SNPs with the transcript expression with and without PCs adjustment shares extremely high correlation of 0.995

(sFigure 2a). An even higher correlation was observed in eQTL predicted transcript expression for the GWAS subjects (with vs. without PCs adjustment), 0.9999 (sFigure 2b). We then used the newly predicted transcript expression for the iGWAS analyses. The results of the 55 candidate transcripts are very similar to our previous analyses (sTables 4 and 5).

The reason that we did not adopt this strategy as our main analyses is as follows. The purpose of building eQTL models is for prediction, i.e., to predict the unknown gene expression pattern for the GWAS subjects. The adjustment of the population stratification by PCs is to seek the prediction on top of the ancestry, which may limit the performance of the prediction. The adjustment of population stratification by PCs is due to our concern about the *confounding* by ancestry in relation to the glioma risk, not the *variability* by ancestry. To predict the expression pattern based on the eQTL models adjusting for PCs tends to lose both of them, but our current strategy (not adjusting for PCs in eQTL analyses but adjusting for them in GWAS) preserves the variability and maximizes the power of predicting gene expression but still accounts for the potential confounding in the iGWAS analyses.

IV. Exploratory validation of TCGA low-grade glioma (LGG)

We ranked the expression values of the four candidate genes (*DRD5*, *WDR1*, *NOMO1*, *PDXDC1*) in LGG tumor and normal tissue with respect to their own transcriptome, and compared whether the ranks between the LGG and normal tissues were significantly different. With this analysis, we were able to validate the two most significant genes, *DRD5* and *WDR1* (sFigure 10): *DRD5* has much lower expression level, and *WDR1* has higher expression in LGG compared to the normal tissue. This exploratory analysis is preliminary due to the lack of matched normal tissue for LGG tumor, and has the following limitations. First, the gene expression profile of the normal tissue and the LGG tumor tissue was not derived from the same project; the technical difference may contribute bias to our analyses. Secondly, the two

expression profiles were measured with different technology for expression profiling. Although we compared the ranking within their own transcriptome, the comparison with ranking does not necessarily reflect the comparison with the absolute values and it still requires assumptions to draw a valid conclusion.

V. Discussion of *PDXDC1* and *WDR1*

Association of *PDXDC1* with lipid metabolism was reported in genome-wide association studies⁷⁻⁹, and *PDXDC1* was also found significantly mutated in a subtype of non-clear cell renal carcinoma¹⁰. Unlike our findings in transcription, its protein expression in both normal tissue of cerebral cortex and glioma tissue is not detectable^{11;12}. *WDR1* encodes a protein containing 9 WD repeats, which are approximately 30-40 amino acid domains with conserved residues and involved in protein-protein interactions; *WDR1* protein may help induce the disassembly of actin filaments¹³. Protein expression of *WDR1* is associated with breast cancer¹⁴, thyroid cancer¹⁵ and ovarian cancer¹⁶. In contrast to our findings in transcription, protein expression ranges from medium to high in both normal brain cerebral cortex and glioma tissue^{11;}

¹².

sTable 1. Demographic characteristics of the study population.

%		GWAS-case (n=556)	GWAS-control (n=3647)	eQTL subjects (n=354)	TCGA case (n=473)	TCGA control (n=10)
Age	<30	2.2	0.1	31.4	4.9	0
	30-39	2.3	0.3	11.3	8.1	0
	40-49	4.1	3.9	15.8	14.1	0
	50-59	14.7	4.4	7.1	27.7	0
	60-69	35.6	18.3	5.1	25.3	33.3
	70-79	32.4	52.6	7.9	16.3	66.7
	80-	8.6	20.4	21.5	3.7	0
Gender	Female	43.2	29.3	33.1	38.6	50
	Male	56.8	70.7	66.9	61.4	50
Race	Caucasian	-	-	100	85.1	75
	African American	-	-	0	8.6	25
	Asian	-	-	0	2.2	0
	Other	-	-	0	4.2	0

sTable 2. The iGWAS result of the 40 Ubiquitin Specific Peptidase 17-Like Family Members. They are all discovered at the significance level of omnibus $p < 0.001$ and validated at the level of omnibus $p < 0.001$.

Illumina ID - Ensembl Gene ID	HGNC Symbol	Chromosome	Start Position	End Position	No. of SNPs	Omnibus p-value		
						Discovery	Validation	Combined
ILMN_1684499-ENSG00000232399	USP17L13	4	9212383	9228214	20	7.06E-47	3.19E-14	1.02E-59
ILMN_1684499-ENSG00000231396	USP17L10	4	9212383	9213975	17	6.96E-47	3.16E-14	9.74E-60
ILMN_2335123-ENSG00000231396	USP17L10	4	9212383	9213975	17	1.77E-49	6.54E-19	6.49E-67
ILMN_1684499-ENSG00000233136	USP17L11	4	9217131	9218723	17	7.09E-47	3.23E-14	1.10E-59
ILMN_2335123-ENSG00000233136	USP17L11	4	9217131	9218723	17	1.78E-49	6.57E-19	6.63E-67
ILMN_1684499-ENSG00000227551	USP17L12	4	9221878	9223470	19	7.06E-47	3.19E-14	1.02E-59
ILMN_2335123-ENSG00000227551	USP17L12	4	9221878	9223470	19	1.77E-49	6.54E-19	6.49E-67
ILMN_1684499-ENSG00000223569	USP17L15	4	9236111	9237700	13	7.06E-47	3.19E-14	1.02E-59
ILMN_2335123-ENSG00000223569	USP17L15	4	9236111	9237700	13	1.80E-49	6.68E-19	6.49E-67
ILMN_1684499-ENSG00000250231	USP17L16P	4	9240856	9242448	13	7.06E-47	3.19E-14	1.02E-59
ILMN_1684499-ENSG00000249104	USP17L17	4	9245605	9247197	13	6.97E-47	3.13E-14	9.42E-60
ILMN_1684499-ENSG00000250844	USP17L18	4	9250356	9251948	13	7.09E-47	3.21E-14	1.04E-59
ILMN_2335123-ENSG00000250844	USP17L18	4	9250356	9251948	13	1.80E-49	6.68E-19	6.49E-67
ILMN_1684499-ENSG00000248920	USP17L19	4	9255104	9256696	13	7.14E-47	3.31E-14	1.19E-59
ILMN_2335123-ENSG00000248920	USP17L19	4	9255104	9256696	13	1.77E-49	6.44E-19	6.58E-67
ILMN_1684499-ENSG00000250745	USP17L20	4	9259850	9261442	14	7.09E-47	3.21E-14	1.04E-59
ILMN_2335123-ENSG00000250745	USP17L20	4	9259850	9261442	14	1.81E-49	6.70E-19	6.44E-67
ILMN_1684499-ENSG00000249811	USP17L21	4	9264598	9266190	14	7.17E-47	3.27E-14	1.13E-59
ILMN_2335123-ENSG00000249811	USP17L21	4	9264598	9266190	14	1.79E-49	6.63E-19	6.55E-67
ILMN_1684499-ENSG00000248933	USP17L22	4	9269345	9270937	14	7.09E-47	3.23E-14	1.10E-59
ILMN_2335123-ENSG00000248933	USP17L22	4	9269345	9270937	14	1.76E-49	6.43E-19	6.62E-67
ILMN_1684499-ENSG00000232264	USP17L24	4	9326891	9328483	21	7.06E-47	3.19E-14	1.02E-59
ILMN_2335123-ENSG00000232264	USP17L24	4	9326891	9328483	21	8.75E-23	7.24E-09	5.27E-32
ILMN_1684499-ENSG00000230430	USP17L25	4	9331637	9333229	22	6.97E-47	3.13E-14	9.42E-60
ILMN_2335123-ENSG00000230430	USP17L25	4	9331637	9333229	22	6.95E-19	2.66E-07	2.14E-26
ILMN_1684499-ENSG00000229579	USP17L26	4	9336384	9337976	24	7.09E-47	3.21E-14	1.04E-59

ILMN_2335123-ENSG00000229579	USP17L26	4	9336384	9337976	24	3.28E-18	1.08E-06	7.10E-25
ILMN_1684499-ENSG00000227140	USP17L5	4	9341129	9342721	24	7.06E-47	3.19E-14	1.02E-59
ILMN_2335123-ENSG00000227140	USP17L5	4	9341129	9342721	24	3.15E-18	1.07E-06	7.22E-25
ILMN_1684499-ENSG00000235780	USP17L27	4	9345874	9347466	25	7.17E-47	3.27E-14	1.13E-59
ILMN_2335123-ENSG00000235780	USP17L27	4	9345874	9347466	25	3.43E-17	4.07E-06	4.34E-23
ILMN_1684499-ENSG00000231051	USP17L28	4	9350619	9352211	26	7.27E-47	3.33E-14	1.24E-59
ILMN_2335123-ENSG00000231051	USP17L28	4	9350619	9352211	26	2.77E-17	3.90E-06	4.60E-23
ILMN_1684499-ENSG00000231637	USP17L29	4	9355364	9356956	26	6.92E-47	3.11E-14	8.99E-60
ILMN_2335123-ENSG00000231637	USP17L29	4	9355364	9356956	26	2.97E-17	3.95E-06	4.58E-23
ILMN_1684499-ENSG00000251694	USP17L9P	4	9360109	9361701	27	7.17E-47	3.27E-14	1.13E-59
ILMN_2335123-ENSG00000251694	USP17L9P	4	9360109	9361701	27	4.00E-15	2.53E-05	3.45E-20
ILMN_1684499-ENSG00000228856	USP17L30	4	9364855	9366447	30	6.92E-47	3.11E-14	8.99E-60
ILMN_2335123-ENSG00000228856	USP17L30	4	9364855	9366447	30	2.32E-13	0.000116	1.49E-17
ILMN_2335123-ENSG00000205946	USP17L6P	4	9369600	9370796	30	2.39E-13	0.000116	1.47E-17

sTable 3. The p-values of the 55 validated transcripts in SNP-only models, main effect-only models and interaction models.

Illumina ID - Ensembl ID	HGNC Symbol	Ch	Discovery Set			Validation Set			Combined		
			Interac- tion	Main Effect	SNP only	Interaction	Main Effect	SNP only	Interac- tion	Main Effect	SNP only
ILMN_1684499-ENSG00000232399	USP17L13	4	3.52E-37	5.35E-32	8.18E-46	7.66E-11	1.79E-09	2.15E-13	9.03E-46	2.68E-39	7.58E-57
ILMN_1684499-ENSG00000231396	USP17L10	4	4.21E-37	6.89E-32	8.18E-46	8.06E-11	1.92E-09	2.15E-13	1.15E-45	3.74E-39	7.58E-57
ILMN_2335123-ENSG00000231396	USP17L10	4	2.03E-47	2.29E-45	1.56E-47	2.23E-18	3.50E-17	8.50E-19	7.20E-68	1.66E-64	5.16E-68
ILMN_1684499-ENSG00000233136	USP17L11	4	2.43E-37	3.17E-32	8.18E-46	6.90E-11	1.54E-09	2.15E-13	5.51E-46	1.34E-39	7.58E-57
ILMN_2335123-ENSG00000233136	USP17L11	4	2.28E-47	2.68E-45	1.56E-47	2.29E-18	3.64E-17	8.50E-19	8.45E-68	2.05E-64	5.16E-68
ILMN_1684499-ENSG00000227551	USP17L12	4	3.52E-37	5.35E-32	8.18E-46	7.66E-11	1.79E-09	2.15E-13	9.03E-46	2.68E-39	7.58E-57
ILMN_2335123-ENSG00000227551	USP17L12	4	2.03E-47	2.29E-45	1.56E-47	2.23E-18	3.50E-17	8.50E-19	7.20E-68	1.66E-64	5.16E-68
ILMN_1684499-ENSG00000223569	USP17L15	4	3.52E-37	5.35E-32	8.18E-46	7.66E-11	1.79E-09	2.15E-13	9.03E-46	2.68E-39	7.58E-57
ILMN_2335123-ENSG00000223569	USP17L15	4	2.70E-47	3.32E-45	1.56E-47	2.38E-18	3.85E-17	8.50E-19	1.06E-67	2.77E-64	5.16E-68
ILMN_1684499-ENSG00000250231	USP17L16P	4	3.52E-37	5.35E-32	8.18E-46	7.66E-11	1.79E-09	2.15E-13	9.03E-46	2.68E-39	7.58E-57
ILMN_1684499-ENSG00000249104	USP17L17	4	5.01E-37	8.83E-32	8.18E-46	8.47E-11	2.06E-09	2.15E-13	1.44E-45	5.18E-39	7.58E-57
ILMN_1684499-ENSG00000250844	USP17L18	4	2.93E-37	4.13E-32	8.18E-46	7.27E-11	1.66E-09	2.15E-13	7.07E-46	1.90E-39	7.58E-57
ILMN_2335123-ENSG00000250844	USP17L18	4	2.70E-47	3.32E-45	1.56E-47	2.38E-18	3.85E-17	8.50E-19	1.06E-67	2.77E-64	5.16E-68
ILMN_1684499-ENSG00000248920	USP17L19	4	1.66E-37	1.86E-32	8.18E-46	6.19E-11	1.32E-09	2.15E-13	3.32E-46	6.59E-40	7.58E-57
ILMN_2335123-ENSG00000248920	USP17L19	4	1.76E-47	1.90E-45	1.56E-47	2.15E-18	3.33E-17	8.50E-19	5.93E-68	1.29E-64	5.16E-68
ILMN_1684499-ENSG00000250745	USP17L20	4	2.93E-37	4.13E-32	8.18E-46	7.27E-11	1.66E-09	2.15E-13	7.07E-46	1.90E-39	7.58E-57
ILMN_2335123-ENSG00000250745	USP17L20	4	2.81E-47	3.51E-45	1.56E-47	2.41E-18	3.91E-17	8.50E-19	1.12E-67	2.98E-64	5.16E-68
ILMN_1684499-ENSG00000249811	USP17L21	4	2.01E-37	2.43E-32	8.18E-46	6.54E-11	1.43E-09	2.15E-13	4.28E-46	9.42E-40	7.58E-57
ILMN_2335123-ENSG00000249811	USP17L21	4	2.48E-47	2.98E-45	1.56E-47	2.34E-18	3.74E-17	8.50E-19	9.45E-68	2.38E-64	5.16E-68
ILMN_1684499-ENSG00000248933	USP17L22	4	2.43E-37	3.17E-32	8.18E-46	6.90E-11	1.54E-09	2.15E-13	5.51E-46	1.34E-39	7.58E-57
ILMN_2335123-ENSG00000248933	USP17L22	4	1.70E-47	1.82E-45	1.56E-47	2.14E-18	3.30E-17	8.50E-19	5.68E-68	1.21E-64	5.16E-68
ILMN_1684499-ENSG00000232264	USP17L24	4	3.52E-37	5.35E-32	8.18E-46	7.66E-11	1.79E-09	2.15E-13	9.03E-46	2.68E-39	7.58E-57
ILMN_2335123-ENSG00000232264	USP17L24	4	2.11E-19	5.42E-17	9.78E-23	4.73E-08	3.54E-07	6.13E-09	9.11E-27	2.25E-23	3.94E-31
ILMN_1684499-ENSG00000230430	USP17L25	4	5.01E-37	8.83E-32	8.18E-46	8.47E-11	2.06E-09	2.15E-13	1.44E-45	5.18E-39	7.58E-57
ILMN_2335123-ENSG00000230430	USP17L25	4	2.28E-16	2.09E-14	4.07E-19	1.11E-06	5.65E-06	2.01E-07	3.65E-22	1.99E-19	9.72E-26
ILMN_1684499-ENSG00000229579	USP17L26	4	2.93E-37	4.13E-32	8.18E-46	7.27E-11	1.66E-09	2.15E-13	7.07E-46	1.90E-39	7.58E-57

ILMN_2335123-ENSG00000229579	USP17L26	4	5.84E-16	3.20E-14	3.37E-18	2.55E-06	9.21E-06	7.71E-07	1.55E-21	3.77E-19	2.31E-24
ILMN_1684499-ENSG00000227140	USP17L5	4	3.52E-37	5.35E-32	8.18E-46	7.66E-11	1.79E-09	2.15E-13	9.03E-46	2.68E-39	7.58E-57
ILMN_2335123-ENSG00000227140	USP17L5	4	1.50E-15	1.14E-13	3.37E-18	3.71E-06	1.55E-05	7.71E-07	6.10E-21	2.39E-18	2.31E-24
ILMN_1684499-ENSG00000235780	USP17L27	4	2.01E-37	2.43E-32	8.18E-46	6.54E-11	1.43E-09	2.15E-13	4.28E-46	9.42E-40	7.58E-57
ILMN_2335123-ENSG00000235780	USP17L27	4	4.29E-15	1.52E-13	4.95E-17	7.59E-06	2.16E-05	2.99E-06	3.11E-20	3.93E-18	1.19E-22
ILMN_1684499-ENSG00000231051	USP17L28	4	1.37E-37	1.41E-32	8.18E-46	5.86E-11	1.23E-09	2.15E-13	2.57E-46	4.60E-40	7.58E-57
ILMN_2335123-ENSG00000231051	USP17L28	4	1.30E-13	1.54E-11	4.95E-17	2.82E-05	0.00013364	2.99E-06	4.07E-18	2.89E-15	1.19E-22
ILMN_1684499-ENSG00000231637	USP17L29	4	5.94E-37	1.12E-31	8.18E-46	8.88E-11	2.21E-09	2.15E-13	1.81E-45	7.10E-39	7.58E-57
ILMN_2335123-ENSG00000231637	USP17L29	4	4.45E-14	3.59E-12	4.95E-17	1.87E-05	7.58E-05	2.99E-06	8.83E-19	3.64E-16	1.19E-22
ILMN_1684499-ENSG00000251694	USP17L9P	4	2.01E-37	2.43E-32	8.18E-46	6.54E-11	1.43E-09	2.15E-13	4.28E-46	9.42E-40	7.58E-57
ILMN_2335123-ENSG00000251694	USP17L9P	4	2.50E-14	2.76E-13	3.82E-15	1.67E-05	2.93E-05	1.65E-05	4.73E-19	1.07E-17	7.22E-20
ILMN_1684499-ENSG00000228856	USP17L30	4	5.94E-37	1.12E-31	8.18E-46	8.88E-11	2.21E-09	2.15E-13	1.81E-45	7.10E-39	7.58E-57
ILMN_2335123-ENSG00000228856	USP17L30	4	1.67E-11	3.59E-10	1.98E-13	0.00021852	0.00054221	7.48E-05	5.57E-15	3.32E-13	2.22E-17
ILMN_2335123-ENSG00000205946	USP17L6P	4	7.45E-12	1.20E-10	1.98E-13	0.00016193	0.0003549	7.48E-05	1.79E-15	7.05E-14	2.22E-17
ILMN_2079225-ENSG00000250884	OR7E85P	4	2.58E-47	2.96E-50	7.56E-37	2.08E-15	3.88E-16	2.04E-12	6.31E-62	1.72E-65	1.79E-48
ILMN_1738406-ENSG00000109667	SLC2A9	4	1.32E-18	1.76E-21	5.18E-10	6.26E-05	1.19E-05	0.004389	4.15E-23	1.36E-26	1.07E-12
ILMN_1723803-ENSG00000109667	SLC2A9	4	1.76E-58	7.12E-54	6.75E-58	1.50E-17	1.34E-16	8.29E-17	1.08E-73	1.04E-67	3.68E-73
ILMN_1689043-ENSG00000169676	DRD5	4	3.65E-46	2.64E-59	1.08E-15	2.98E-12	1.45E-15	0.000178	1.32E-59	6.44E-77	3.11E-20
ILMN_1780036-ENSG00000071127	WDR1	4	7.16E-40	3.15E-44	6.27E-25	1.50E-12	2.40E-13	9.99E-09	1.00E-52	3.35E-57	3.14E-34
ILMN_1675844-ENSG00000071127	WDR1	4	1.32E-52	2.42E-59	1.12E-32	4.30E-17	8.76E-19	3.40E-11	1.18E-70	2.93E-79	7.84E-44
ILMN_1804935-ENSG00000093134	VNN3	6	2.44E-08	3.39E-08	1.04E-07	4.43E-05	2.36E-05	0.00041	6.56E-13	4.86E-13	4.38E-11
ILMN_2096747-ENSG00000221500	SNORD100	6	2.23E-09	4.88E-12	0.000591	0.00405293	0.00040858	0.197477	5.67E-12	3.64E-16	0.000737
ILMN_2096747-ENSG00000200534	SNORA33	6	2.91E-09	7.54E-12	0.000591	0.00448741	0.00048439	0.197477	8.48E-12	7.06E-16	0.000737
ILMN_2126957-ENSG00000103512	NOMO1	16	9.51E-20	7.88E-20	8.72E-17	2.35E-07	5.03E-08	3.12E-05	2.71E-25	3.93E-26	6.40E-20
ILMN_1702114-ENSG00000103512	NOMO1	16	4.52E-18	7.06E-18	1.21E-17	1.32E-05	1.63E-05	1.40E-05	7.89E-22	1.87E-21	1.45E-21
ILMN_1703969-ENSG00000179889	PDXDC1	16	4.70E-19	6.88E-19	6.55E-16	4.30E-06	1.02E-06	0.000326	4.77E-24	1.27E-24	1.70E-18
ILMN_1815552-ENSG00000157045	NTAN1	16	8.20E-14	5.95E-12	3.48E-15	0.00374158	0.01380299	0.000529	3.02E-15	1.32E-12	7.63E-18
ILMN_1728645-ENSG00000197457	STMN3	20	4.29E-05	0.00062463	6.76E-07	0.00139136	0.00515311	0.000214	1.57E-08	1.61E-06	1.86E-11
ILMN_2344079-ENSG00000203896	LIME1	20	6.79E-05	0.0007056	4.59E-06	0.00101493	0.00287834	0.000401	2.26E-08	1.08E-06	4.37E-10

sTable 4. The p-values of the 55 validated transcripts in SNP-only models, main effect-only models and interaction models. Results of sensitivity analyses by adjusting for population stratification in eQTL analyses.

Illumina ID - Ensembl ID	HGNC Symbol	Ch	Omnibus p-value		
			Discovery	Validation	Combined
ILMN_1684499-ENSG00000232399	USP17L13	4	2.85E-51	1.27E-13	9.51E-71
ILMN_1684499-ENSG00000231396	USP17L10	4	2.58E-51	1.27E-13	9.15E-71
ILMN_2335123-ENSG00000231396	USP17L10	4	2.46E-51	6.23E-19	1.28E-70
ILMN_1684499-ENSG00000233136	USP17L11	4	2.91E-51	1.25E-13	8.19E-71
ILMN_2335123-ENSG00000233136	USP17L11	4	2.02E-51	6.79E-19	1.21E-70
ILMN_1684499-ENSG00000227551	USP17L12	4	2.85E-51	1.27E-13	9.51E-71
ILMN_2335123-ENSG00000227551	USP17L12	4	2.46E-51	6.23E-19	1.28E-70
ILMN_1684499-ENSG00000223569	USP17L15	4	2.85E-51	1.27E-13	9.51E-71
ILMN_2335123-ENSG00000223569	USP17L15	4	2.23E-51	7.17E-19	1.22E-70
ILMN_1684499-ENSG00000250231	USP17L16P	4	2.85E-51	1.27E-13	9.51E-71
ILMN_1684499-ENSG00000249104	USP17L17	4	2.08E-51	1.25E-13	1.14E-70
ILMN_1684499-ENSG00000250844	USP17L18	4	2.67E-51	1.28E-13	8.34E-71
ILMN_2335123-ENSG00000250844	USP17L18	4	2.23E-51	7.17E-19	1.22E-70
ILMN_1684499-ENSG00000248920	USP17L19	4	4.31E-51	1.25E-13	7.84E-71
ILMN_2335123-ENSG00000248920	USP17L19	4	2.41E-51	5.67E-19	1.32E-70
ILMN_1684499-ENSG00000250745	USP17L20	4	2.67E-51	1.28E-13	8.34E-71
ILMN_2335123-ENSG00000250745	USP17L20	4	2.21E-51	7.26E-19	1.22E-70
ILMN_1684499-ENSG00000249811	USP17L21	4	4.16E-51	1.24E-13	7.86E-71
ILMN_2335123-ENSG00000249811	USP17L21	4	2.12E-51	6.92E-19	1.22E-70
ILMN_1684499-ENSG00000248933	USP17L22	4	2.91E-51	1.25E-13	8.19E-71
ILMN_2335123-ENSG00000248933	USP17L22	4	2.38E-51	5.59E-19	1.32E-70
ILMN_1684499-ENSG00000232264	USP17L24	4	2.85E-51	1.27E-13	9.51E-71
ILMN_2335123-ENSG00000232264	USP17L24	4	1.23E-24	3.32E-09	8.05E-35
ILMN_1684499-ENSG00000230430	USP17L25	4	2.08E-51	1.25E-13	1.14E-70
ILMN_2335123-ENSG00000230430	USP17L25	4	3.38E-20	1.82E-07	3.83E-29
ILMN_1684499-ENSG00000229579	USP17L26	4	2.67E-51	1.28E-13	8.34E-71

ILMN_2335123-ENSG00000229579	USP17L26	4	3.13E-20	1.26E-06	2.49E-27
ILMN_1684499-ENSG00000227140	USP17L5	4	2.85E-51	1.27E-13	9.51E-71
ILMN_2335123-ENSG00000227140	USP17L5	4	3.42E-20	1.10E-06	2.21E-27
ILMN_1684499-ENSG00000235780	USP17L27	4	4.16E-51	1.24E-13	7.86E-71
ILMN_2335123-ENSG00000235780	USP17L27	4	2.97E-19	4.50E-06	5.45E-25
ILMN_1684499-ENSG00000231051	USP17L28	4	4.22E-51	1.21E-13	9.35E-71
ILMN_2335123-ENSG00000231051	USP17L28	4	2.10E-19	4.47E-06	7.83E-25
ILMN_1684499-ENSG00000231637	USP17L29	4	1.93E-51	1.24E-13	1.25E-70
ILMN_2335123-ENSG00000231637	USP17L29	4	2.36E-19	4.44E-06	6.28E-25
ILMN_1684499-ENSG00000251694	USP17L9P	4	4.16E-51	1.24E-13	7.86E-71
ILMN_2335123-ENSG00000251694	USP17L9P	4	6.57E-17	2.23E-05	2.25E-21
ILMN_1684499-ENSG00000228856	USP17L30	4	1.93E-51	1.24E-13	1.25E-70
ILMN_2335123-ENSG00000228856	USP17L30	4	2.87E-15	0.000124	2.48E-19
ILMN_2335123-ENSG00000205946	USP17L6P	4	2.98E-15	0.000124	3.29E-19
ILMN_2079225-ENSG00000250884	OR7E85P	4	3.43E-57	1.78E-18	7.69E-79
ILMN_1738406-ENSG00000109667	SLC2A9	4	7.38E-22	1.51E-05	3.09E-29
ILMN_1723803-ENSG00000109667	SLC2A9	4	1.80E-71	3.88E-21	4.06E-81
ILMN_1689043-ENSG00000169676	DRD5	4	3.86E-62	5.39E-14	1.02E-64
ILMN_1780036-ENSG00000071127	WDR1	4	2.13E-46	1.48E-13	1.17E-60
ILMN_1675844-ENSG00000071127	WDR1	4	5.84E-78	3.30E-21	4.80E-97
ILMN_1804935-ENSG00000093134	VNN3	6	7.88E-08	6.96E-06	3.02E-12
ILMN_2096747-ENSG00000221500	SNORD100	6	3.50E-11	0.002429	3.36E-13
ILMN_2096747-ENSG00000200534	SNORA33	6	5.70E-11	0.002845	6.13E-13
ILMN_2126957-ENSG00000103512	NOMO1	16	8.76E-24	4.50E-07	1.99E-30
ILMN_1702114-ENSG00000103512	NOMO1	16	9.12E-21	1.77E-05	1.18E-27
ILMN_1703969-ENSG00000179889	PDXDC1	16	9.09E-24	2.82E-06	7.30E-29
ILMN_1815552-ENSG00000157045	NTAN1	16	1.10E-19	0.000159	4.57E-25
ILMN_1728645-ENSG00000197457	STMN3	20	6.50E-07	0.000326	2.71E-10
ILMN_2344079-ENSG00000203896	LIME1	20	2.39E-06	0.000530	3.86E-10

sTable 5. The p-values of the 55 validated transcripts in SNP-only models, main effect-only models and interaction models. Results of sensitivity analyses by adjusting for population stratification in eQTL analyses.

Illumina ID - Ensembl ID	HGNC Symbol	Ch	Discovery Set			Validation Set			Combined		
			Interac- tion	Main Effect	SNP only	Interaction	Main Effect	SNP only	Interac- tion	Main Effect	SNP only
ILMN_1684499-ENSG00000232399	USP17L13	4	1.03E-38	3.64E-33	8.28E-48	2.46E-10	4.95E-09	9.05E-13	5.44E-53	1.51E-45	2.01E-65
ILMN_1684499-ENSG00000231396	USP17L10	4	1.25E-38	4.75E-33	8.28E-48	2.58E-10	5.31E-09	9.05E-13	7.20E-53	2.23E-45	2.01E-65
ILMN_2335123-ENSG00000231396	USP17L10	4	2.64E-47	5.40E-45	4.97E-48	3.95E-18	2.28E-17	9.97E-18	4.44E-63	3.95E-59	2.85E-65
ILMN_1684499-ENSG00000233136	USP17L11	4	6.99E-39	2.10E-33	8.28E-48	2.22E-10	4.28E-09	9.05E-13	3.05E-53	6.71E-46	2.01E-65
ILMN_2335123-ENSG00000233136	USP17L11	4	3.03E-47	6.43E-45	4.97E-48	4.07E-18	2.38E-17	9.97E-18	5.30E-63	4.94E-59	2.85E-65
ILMN_1684499-ENSG00000227551	USP17L12	4	1.03E-38	3.64E-33	8.28E-48	2.46E-10	4.95E-09	9.05E-13	5.44E-53	1.51E-45	2.01E-65
ILMN_2335123-ENSG00000227551	USP17L12	4	2.64E-47	5.40E-45	4.97E-48	3.95E-18	2.28E-17	9.97E-18	4.44E-63	3.95E-59	2.85E-65
ILMN_1684499-ENSG00000223569	USP17L15	4	1.03E-38	3.64E-33	8.28E-48	2.46E-10	4.95E-09	9.05E-13	5.44E-53	1.51E-45	2.01E-65
ILMN_2335123-ENSG00000223569	USP17L15	4	3.66E-47	8.22E-45	4.97E-48	4.24E-18	2.54E-17	9.97E-18	6.77E-63	6.75E-59	2.85E-65
ILMN_1684499-ENSG00000250231	USP17L16P	4	1.03E-38	3.64E-33	8.28E-48	2.46E-10	4.95E-09	9.05E-13	5.44E-53	1.51E-45	2.01E-65
ILMN_1684499-ENSG00000249104	USP17L17	4	1.50E-38	6.16E-33	8.28E-48	2.71E-10	5.69E-09	9.05E-13	9.46E-53	3.26E-45	2.01E-65
ILMN_1684499-ENSG00000250844	USP17L18	4	8.52E-39	2.77E-33	8.28E-48	2.34E-10	4.61E-09	9.05E-13	4.08E-53	1.01E-45	2.01E-65
ILMN_2335123-ENSG00000250844	USP17L18	4	3.66E-47	8.22E-45	4.97E-48	4.24E-18	2.54E-17	9.97E-18	6.77E-63	6.75E-59	2.85E-65
ILMN_1684499-ENSG00000248920	USP17L19	4	4.67E-39	1.19E-33	8.28E-48	1.99E-10	3.69E-09	9.05E-13	1.68E-53	2.92E-46	2.01E-65
ILMN_2335123-ENSG00000248920	USP17L19	4	2.24E-47	4.37E-45	4.97E-48	3.81E-18	2.16E-17	9.97E-18	3.60E-63	3.01E-59	2.85E-65
ILMN_1684499-ENSG00000250745	USP17L20	4	8.52E-39	2.77E-33	8.28E-48	2.34E-10	4.61E-09	9.05E-13	4.08E-53	1.01E-45	2.01E-65
ILMN_2335123-ENSG00000250745	USP17L20	4	3.84E-47	8.74E-45	4.97E-48	4.28E-18	2.58E-17	9.97E-18	7.20E-63	7.30E-59	2.85E-65
ILMN_1684499-ENSG00000249811	USP17L21	4	5.72E-39	1.58E-33	8.28E-48	2.10E-10	3.97E-09	9.05E-13	2.26E-53	4.44E-46	2.01E-65
ILMN_2335123-ENSG00000249811	USP17L21	4	3.33E-47	7.27E-45	4.97E-48	4.15E-18	2.46E-17	9.97E-18	5.98E-63	5.77E-59	2.85E-65
ILMN_1684499-ENSG00000248933	USP17L22	4	6.99E-39	2.10E-33	8.28E-48	2.22E-10	4.28E-09	9.05E-13	3.05E-53	6.71E-46	2.01E-65
ILMN_2335123-ENSG00000248933	USP17L22	4	2.16E-47	4.17E-45	4.97E-48	3.78E-18	2.13E-17	9.97E-18	3.43E-63	2.83E-59	2.85E-65
ILMN_1684499-ENSG00000232264	USP17L24	4	1.03E-38	3.64E-33	8.28E-48	2.46E-10	4.95E-09	9.05E-13	5.44E-53	1.51E-45	2.01E-65
ILMN_2335123-ENSG00000232264	USP17L24	4	5.53E-20	1.30E-17	4.78E-23	6.21E-08	3.38E-07	1.23E-08	9.24E-29	3.06E-25	1.00E-32
ILMN_1684499-ENSG00000230430	USP17L25	4	1.50E-38	6.16E-33	8.28E-48	2.71E-10	5.69E-09	9.05E-13	9.46E-53	3.26E-45	2.01E-65
ILMN_2335123-ENSG00000230430	USP17L25	4	1.47E-16	1.16E-14	4.05E-19	1.52E-06	6.24E-06	3.46E-07	1.70E-23	1.14E-20	7.06E-27

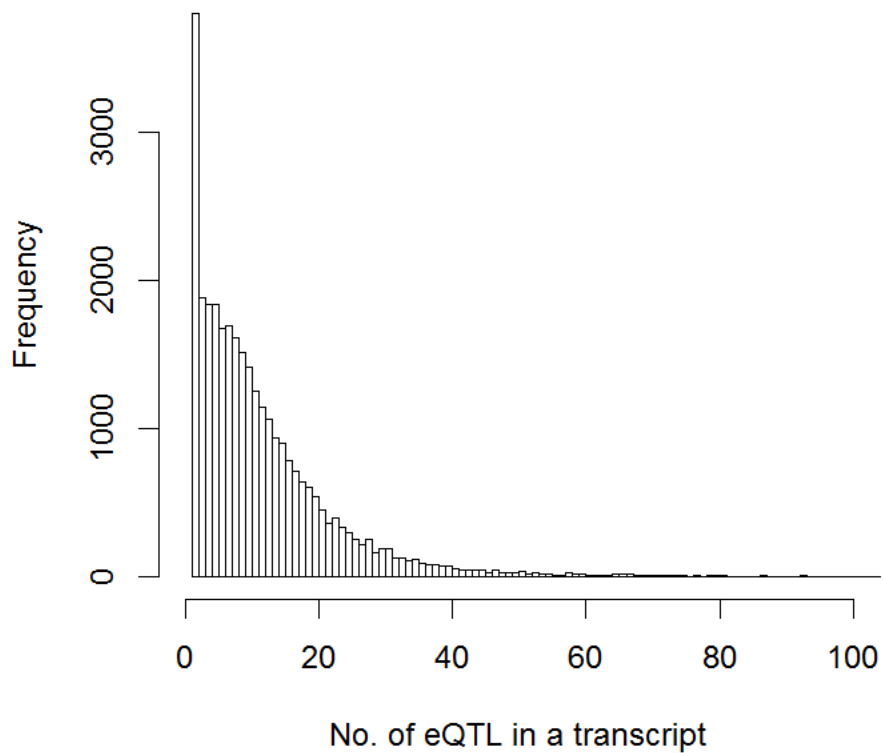
ILMN_1684499-ENSG00000229579	USP17L26	4	8.52E-39	2.77E-33	8.28E-48	2.34E-10	4.61E-09	9.05E-13	4.08E-53	1.01E-45	2.01E-65
ILMN_2335123-ENSG00000229579	USP17L26	4	2.08E-16	1.10E-14	1.67E-18	3.37E-06	9.64E-06	1.36E-06	6.50E-23	1.84E-20	1.82E-25
ILMN_1684499-ENSG00000227140	USP17L5	4	1.03E-38	3.64E-33	8.28E-48	2.46E-10	4.95E-09	9.05E-13	5.44E-53	1.51E-45	2.01E-65
ILMN_2335123-ENSG00000227140	USP17L5	4	5.39E-16	4.03E-14	1.67E-18	4.91E-06	1.66E-05	1.36E-06	2.73E-22	1.29E-19	1.82E-25
ILMN_1684499-ENSG00000235780	USP17L27	4	5.72E-39	1.58E-33	8.28E-48	2.10E-10	3.97E-09	9.05E-13	2.26E-53	4.44E-46	2.01E-65
ILMN_2335123-ENSG00000235780	USP17L27	4	1.08E-15	4.13E-14	1.52E-17	9.32E-06	2.10E-05	5.11E-06	1.75E-21	2.41E-19	1.40E-23
ILMN_1684499-ENSG00000231051	USP17L28	4	3.81E-39	8.97E-34	8.28E-48	1.89E-10	3.42E-09	9.05E-13	1.24E-53	1.92E-46	2.01E-65
ILMN_2335123-ENSG00000231051	USP17L28	4	3.43E-14	4.60E-12	1.52E-17	3.54E-05	0.000141	5.11E-06	2.92E-19	2.54E-16	1.40E-23
ILMN_1684499-ENSG00000231637	USP17L29	4	1.80E-38	7.92E-33	8.28E-48	2.84E-10	6.08E-09	9.05E-13	1.23E-52	4.73E-45	2.01E-65
ILMN_2335123-ENSG00000231637	USP17L29	4	1.16E-14	1.04E-12	1.52E-17	2.33E-05	7.81E-05	5.11E-06	5.86E-20	2.85E-17	1.40E-23
ILMN_1684499-ENSG00000251694	USP17L9P	4	5.72E-39	1.58E-33	8.28E-48	2.10E-10	3.97E-09	9.05E-13	2.26E-53	4.44E-46	2.01E-65
ILMN_2335123-ENSG00000251694	USP17L9P	4	8.47E-15	9.60E-14	1.53E-15	2.07E-05	2.99E-05	2.51E-05	4.07E-20	9.59E-19	1.07E-20
ILMN_1684499-ENSG00000228856	USP17L30	4	1.80E-38	7.92E-33	8.28E-48	2.84E-10	6.08E-09	9.05E-13	1.23E-52	4.73E-45	2.01E-65
ILMN_2335123-ENSG00000228856	USP17L30	4	7.49E-12	1.69E-10	9.61E-14	0.00027	0.000601	0.000106	1.01E-15	6.73E-14	4.72E-18
ILMN_2335123-ENSG00000205946	USP17L6P	4	3.29E-12	5.51E-11	9.61E-14	0.0002	0.00039	0.000106	3.07E-16	1.32E-14	4.72E-18
ILMN_2079225-ENSG00000250884	OR7E85P	4	4.07E-50	4.77E-52	1.70E-40	1.02E-16	3.48E-17	6.05E-14	3.83E-64	1.24E-69	3.44E-48
ILMN_1738406-ENSG00000109667	SLC2A9	4	1.45E-20	6.93E-24	3.37E-11	6.29E-05	1.32E-05	0.003856	4.76E-26	1.05E-29	2.26E-14
ILMN_1723803-ENSG00000109667	SLC2A9	4	4.57E-67	2.13E-62	4.68E-65	4.87E-19	1.47E-18	2.64E-17	1.96E-79	7.26E-73	2.64E-78
ILMN_1689043-ENSG00000169676	DRD5	4	1.16E-47	2.89E-60	1.91E-17	1.20E-10	2.64E-13	0.000252	4.20E-55	1.55E-69	1.58E-20
ILMN_1780036-ENSG00000071127	WDR1	4	1.08E-39	1.01E-43	1.73E-25	4.80E-12	3.94E-13	4.43E-08	3.70E-51	8.92E-55	1.76E-34
ILMN_1675844-ENSG00000071127	WDR1	4	5.35E-66	5.83E-71	1.26E-45	6.04E-18	1.55E-19	2.29E-12	6.22E-85	3.31E-94	1.13E-55
ILMN_1804935-ENSG00000093134	VNN3	6	3.05E-08	4.19E-08	2.19E-07	1.95E-05	1.02E-05	0.000313	3.98E-12	2.28E-12	7.53E-10
ILMN_2096747-ENSG00000221500	SNORD100	6	1.01E-07	4.96E-10	0.004345	0.014624	0.00131	0.511956	1.30E-10	1.10E-14	0.002368
ILMN_2096747-ENSG00000200534	SNORA33	6	1.28E-07	7.28E-10	0.004345	0.016062	0.001542	0.511956	1.83E-10	1.95E-14	0.002368
ILMN_2126957-ENSG00000103512	NOMO1	16	3.21E-21	5.08E-21	1.35E-19	5.36E-07	3.14E-07	7.07E-06	6.24E-29	3.15E-29	3.59E-25
ILMN_1702114-ENSG00000103512	NOMO1	16	5.23E-19	4.61E-19	3.12E-17	2.33E-05	2.25E-05	6.07E-05	1.59E-27	2.04E-27	6.68E-25
ILMN_1703969-ENSG00000179889	PDXDC1	16	3.75E-21	6.02E-21	9.84E-18	7.44E-06	3.09E-06	0.000316	6.47E-26	9.61E-26	8.40E-21
ILMN_1815552-ENSG00000157045	NTAN1	16	1.99E-15	5.49E-13	2.16E-17	0.001191	0.005791	0.000142	1.63E-19	4.04E-16	1.72E-22
ILMN_1728645-ENSG00000197457	STMN3	20	5.69E-05	0.000581	2.55E-06	0.00158	0.005448	0.000306	1.69E-07	5.90E-06	1.44E-09
ILMN_2344079-ENSG00000203896	LIME1	20	5.37E-05	0.000597	4.41E-06	0.001157	0.003581	0.000359	1.39E-08	8.65E-07	2.72E-10

sTable 6. The p-values of the SNPs reported in previous GWAS of glioma.

SNP ID	Gene	Cytoband	p-value
rs1920116	<i>TERC</i>	3q26.2	0.0993
rs2736100	<i>TERT</i>	5p15.33	1.46E-05
rs2853676	<i>TERT</i>	5p15.33	0.00152
rs11979158	<i>EGFR</i>	7p11.2	0.233
rs2252586	<i>EGFR</i>	7p11.2	3.12E-05
rs4295627	<i>CCDC26</i>	8q24.21	0.537
rs10464870	<i>CCDC26</i>	8q24.21	0.208
rs891835	<i>CCDC26</i>	8q24.21	0.535
rs6470745	<i>CCDC26</i>	8q24.21	0.991
rs16904140	<i>CCDC26</i>	8q24.21	0.521
rs4977756	<i>CDKN2BAS</i>	9p21.3	8.63E-05
rs1412829	<i>CDKN2BAS</i>	9p21.3	1.08E-05
rs1063192	<i>CDKN2A/B</i>	9p21.3	1.36E-07
rs2157719	<i>CDKN2A/B</i>	9p21.3	6.44E-07
rs111696067	<i>VTI1A</i>	10q25.2	NA
rs648044	<i>ZBTB16</i>	11q23.2	NA
rs498872	<i>ARCN;PHLDB1</i>	11q23.3	0.710
rs12230172	NA	12q21.2	NA
rs3851634	<i>POLR3B</i>	12q23.3	0.0129
rs1801591	<i>ETFA</i>	15q24.2	0.109
rs2297440	<i>RTEL1</i>	20q13.33	1.01E-08
rs4809324	<i>RTEL1;TNFRSF6B</i>	20q13.33	0.0570
rs6010620	<i>RTEL1;TNFRSF6B</i>	20q13.33	3.36E-08

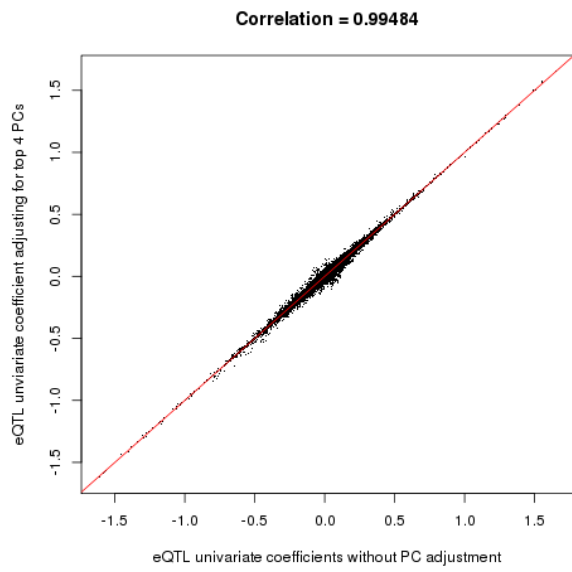
sFigure 1. Distribution of number of eQTL in 30,527 transcripts. 24 transcripts with more than 100 eQTL are not shown in the plot.

Distribution of No. of eQTL in 30,527 transcripts

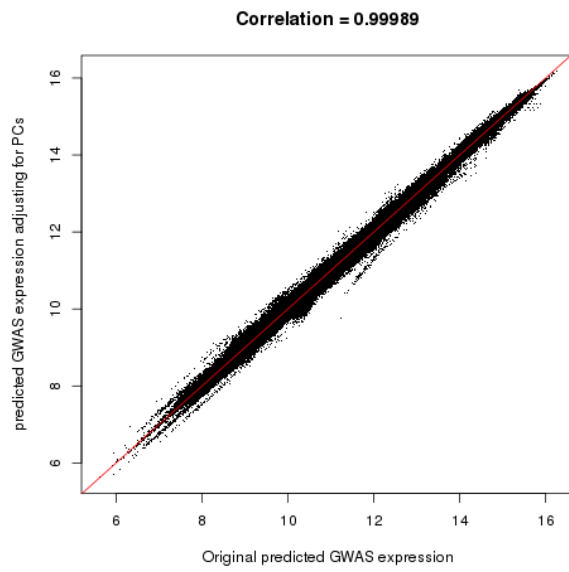


sFigure 2. Comparison of eQTL association (a) and predicted transcript expression (b) with and without adjustment of principal components of population stratification.

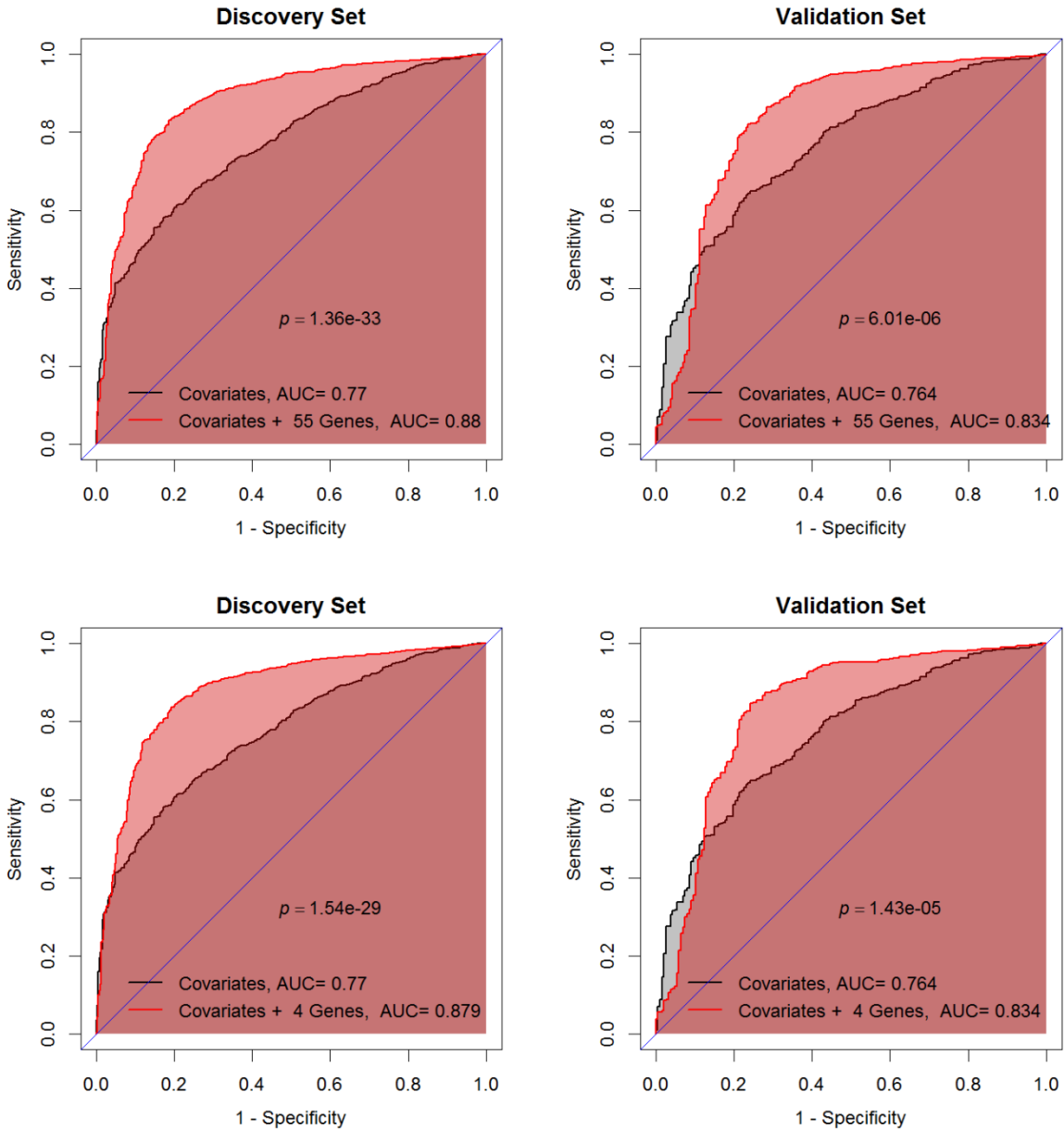
a



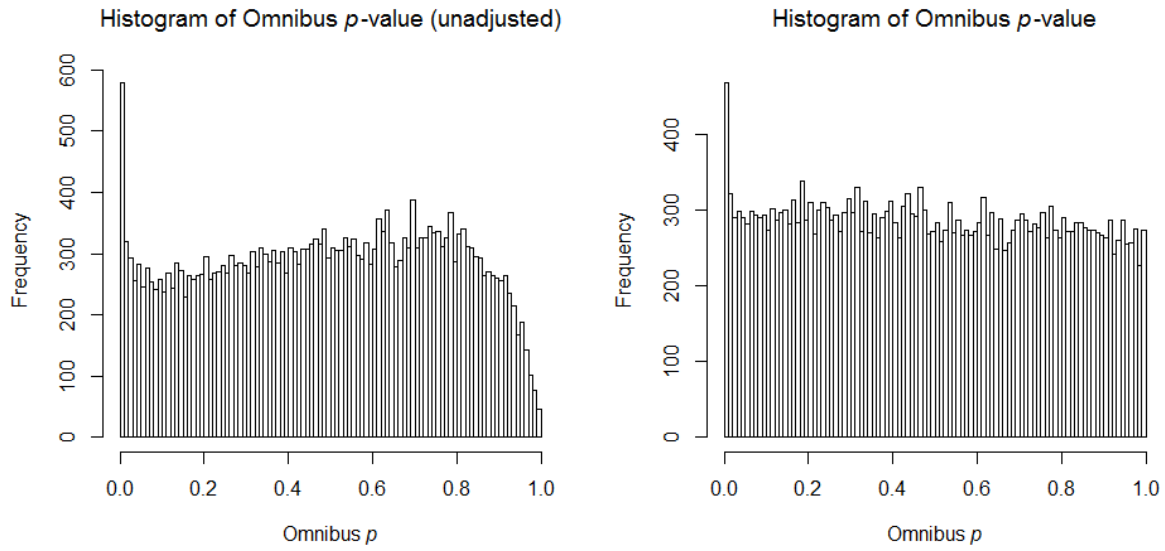
b



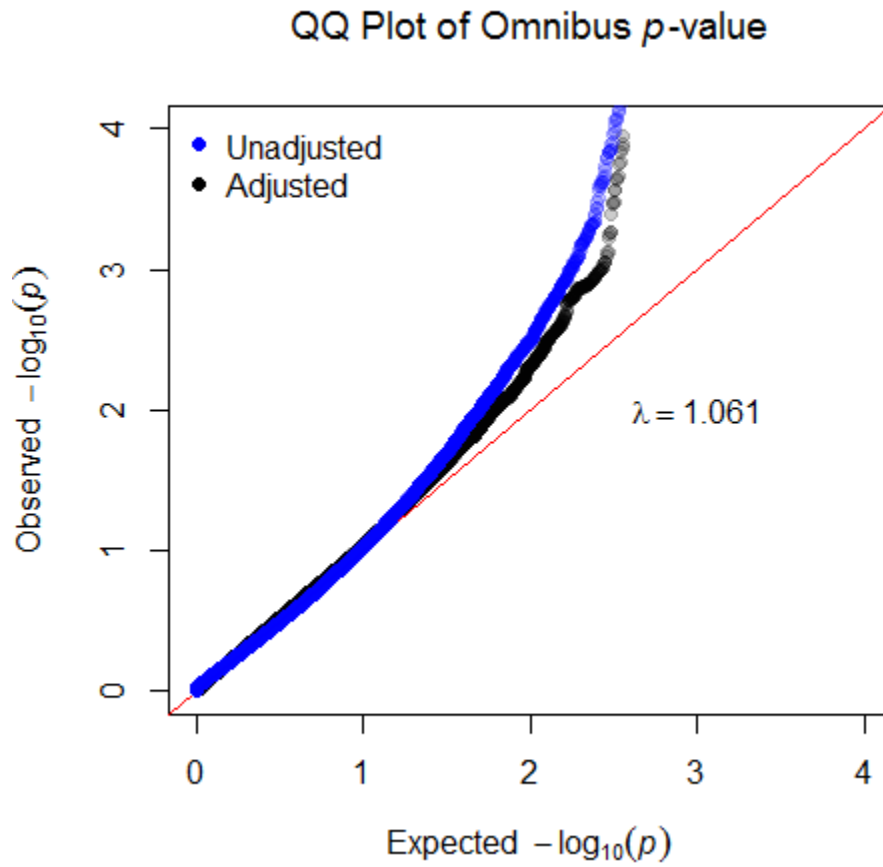
sFigure 3. The gene signature of glioma risk with eQTL analyses adjusting for population stratification. (a) and (b), the ROC curve and its area under the curve (AUC) of the model with only covariates (black curve) and that with covariates and the 55 transcripts (red curve) in Discovery Set (a) and Validation Set (b). (c) and (d), the ROC curve and its area under the curve (AUC) of the model with only covariates (black curve) and that with covariates and the 4 genes: *DRD5*, *WDR1*, *NOMO1* and *PDXDC1* (red curve) in Discovery Set (c) and Validation Set (d).



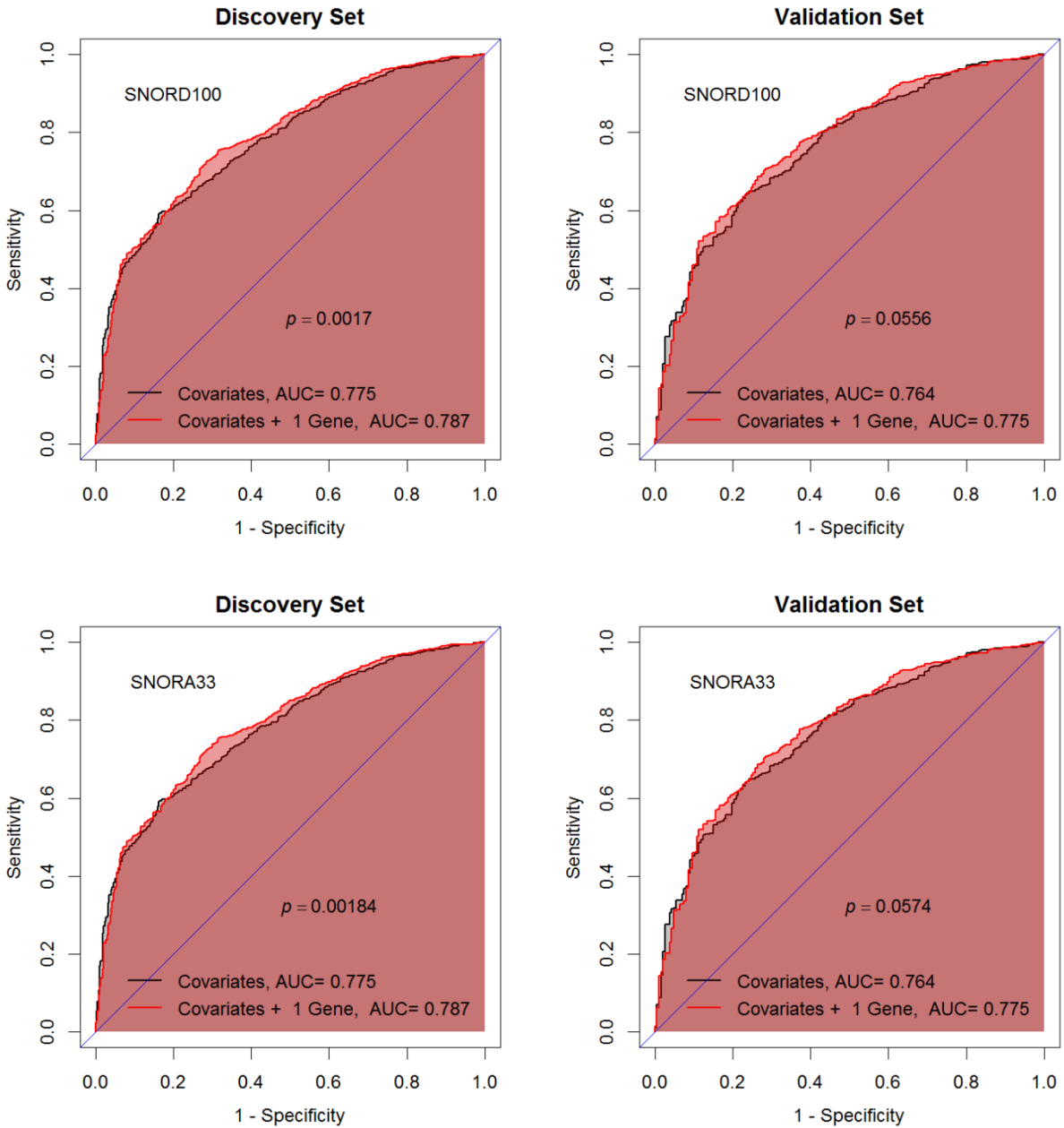
sFigure 4. Histogram of iGWAS omnibus p-value for the association of 30,527 transcripts with glioma risk. Left, p-values without adjusting for age, gender and population stratification; right: adjusted p-values.

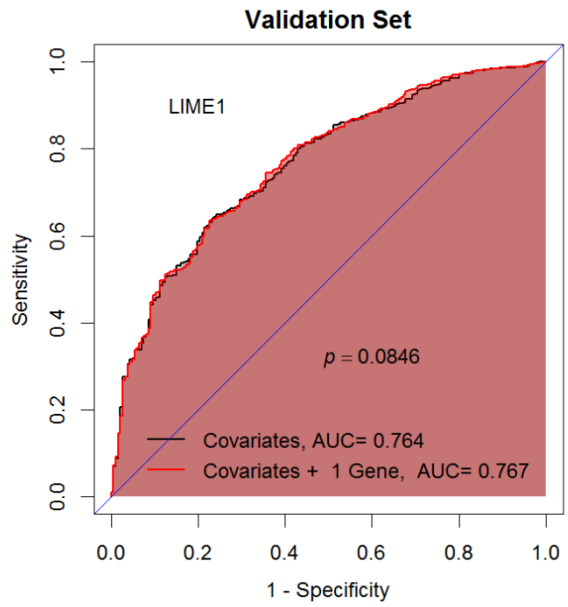
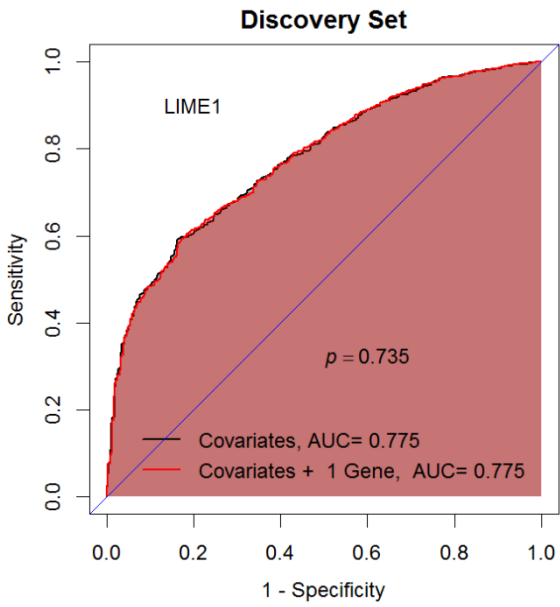
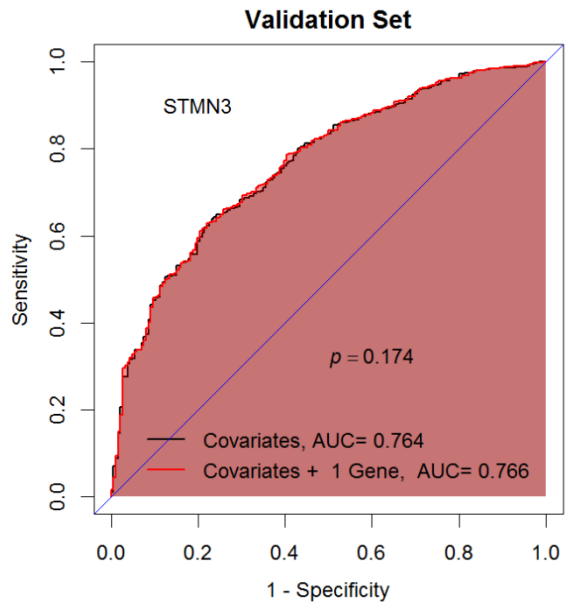
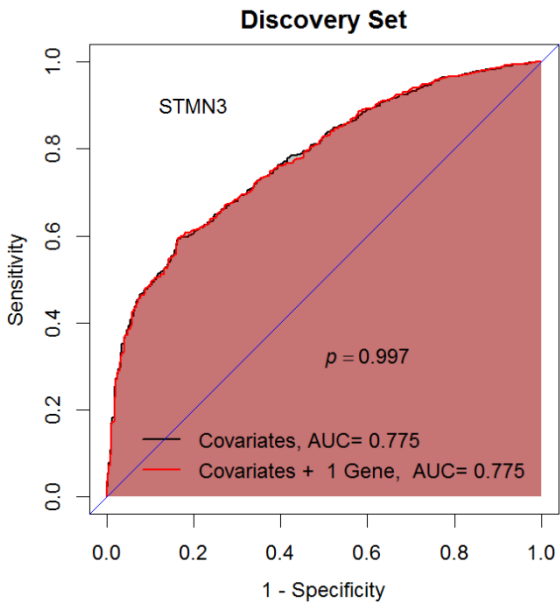


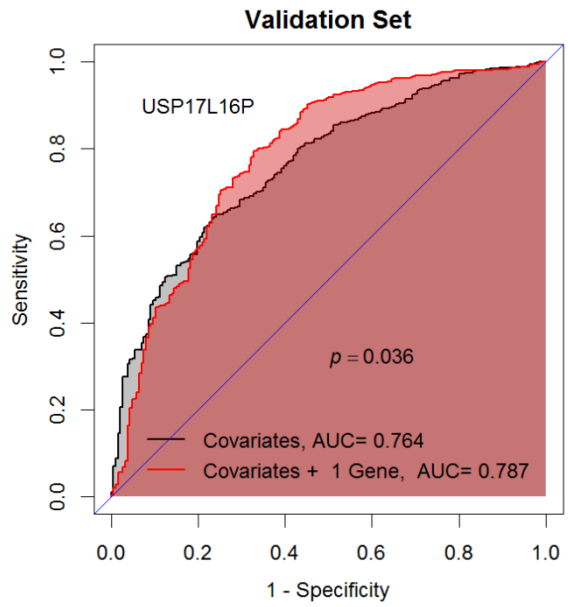
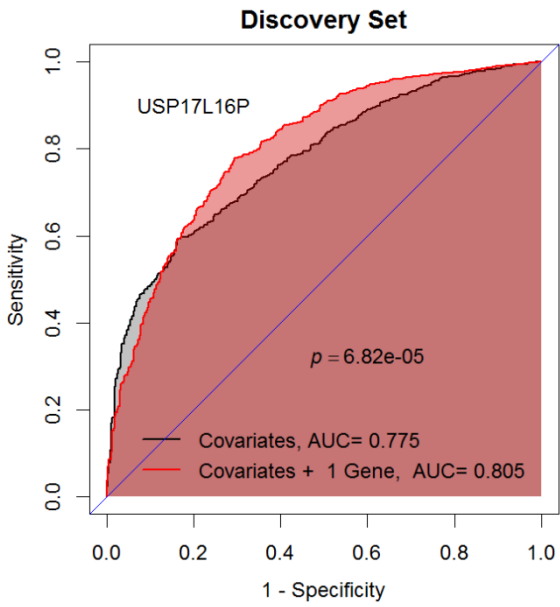
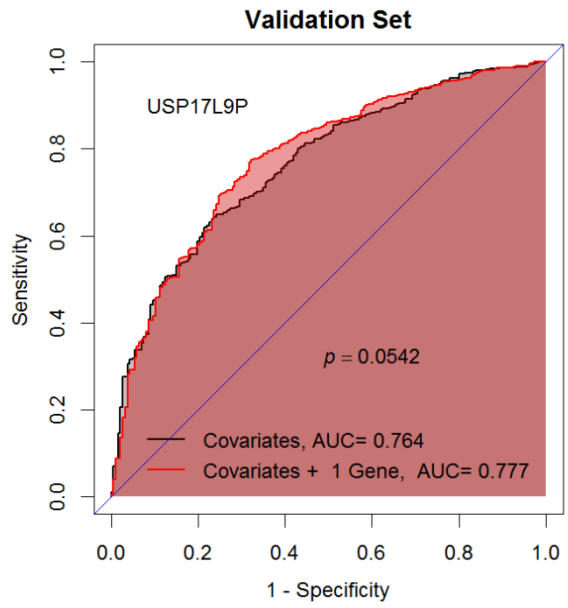
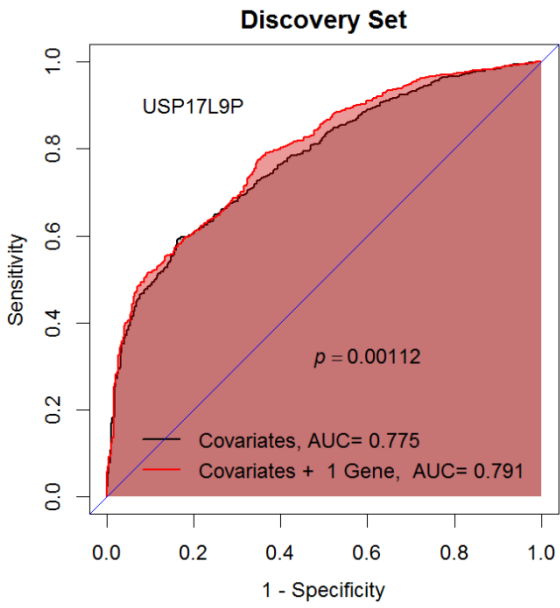
sFigure 5. Quantile-quantile plot of iGWAS omnibus p-value for the association of 30,527 transcripts with glioma risk, with genomic inflation factor λ of 1.061. Blue dots indicate the p-values from analyses without adjusting for age, gender and population stratification.

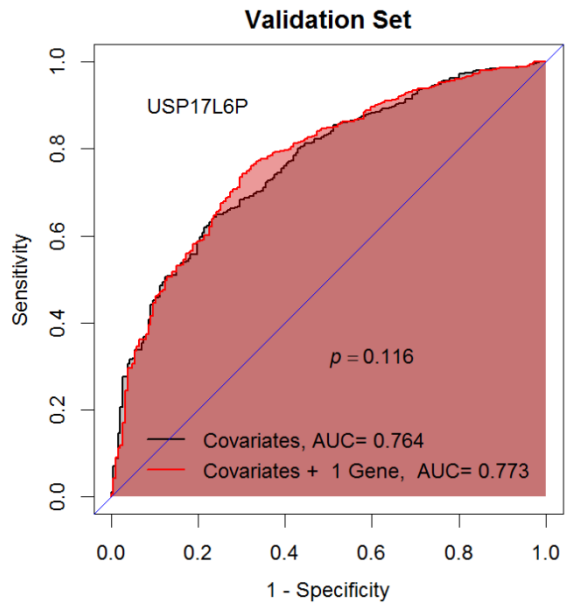
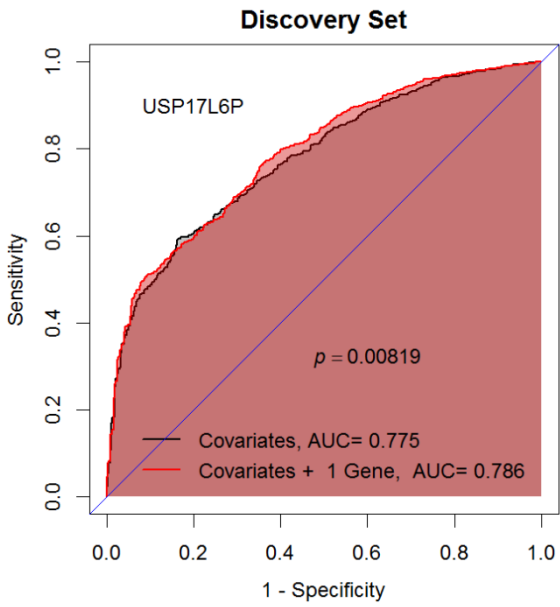
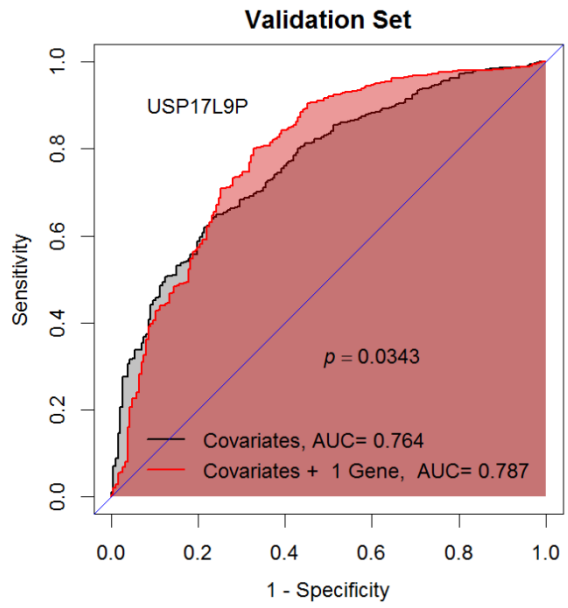
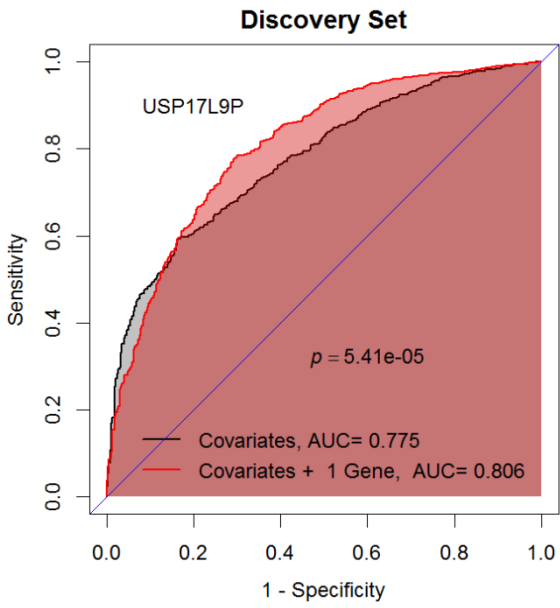


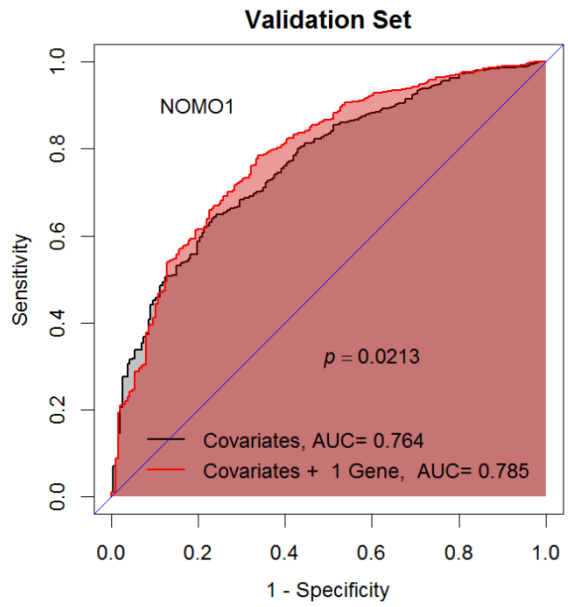
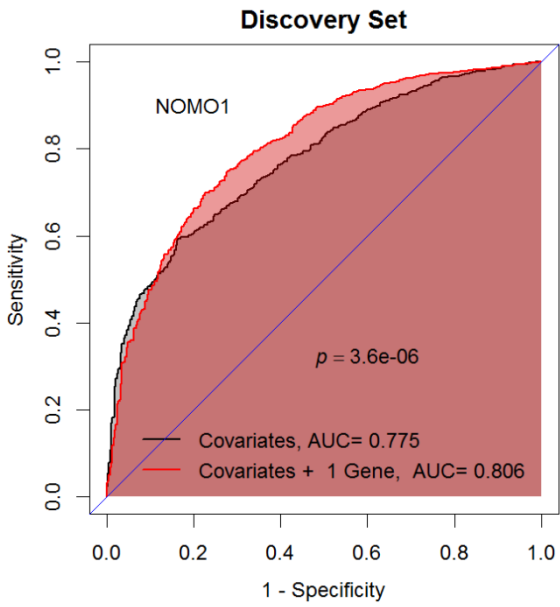
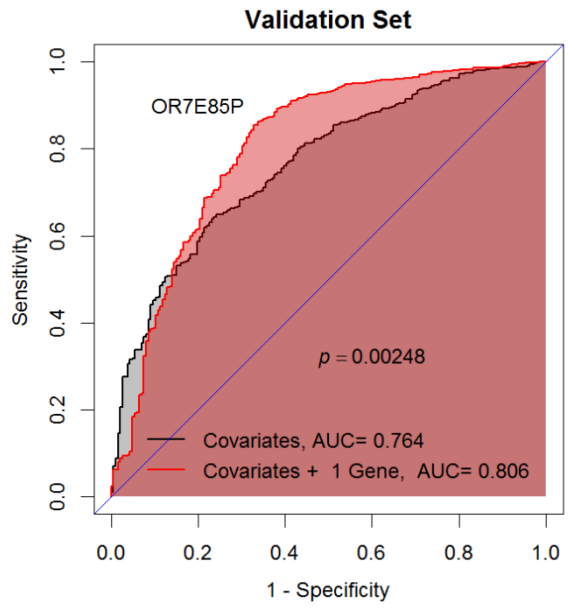
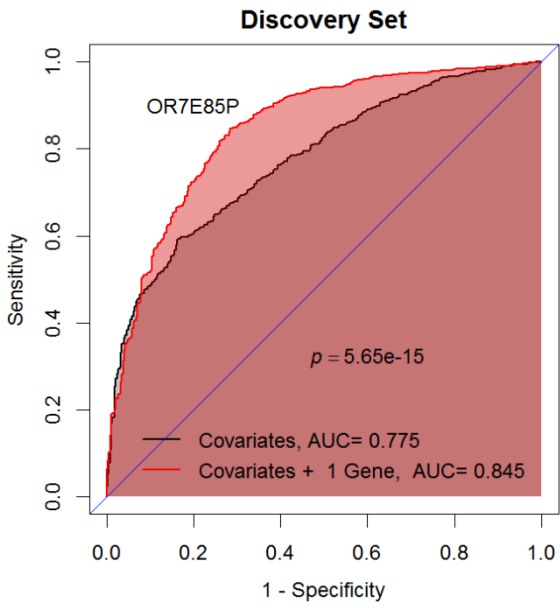
sFigure 6. The ROC curves for the 55 validated transcripts and its AUC of the model with only covariates (black curve) and that with covariates plus the estimated expression values of one transcript (red curve) in Discovery Set (left) and Validation Set (right).

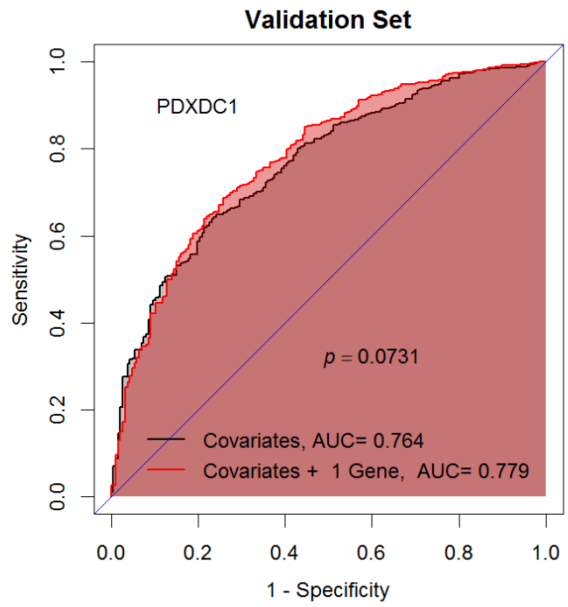
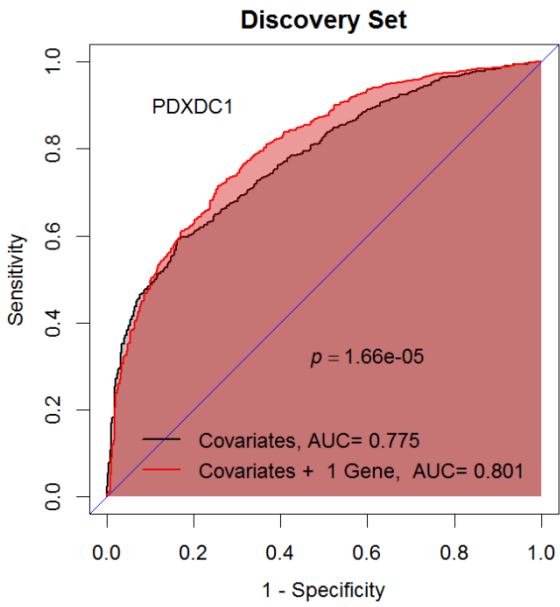
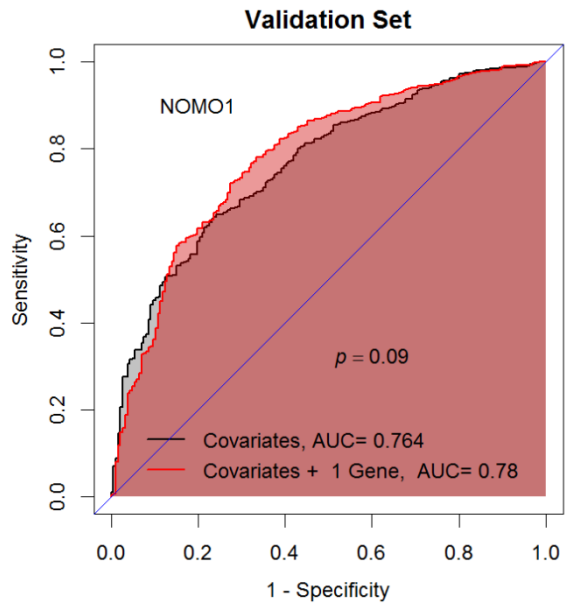
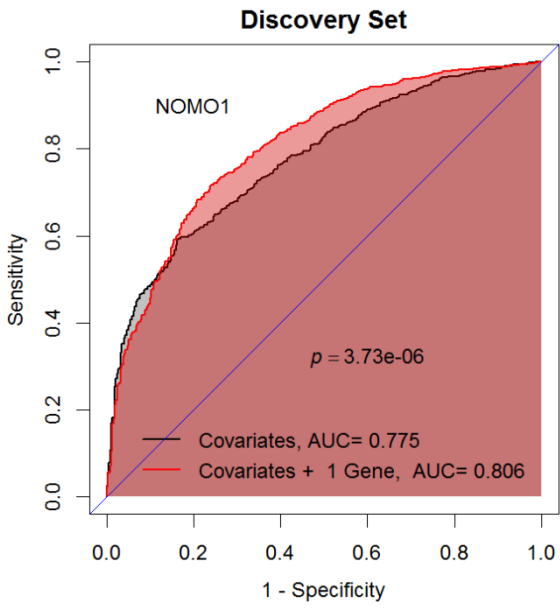


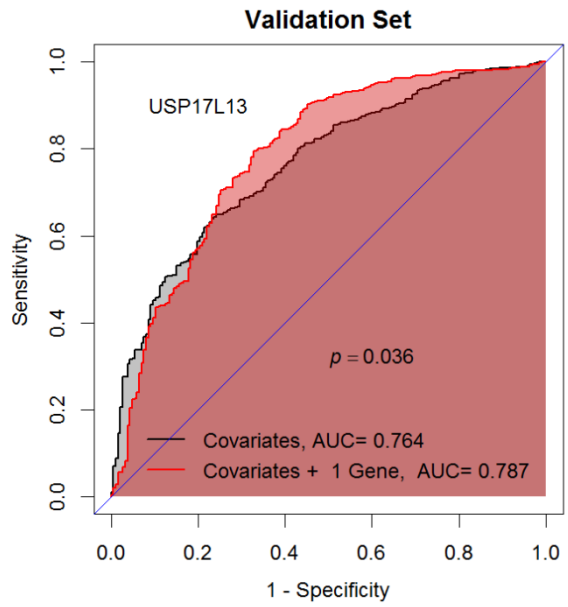
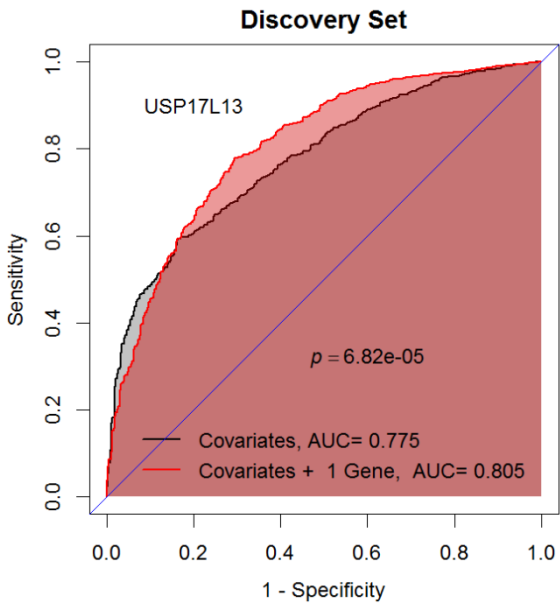
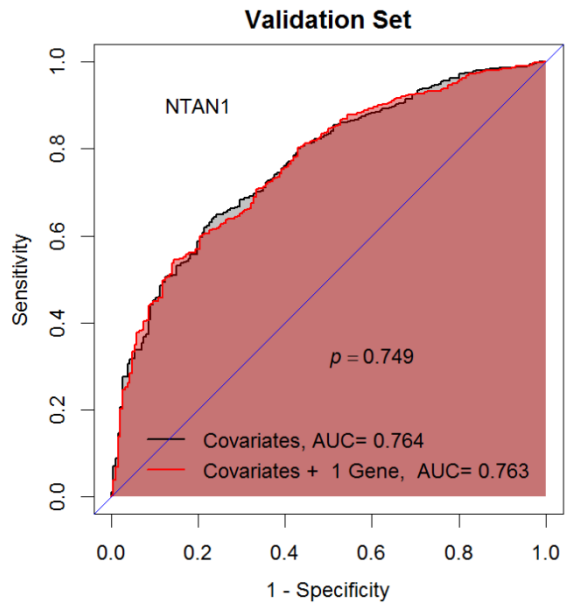
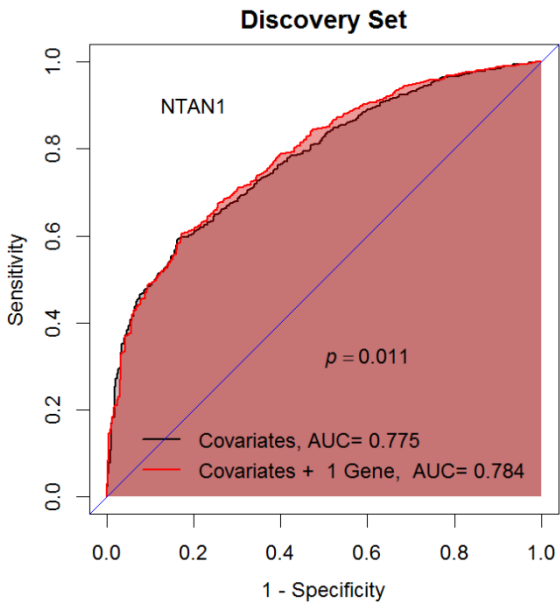


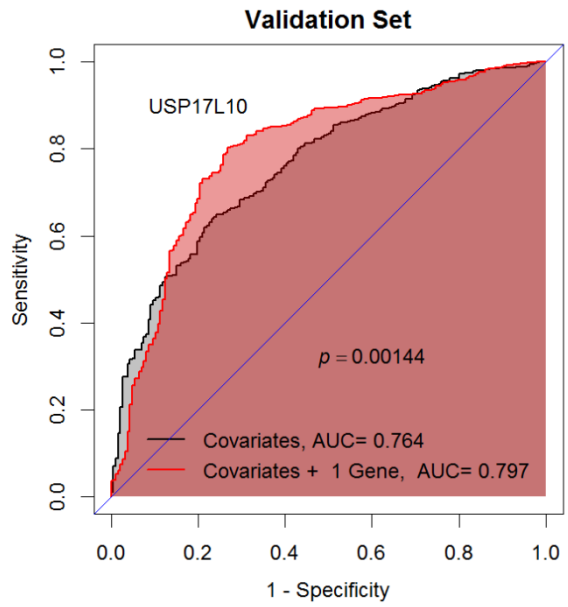
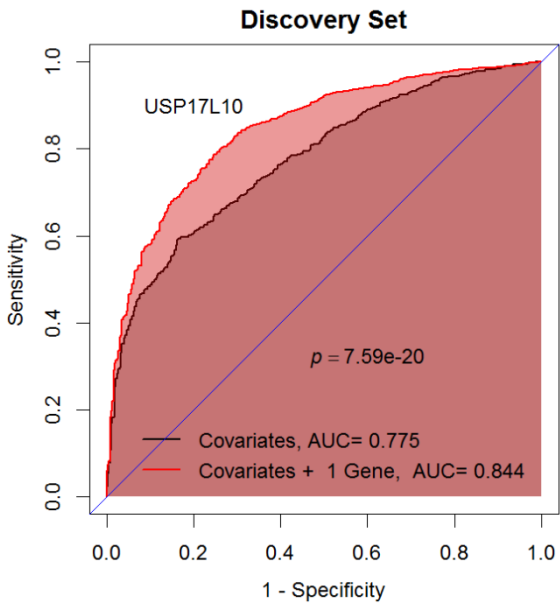
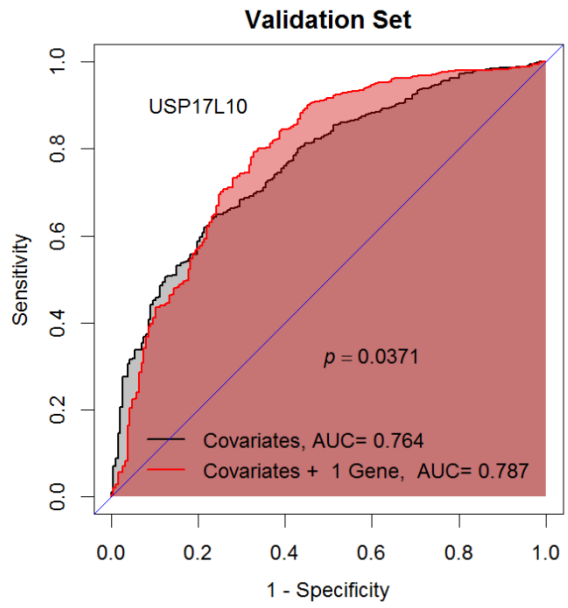
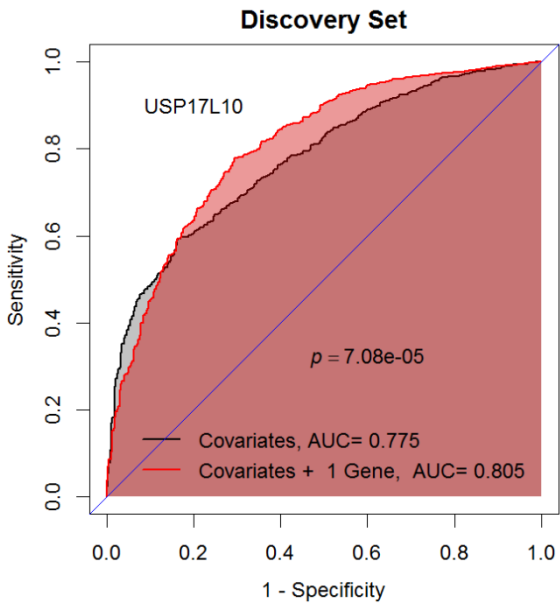


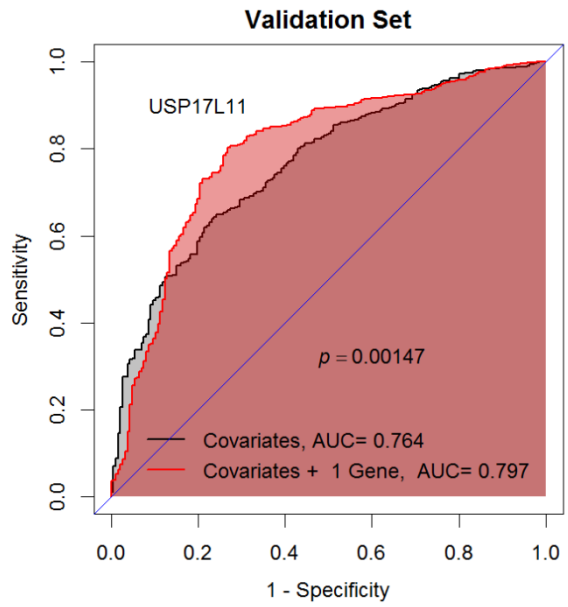
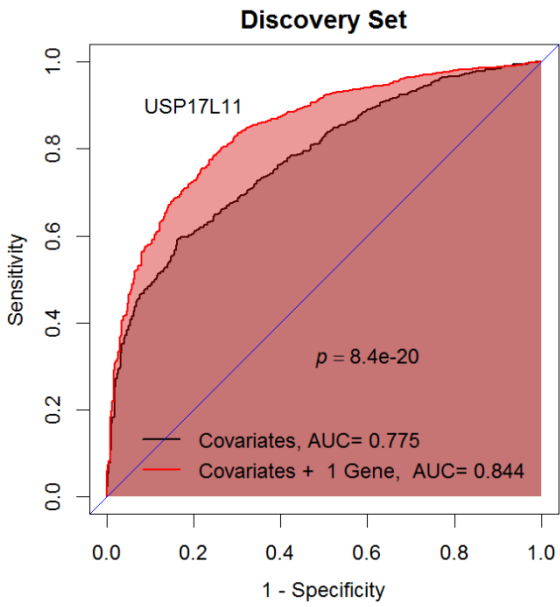
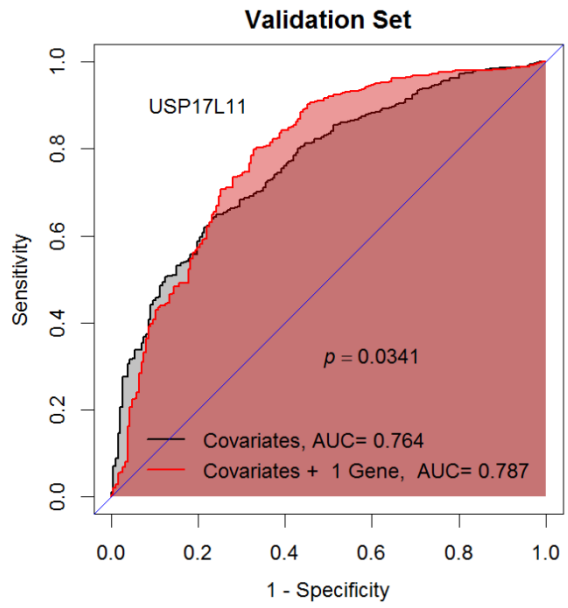
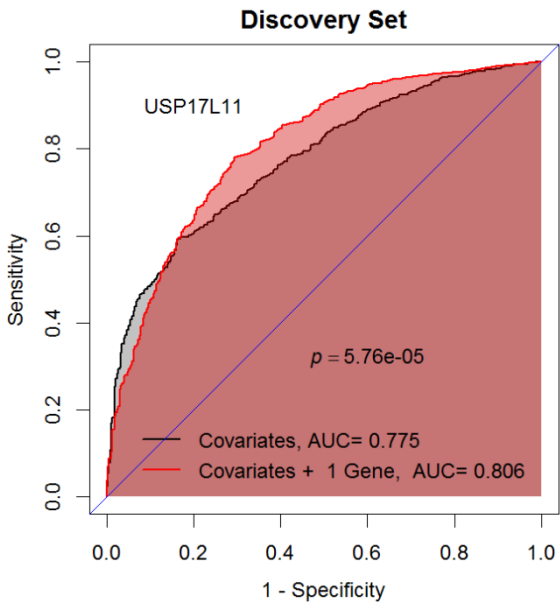


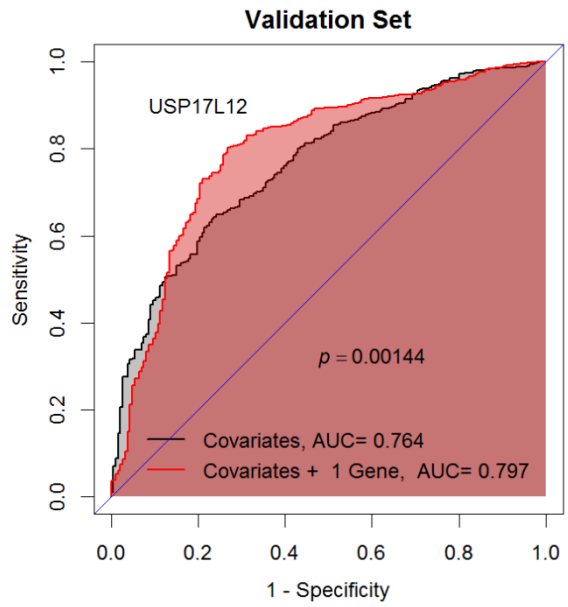
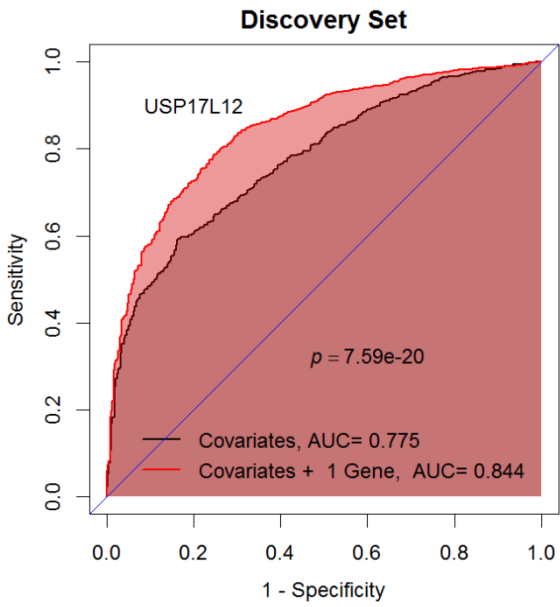
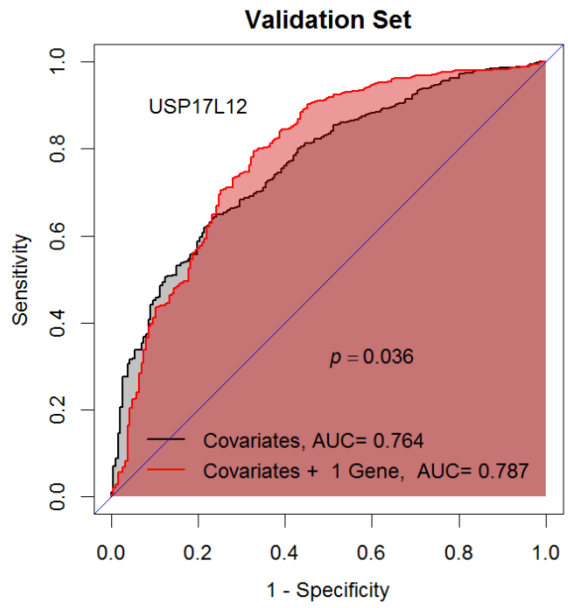
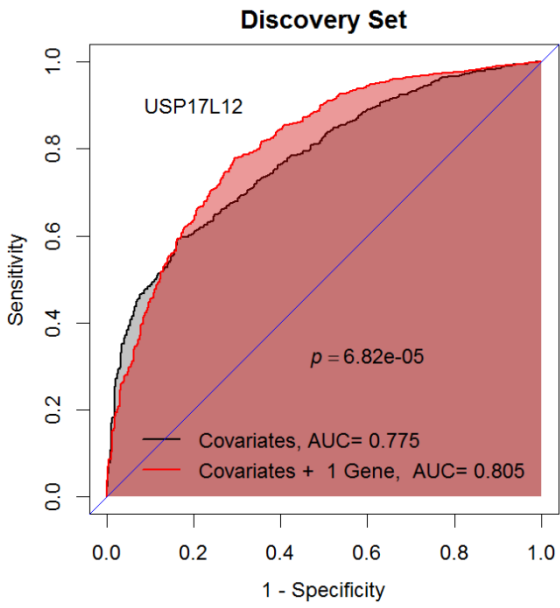


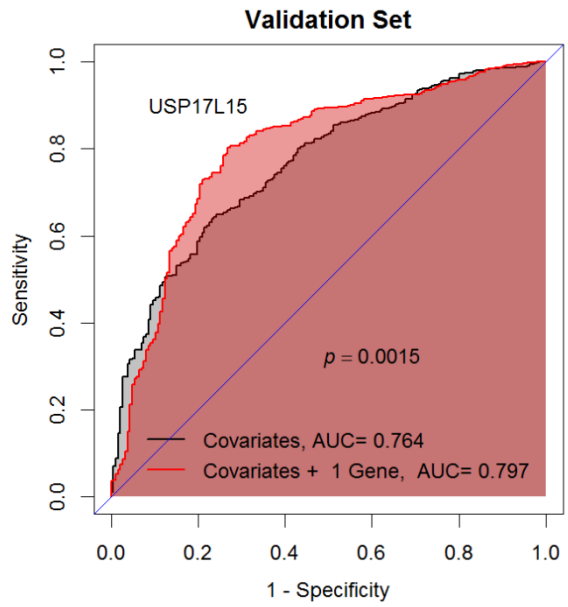
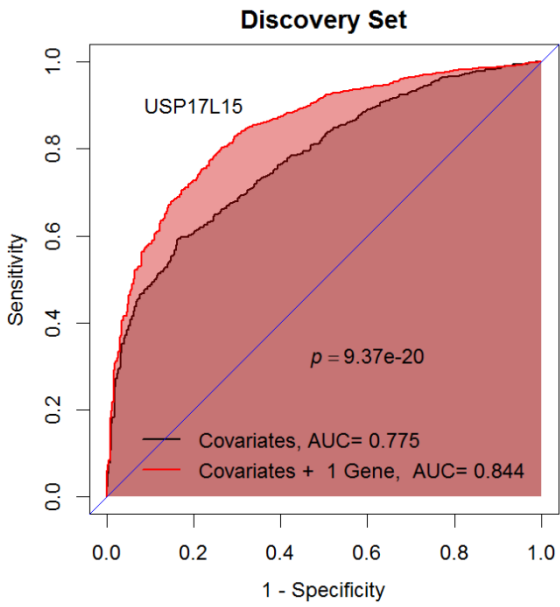
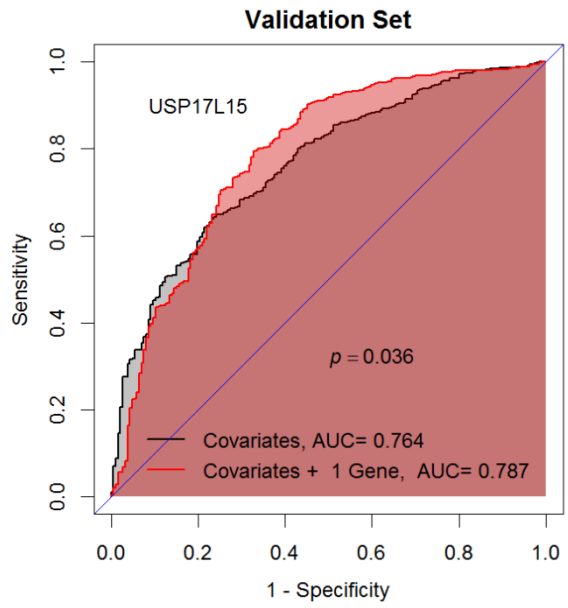
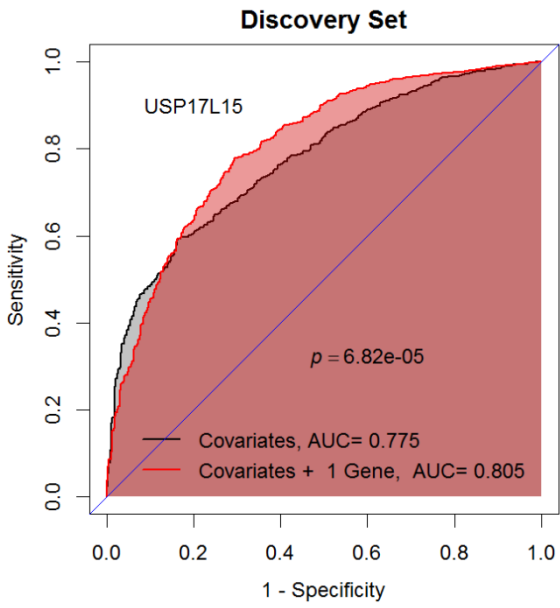


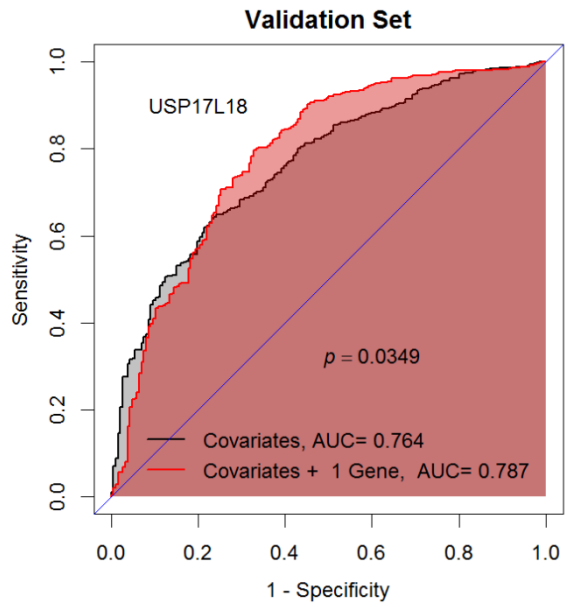
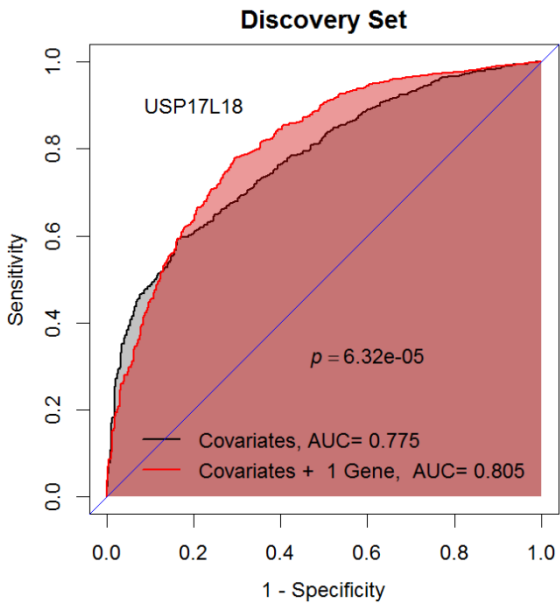
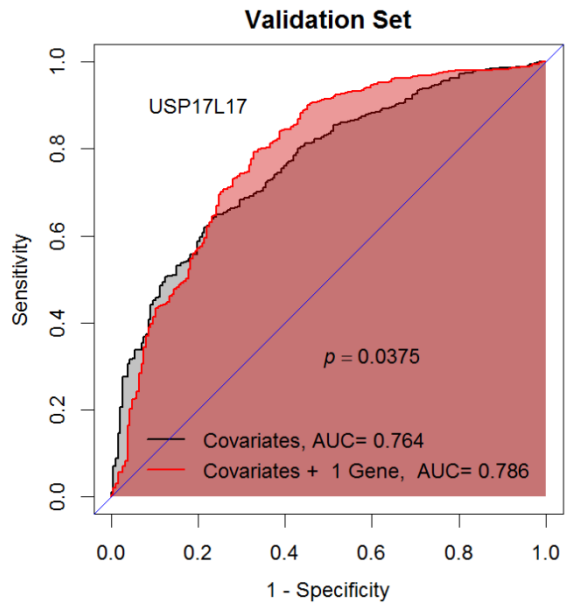
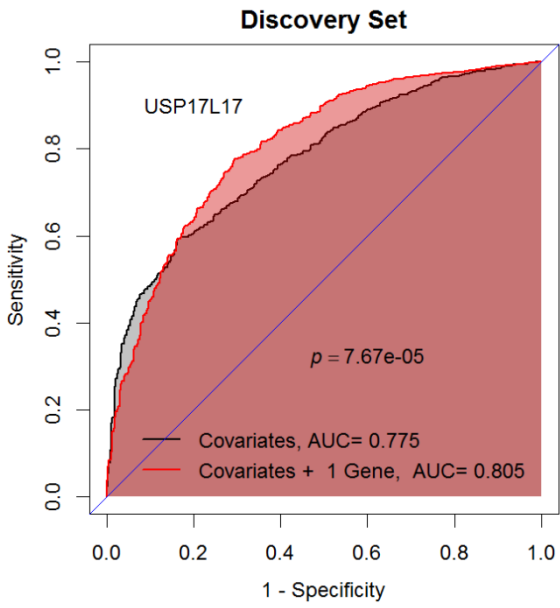


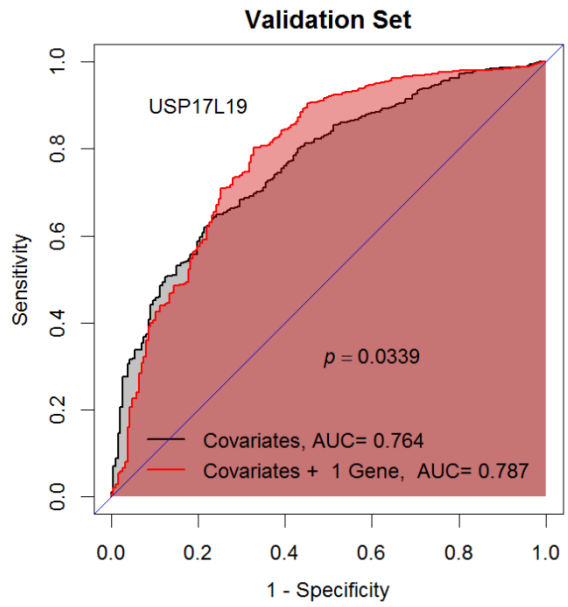
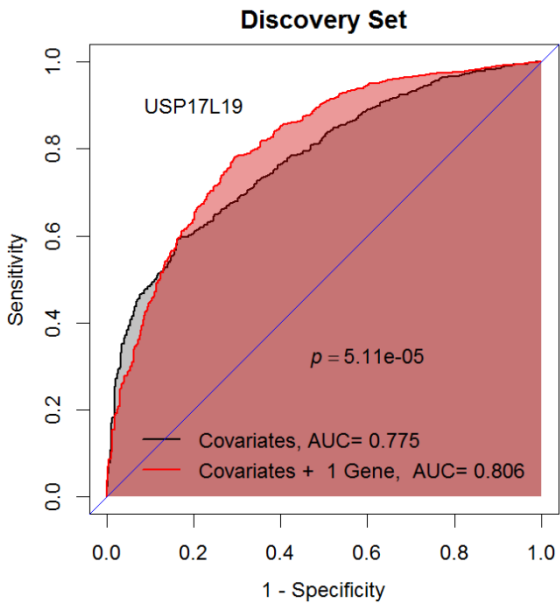
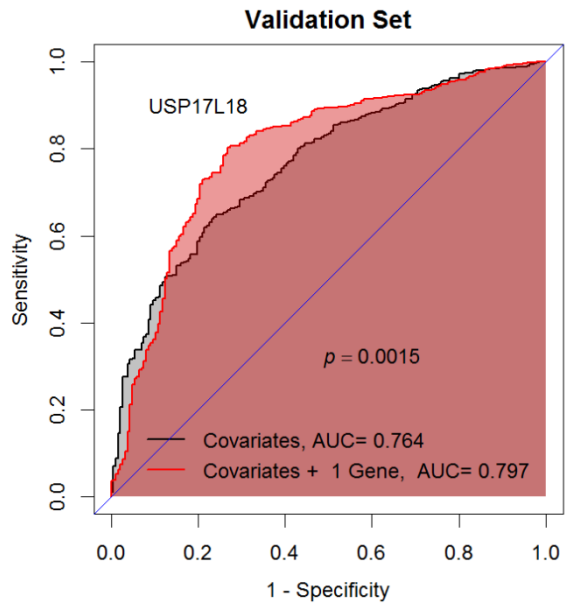
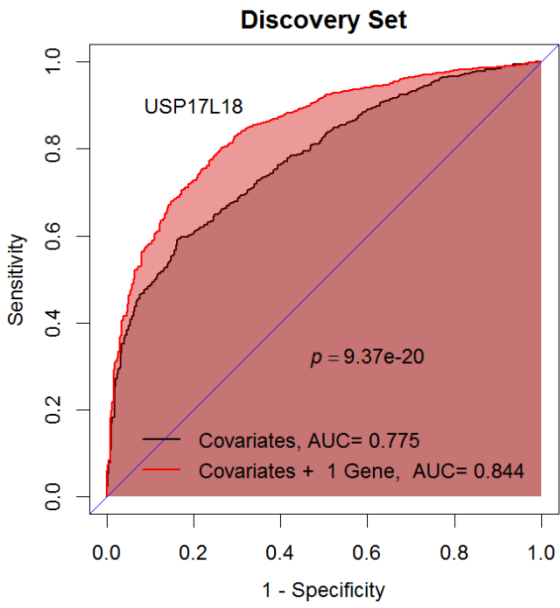


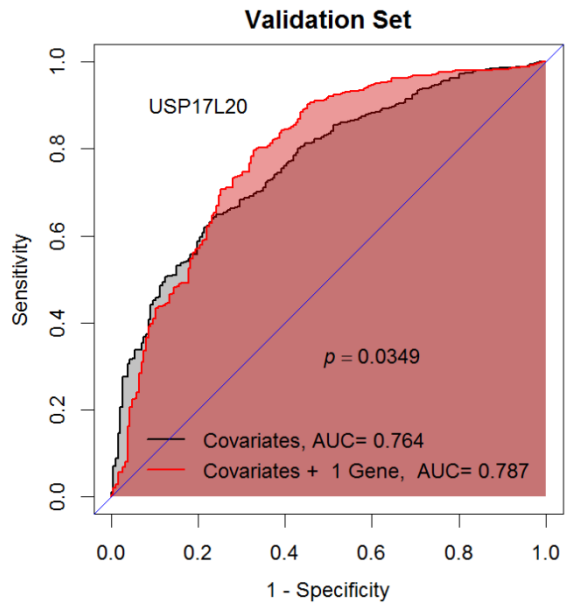
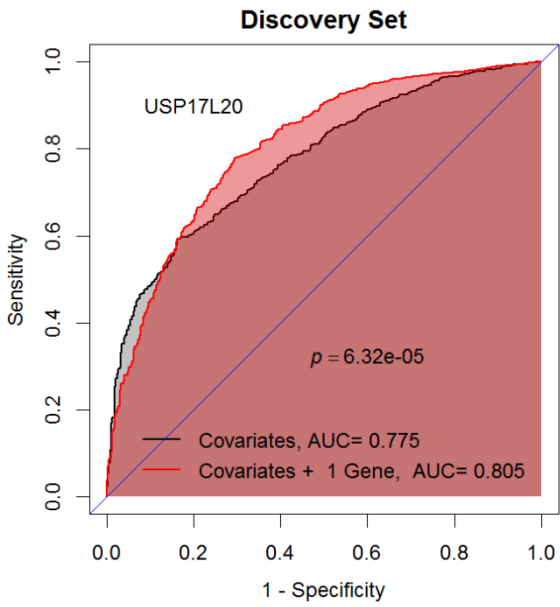
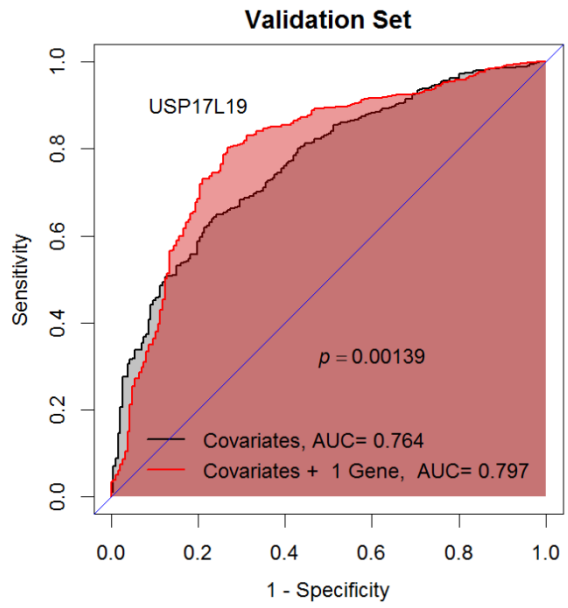
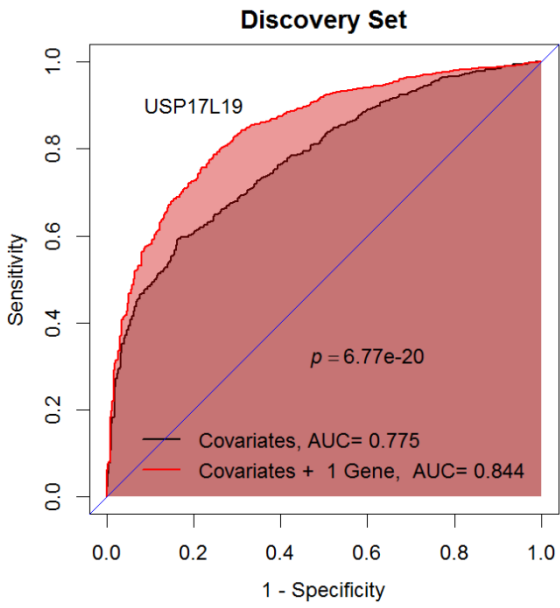


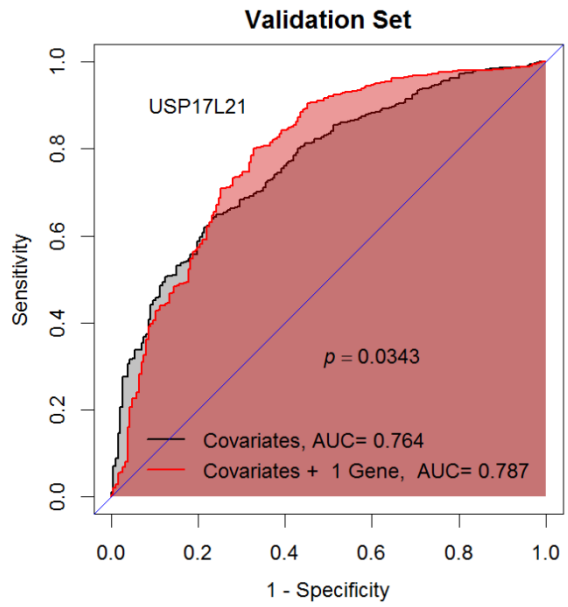
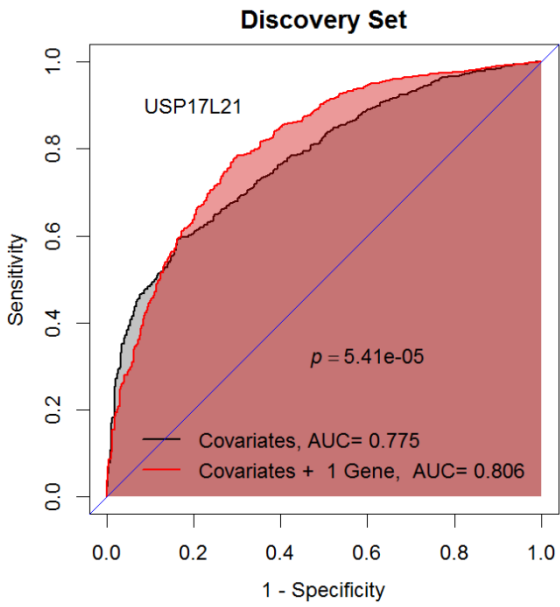
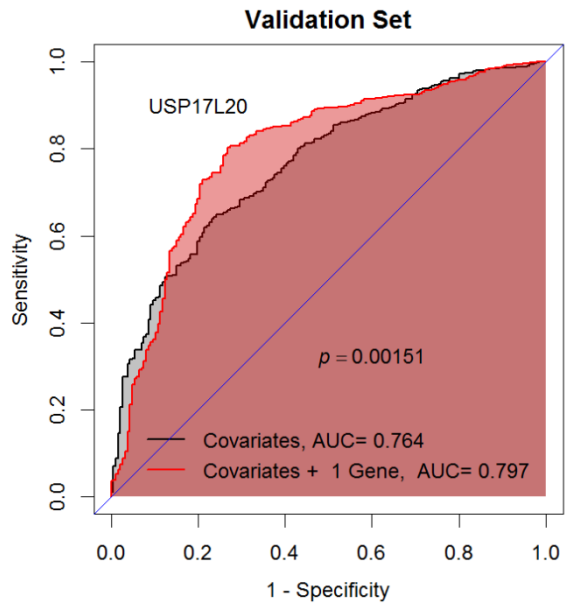
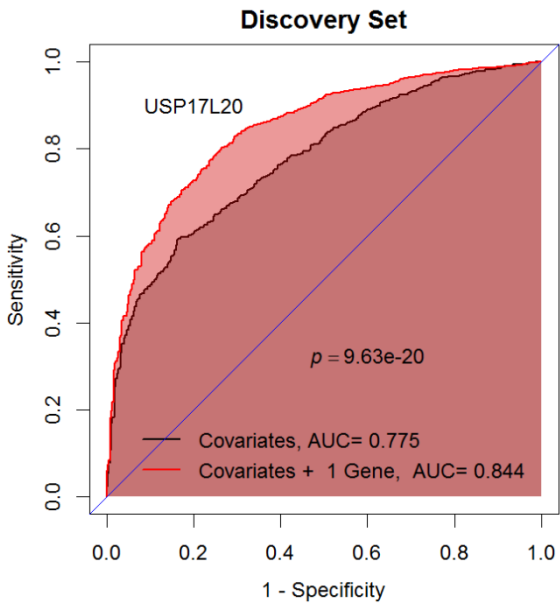


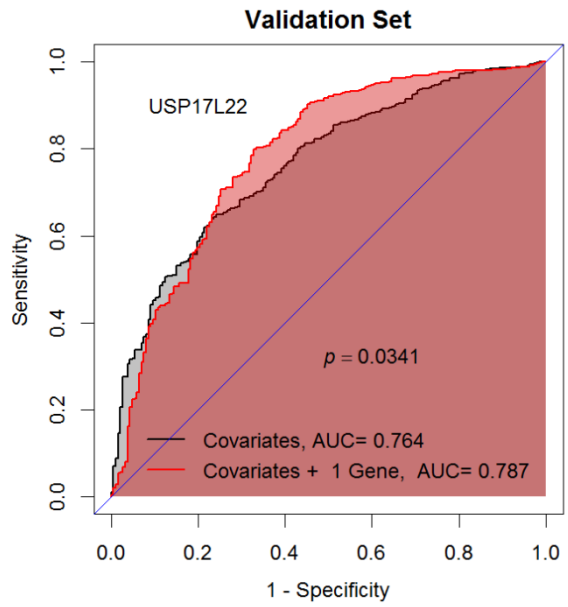
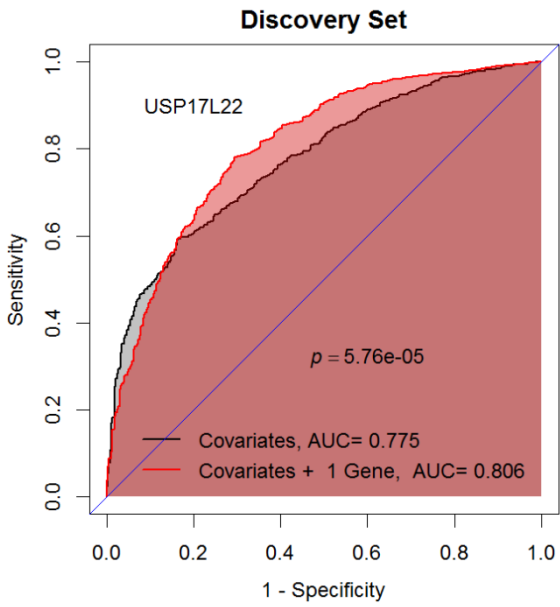
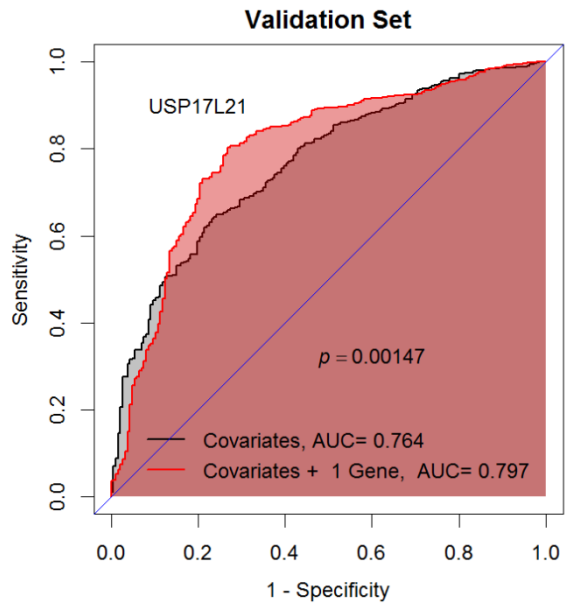
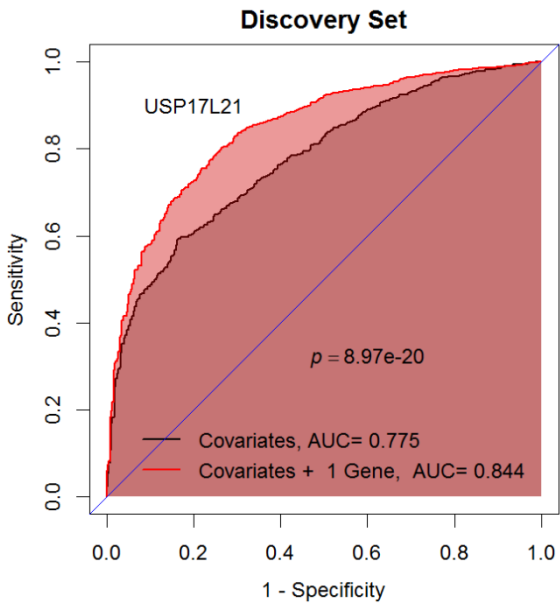


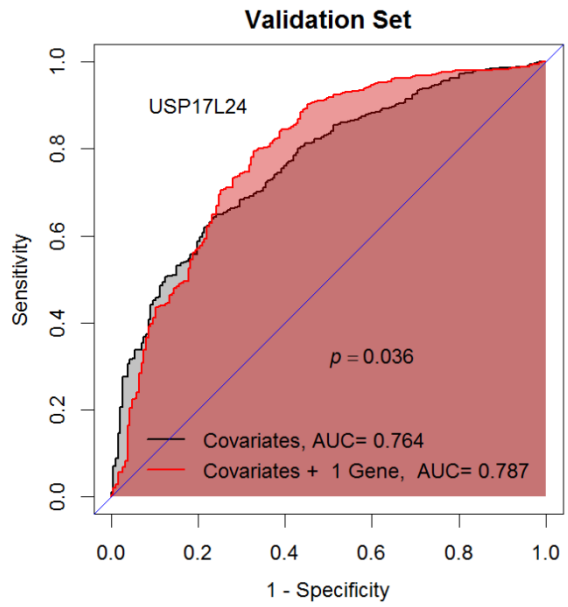
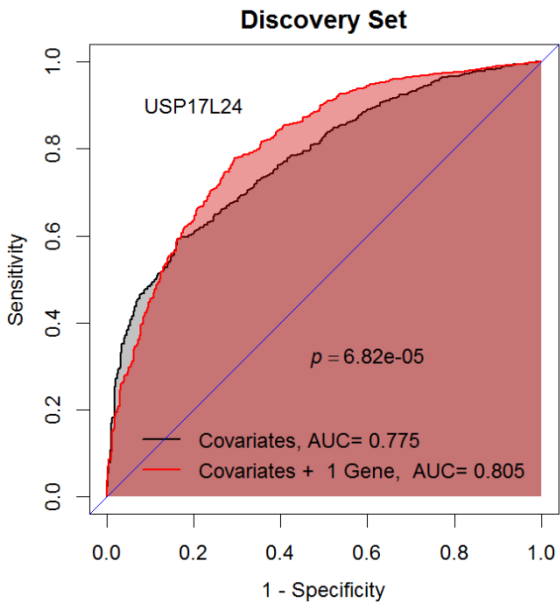
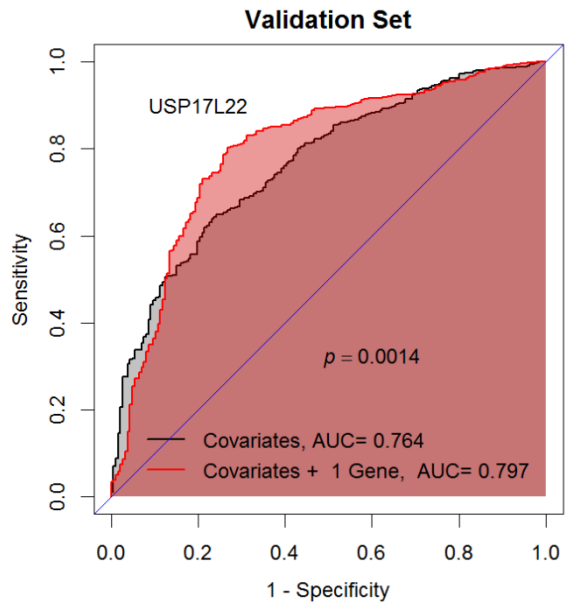
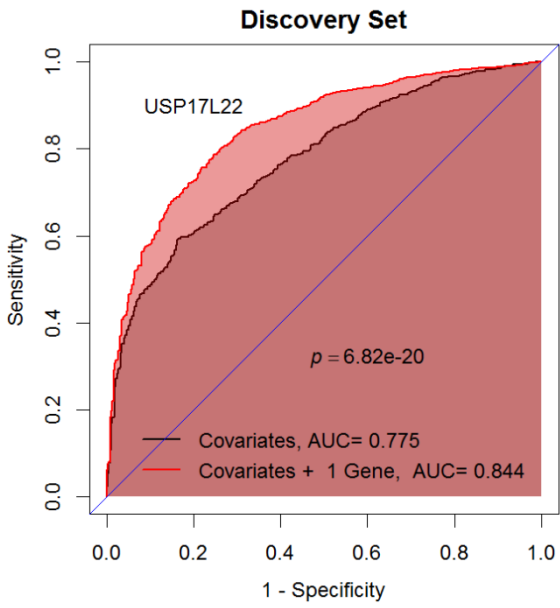


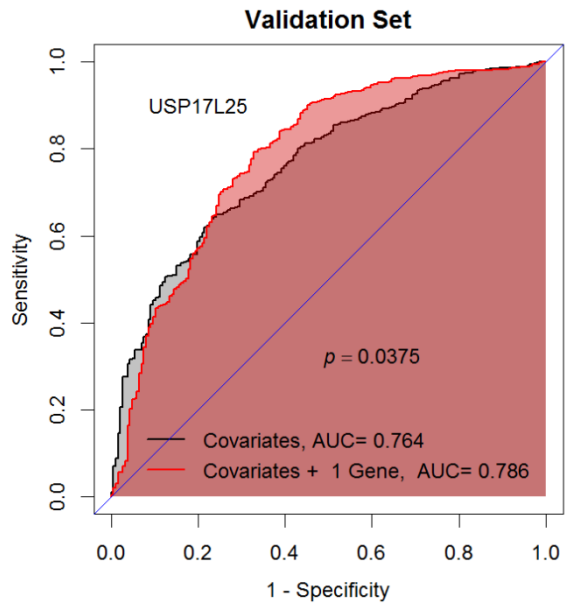
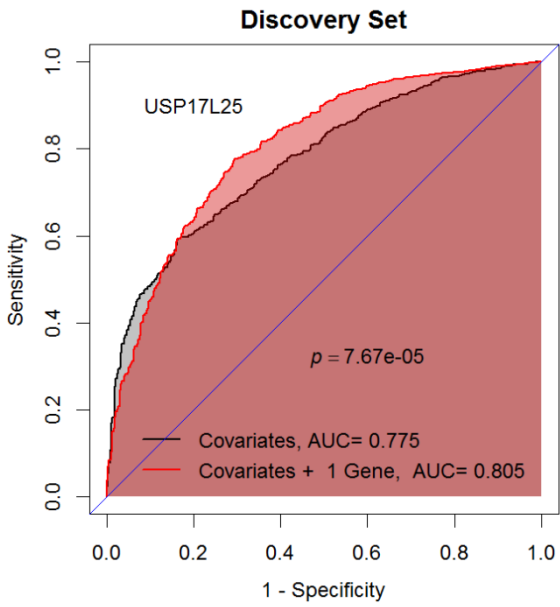
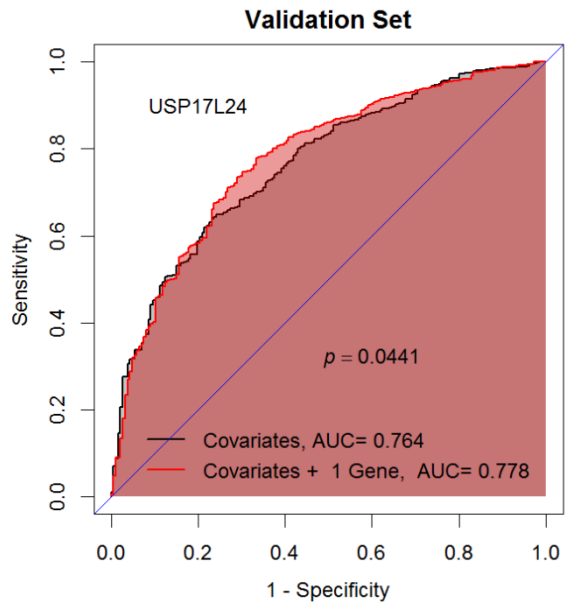
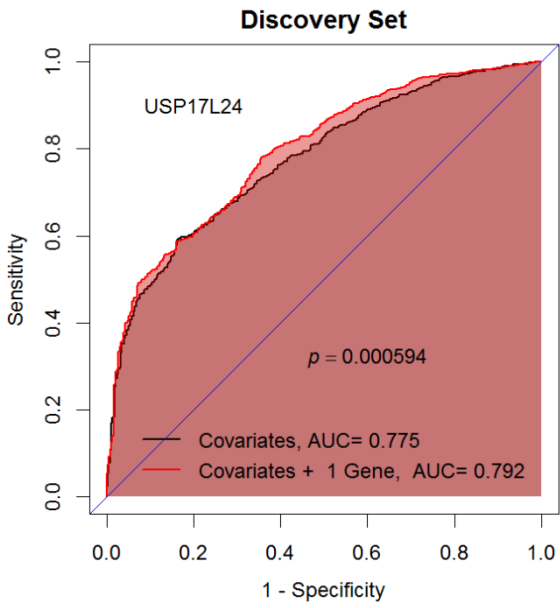


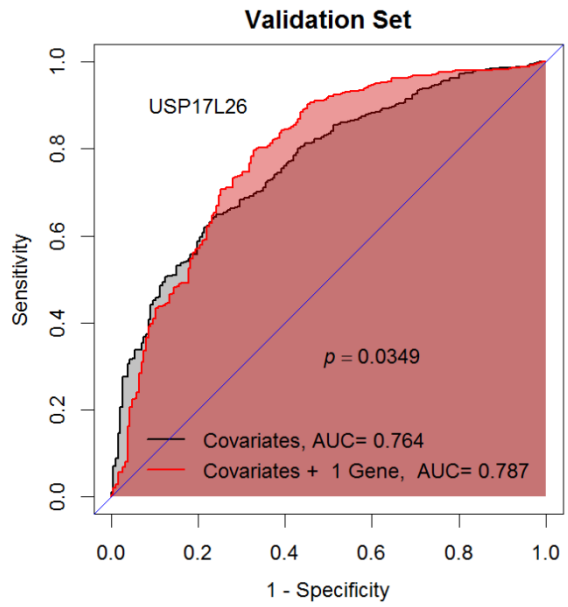
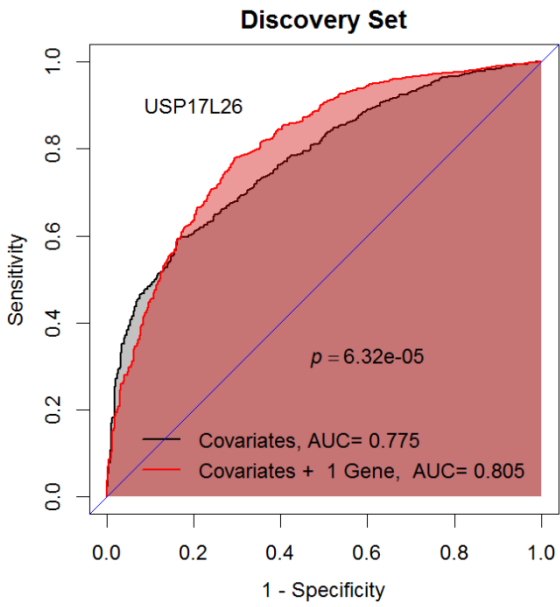
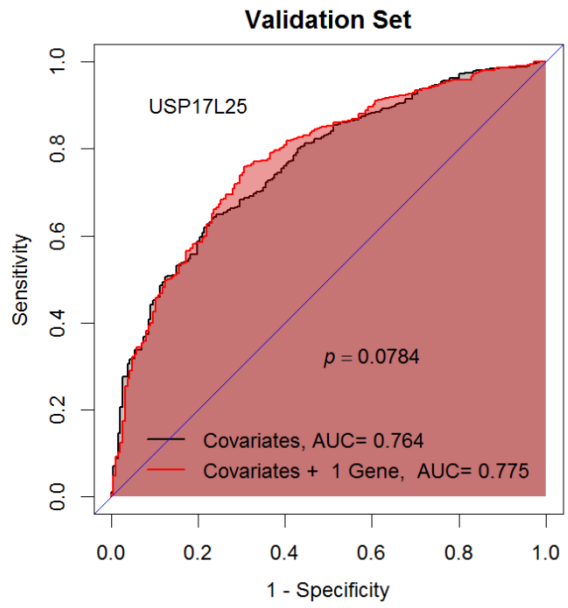
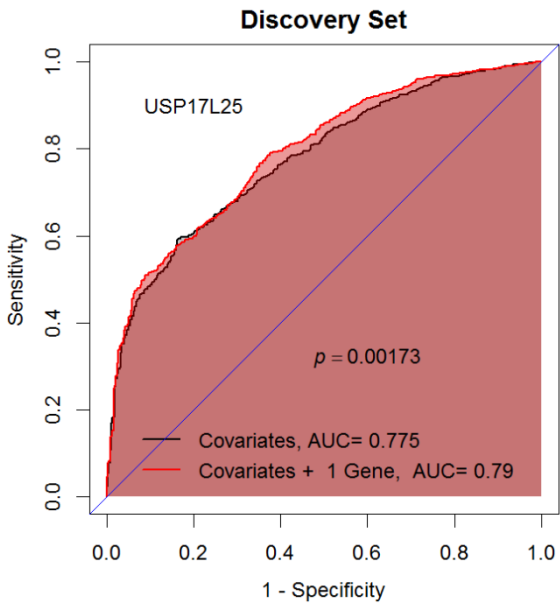


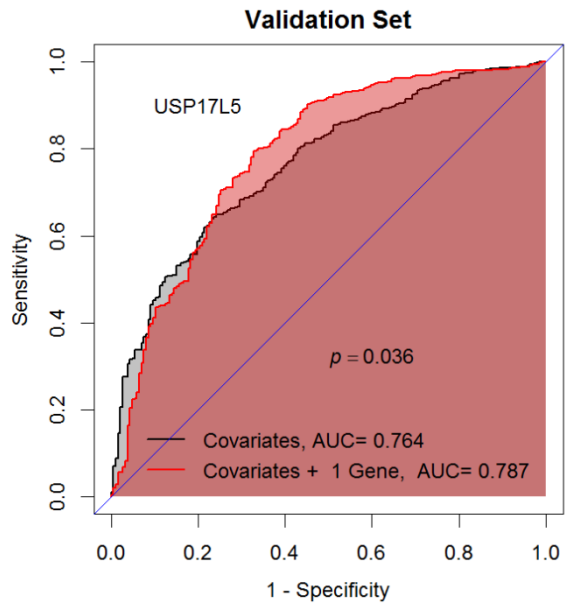
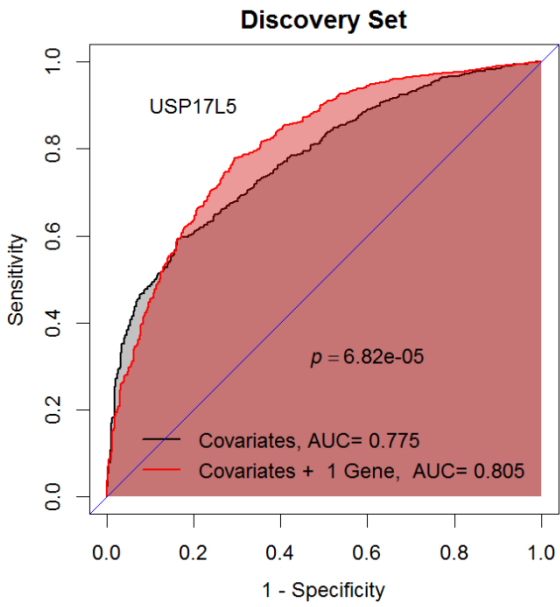
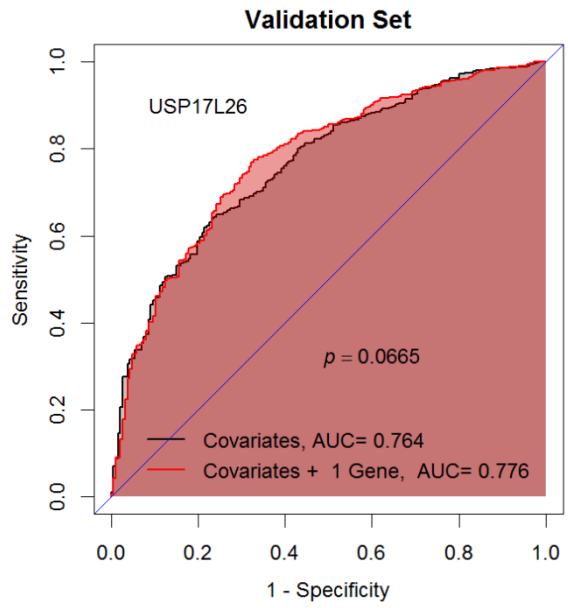
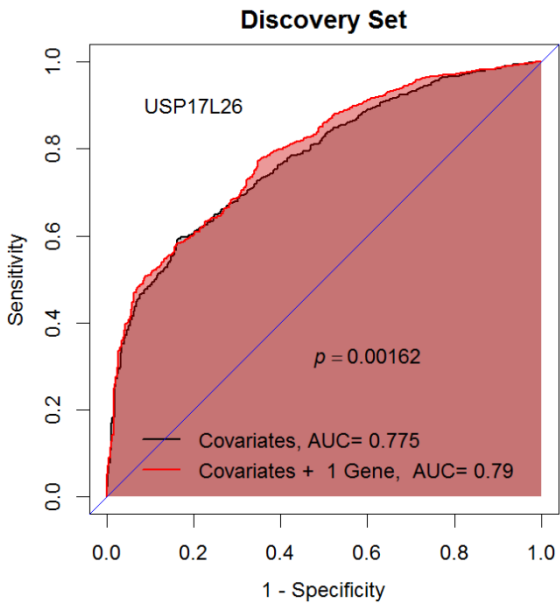


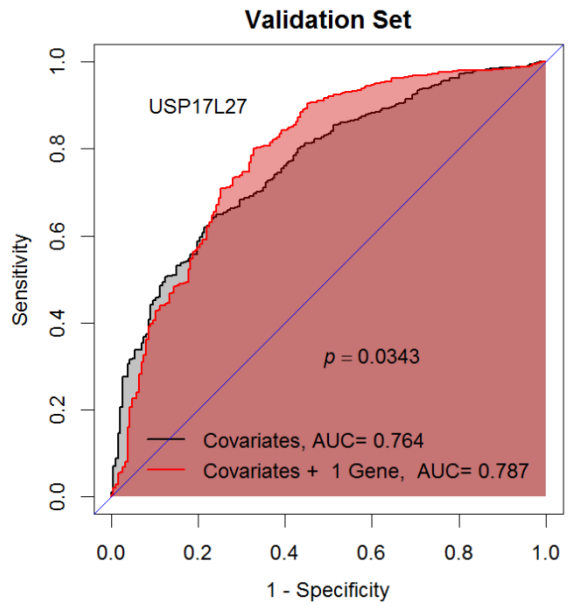
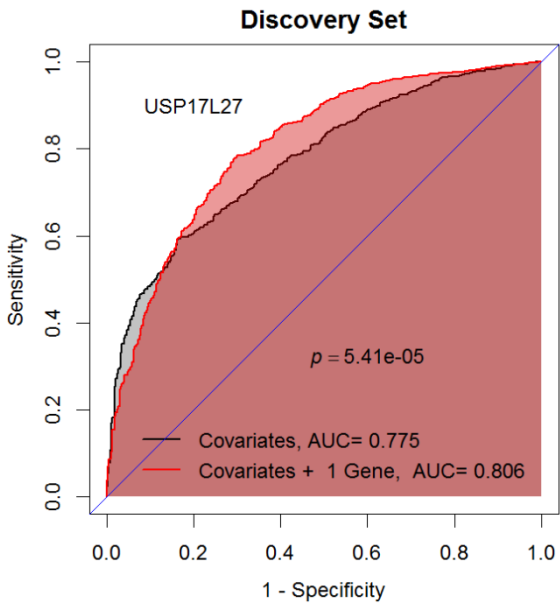
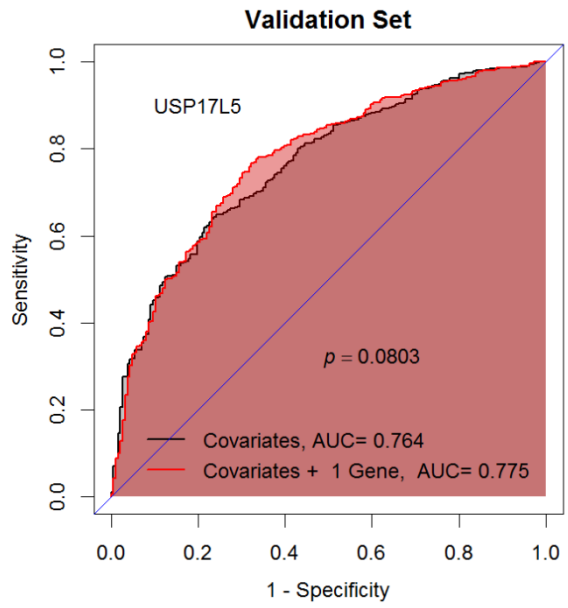
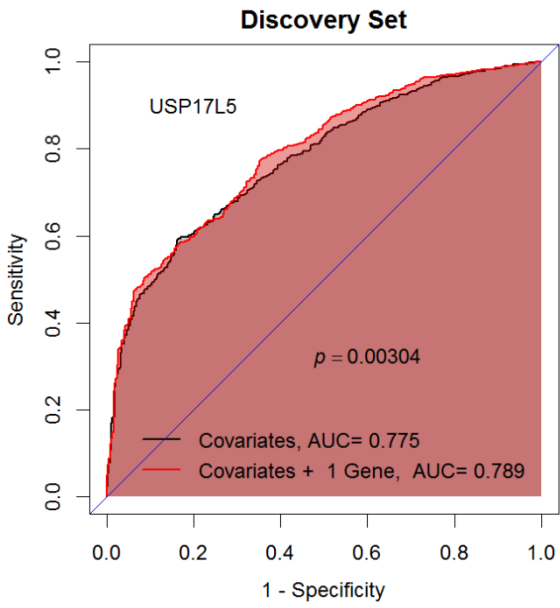


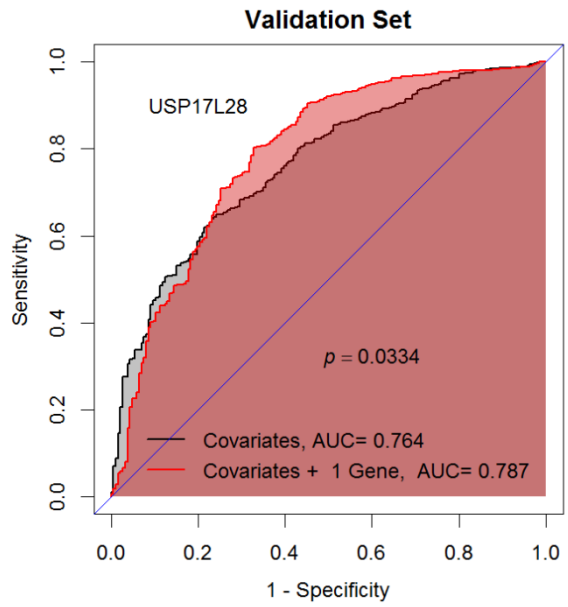
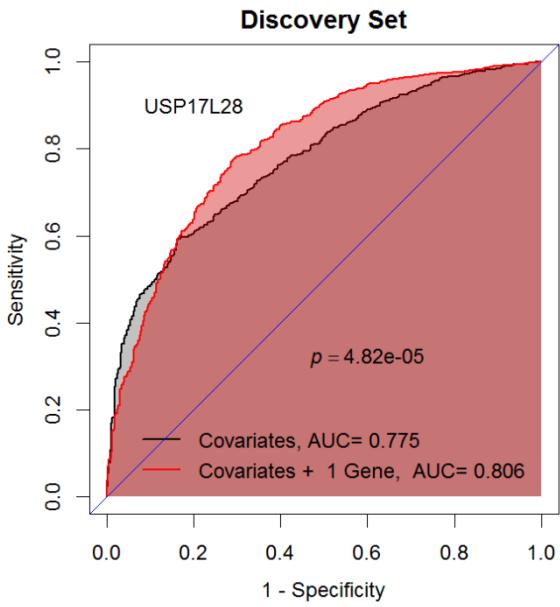
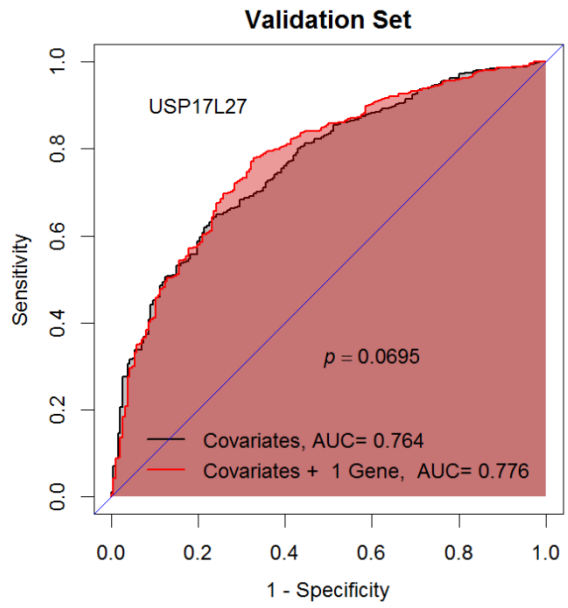
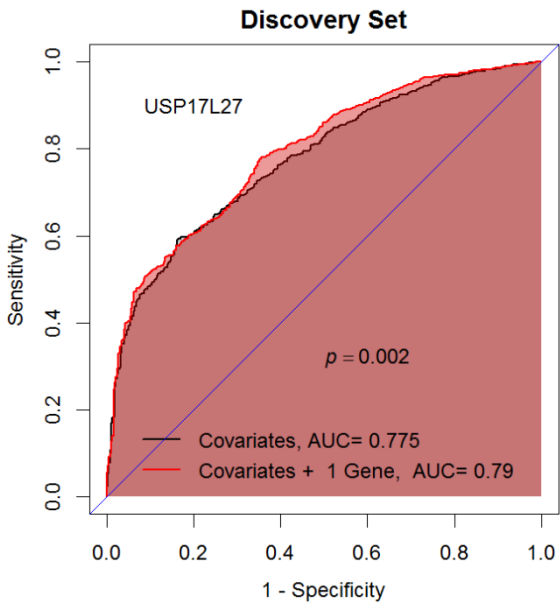


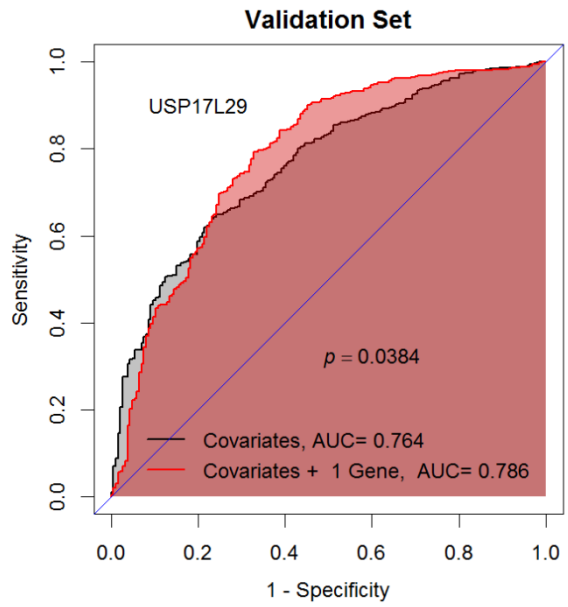
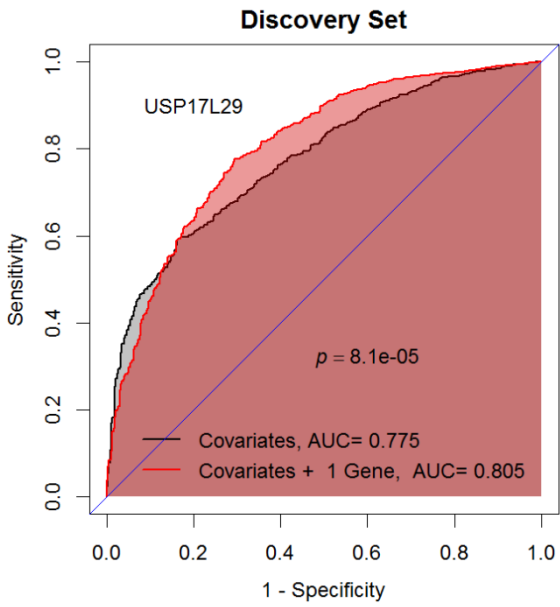
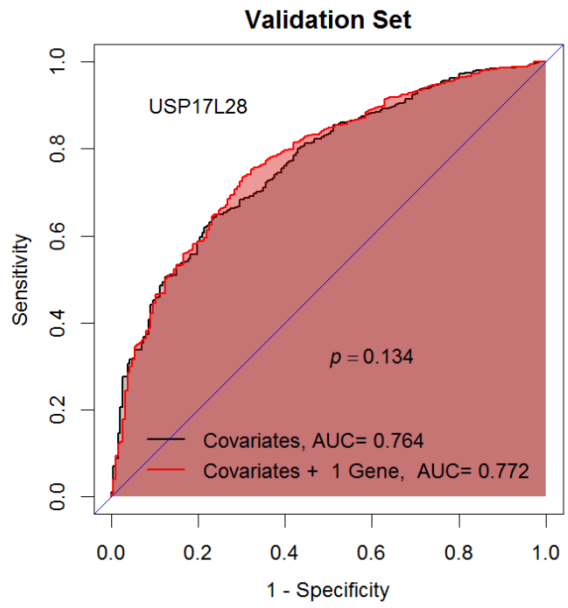
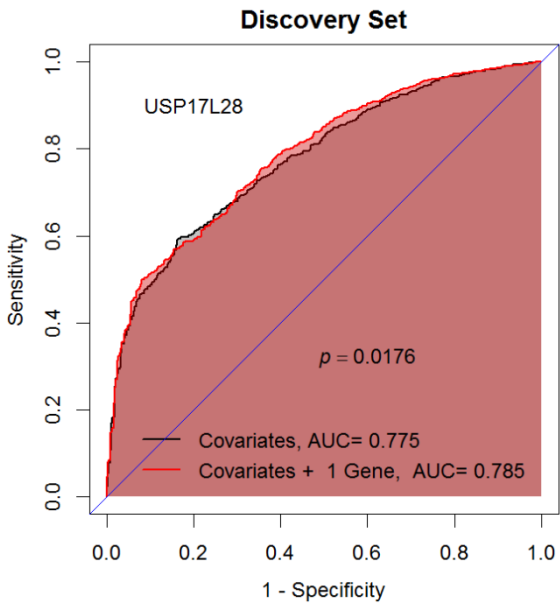


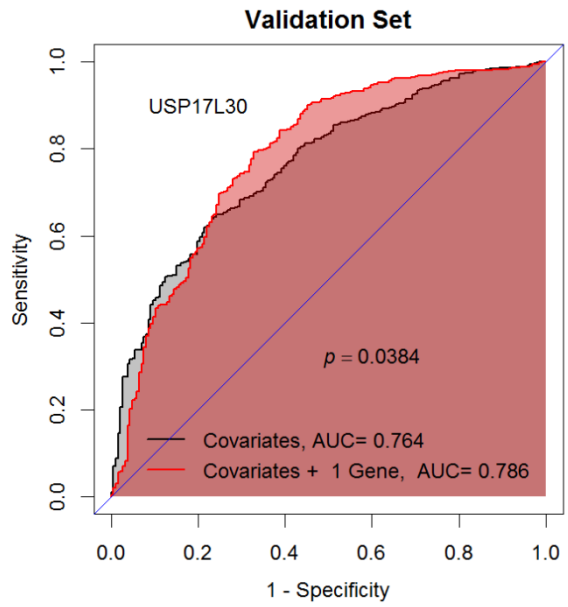
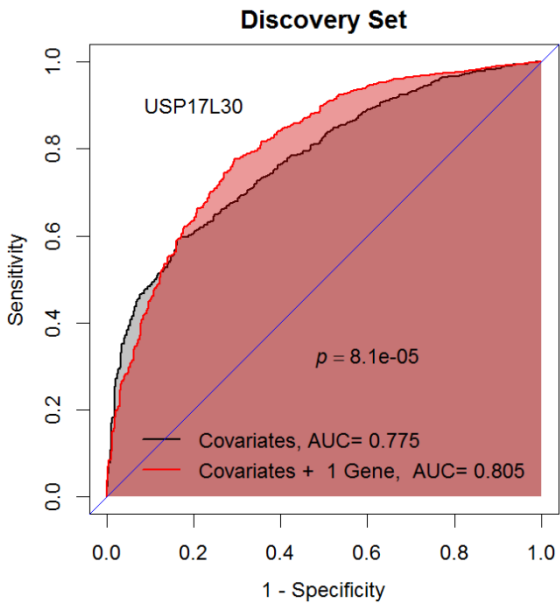
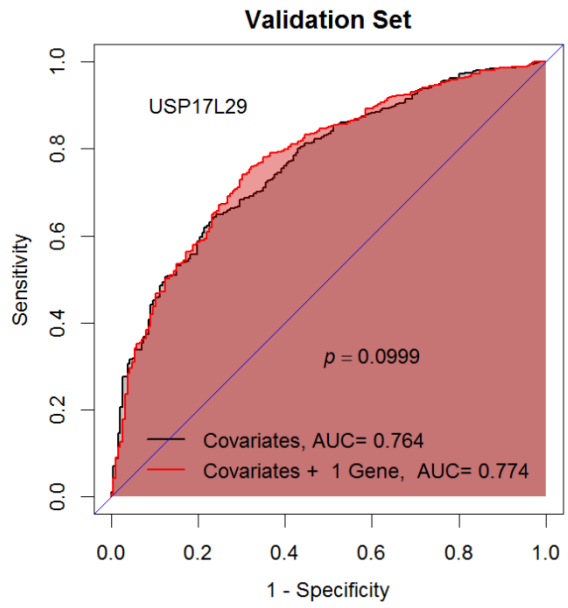
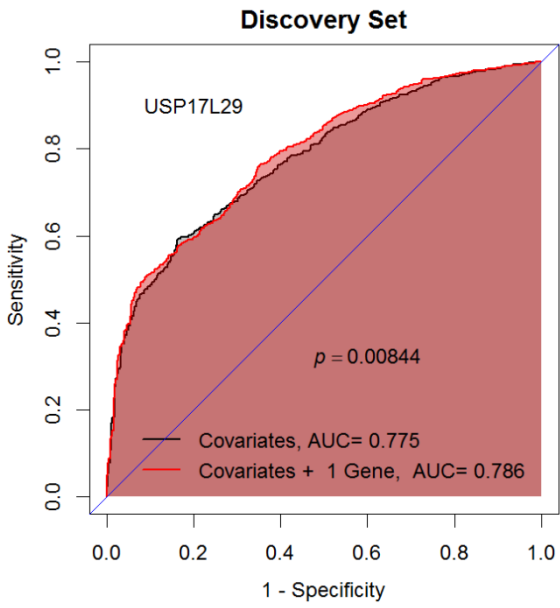


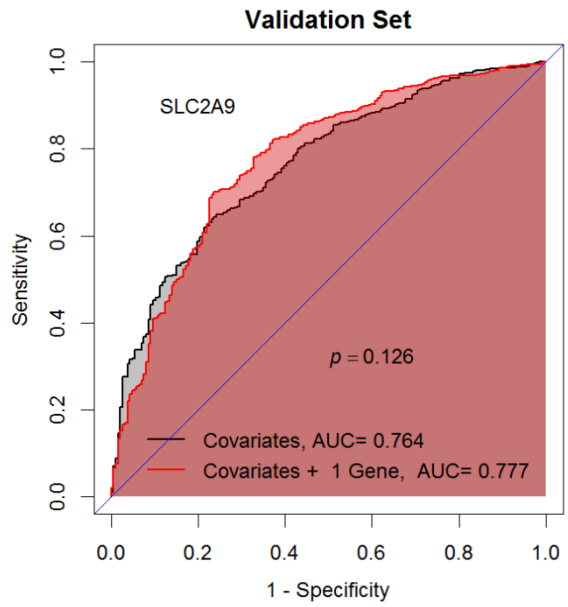
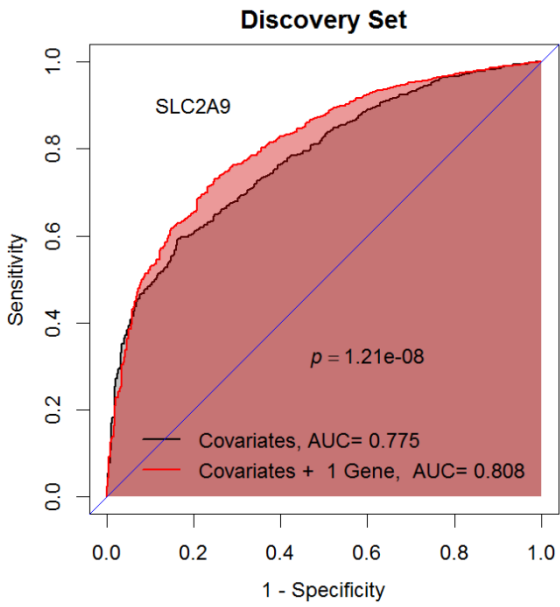
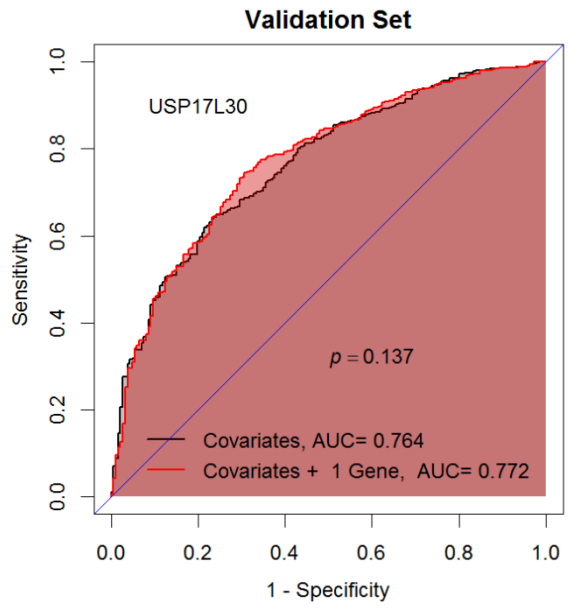
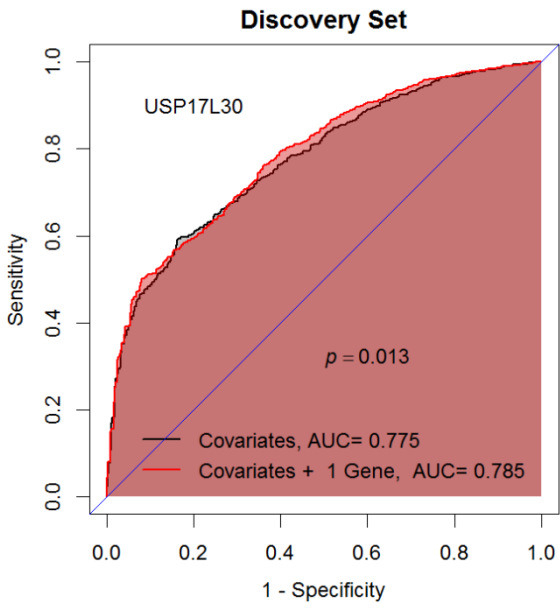


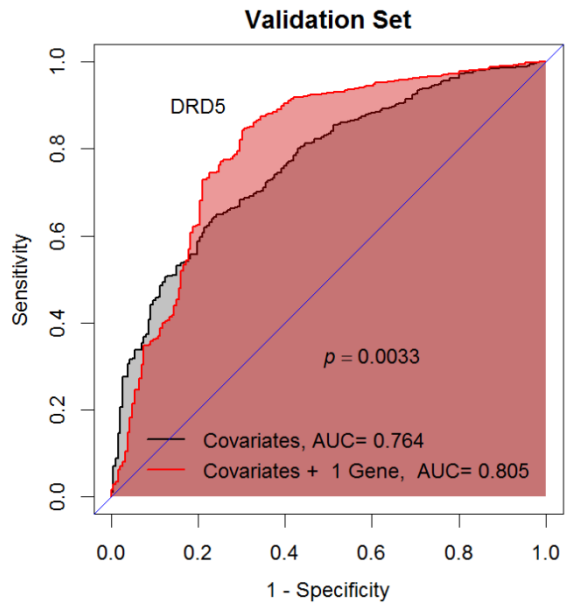
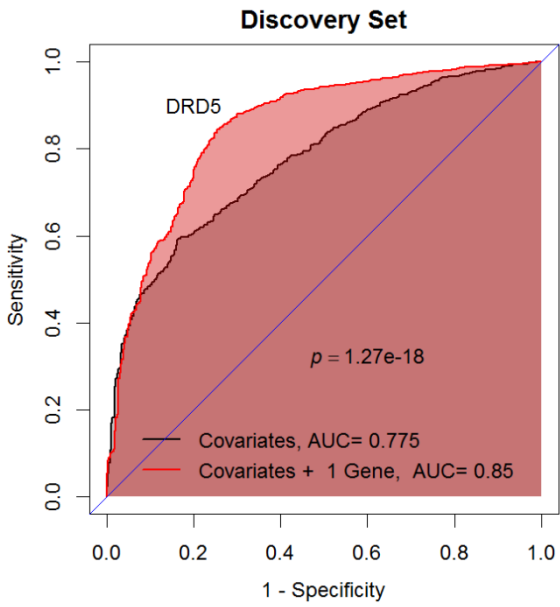
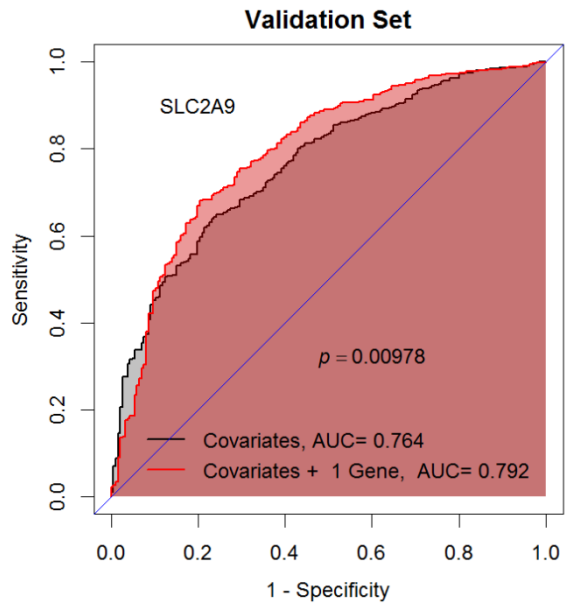
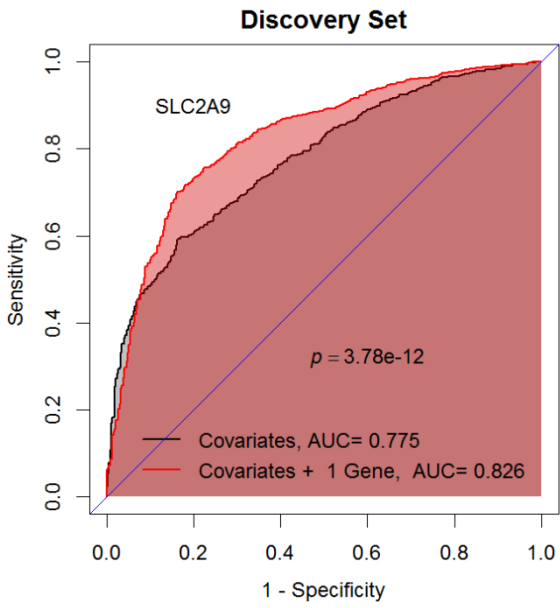


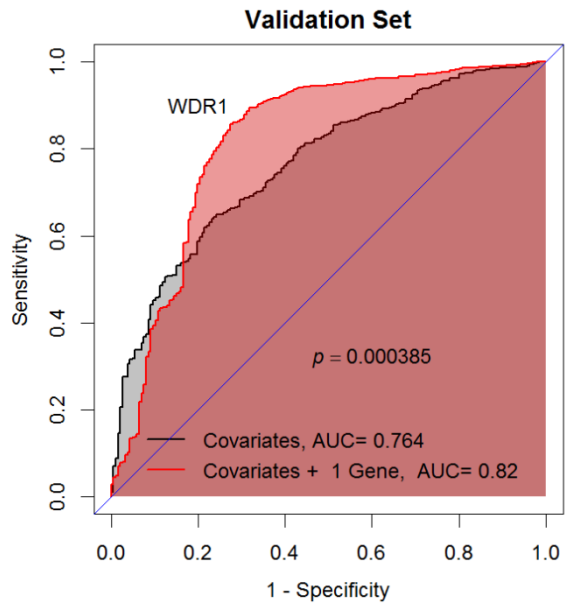
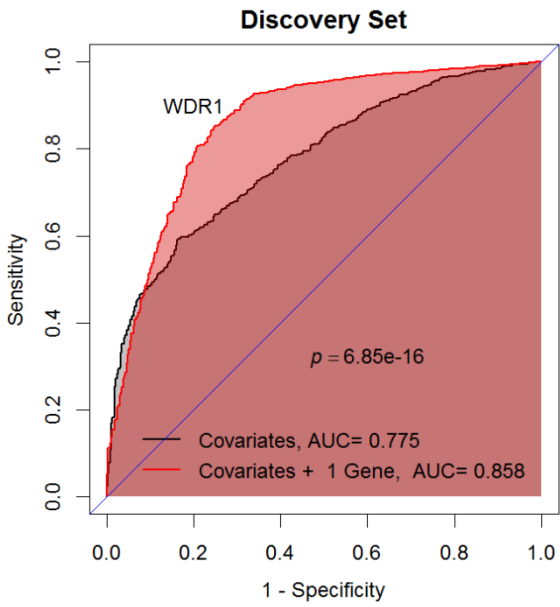
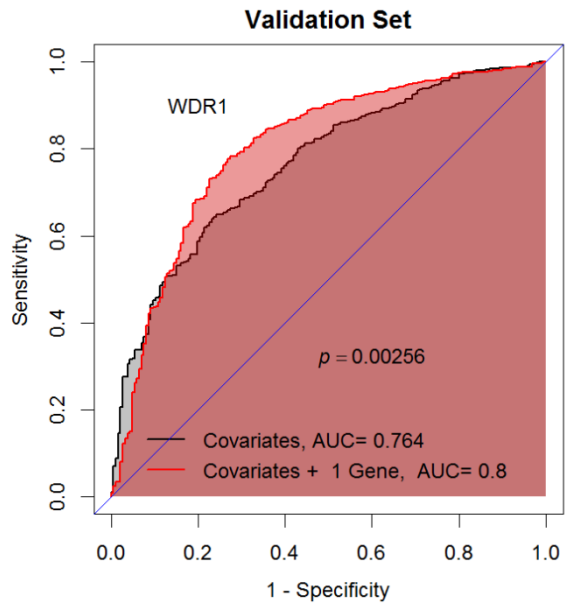
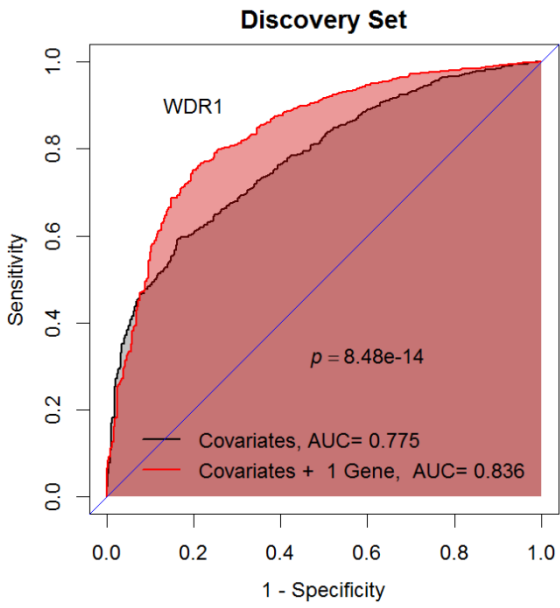


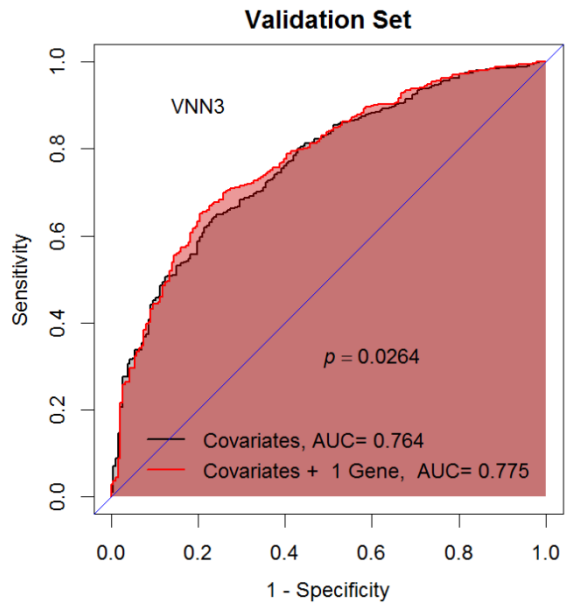
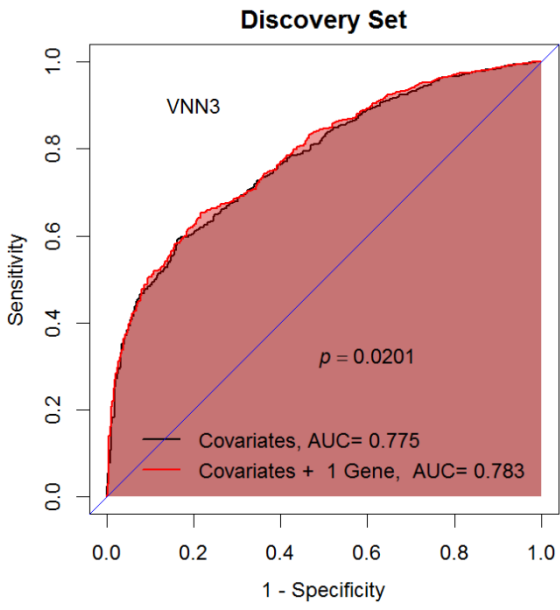






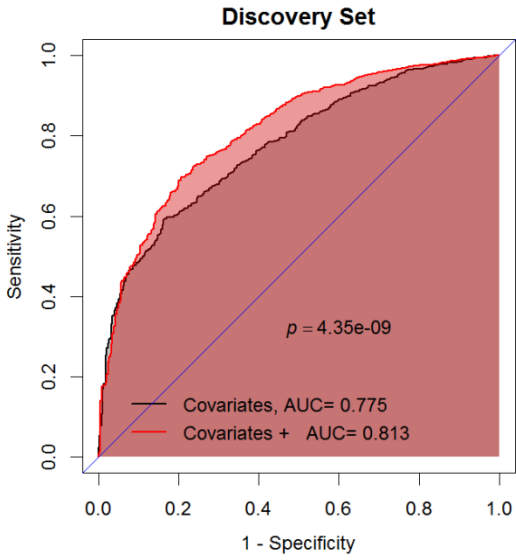




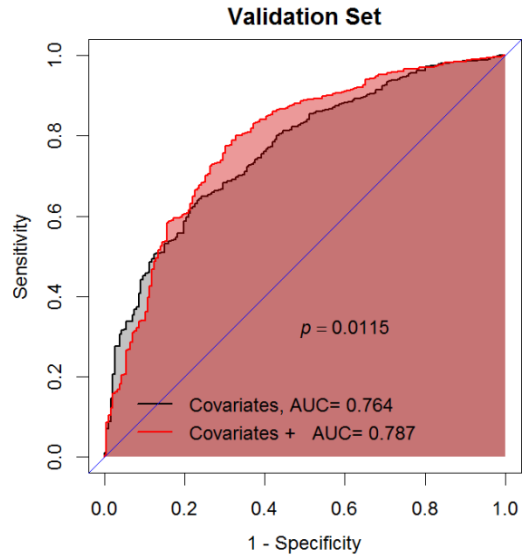


sFigure 7. The ROC curve and its AUC of the model with only covariates (black curve) and that with covariates plus the estimated expression values of LIME1, SLC2A9, STMN3 and VNN3 (red curve) in Discovery Set (a) and Validation Set (b).

a

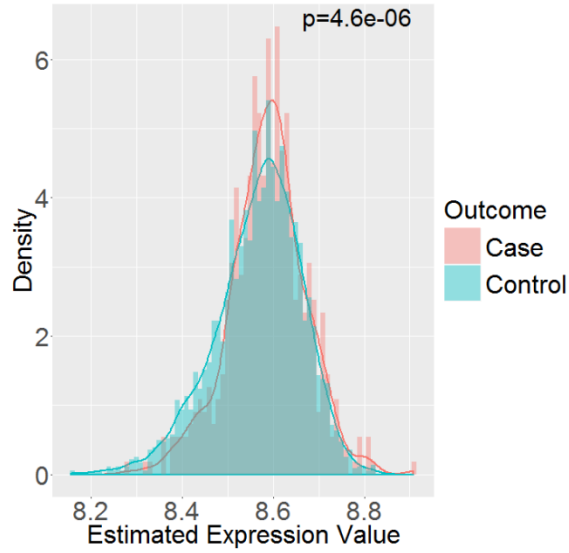


b



sFigure 8. The distribution of estimated expression values of the 55 validated transcripts (see sTable 3) between cases and controls.

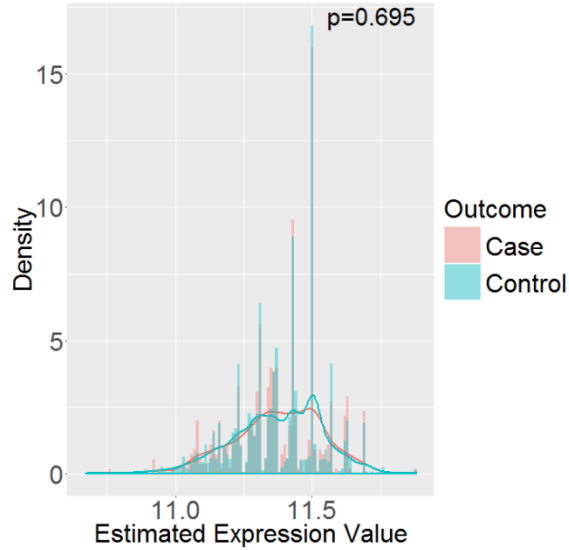
SNORD100 in Glioma GWAS Data



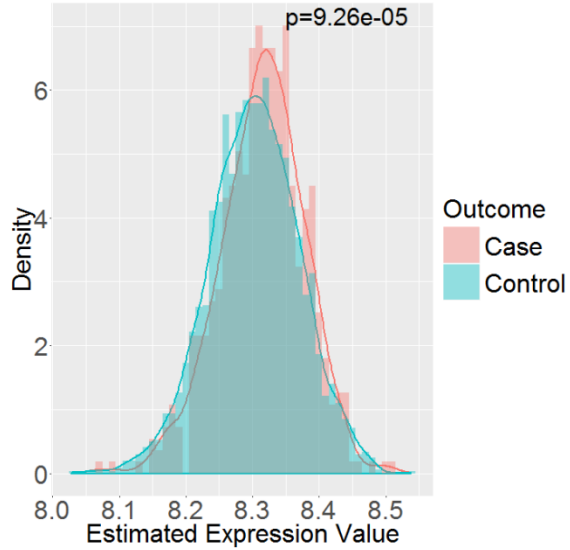
SNORA33 in Glioma GWAS Data



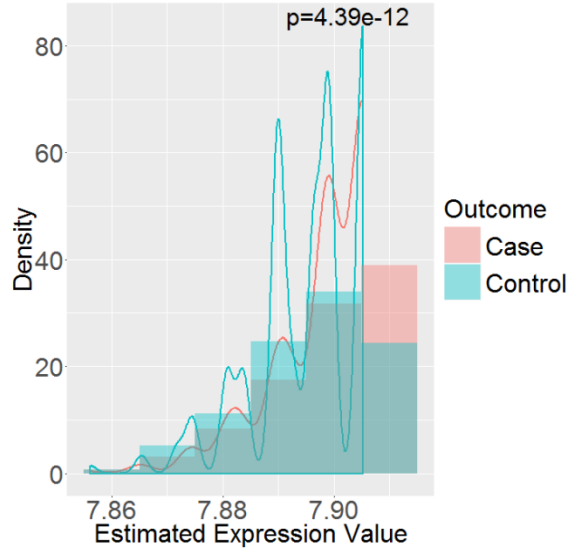
STMN3 in Glioma GWAS Data



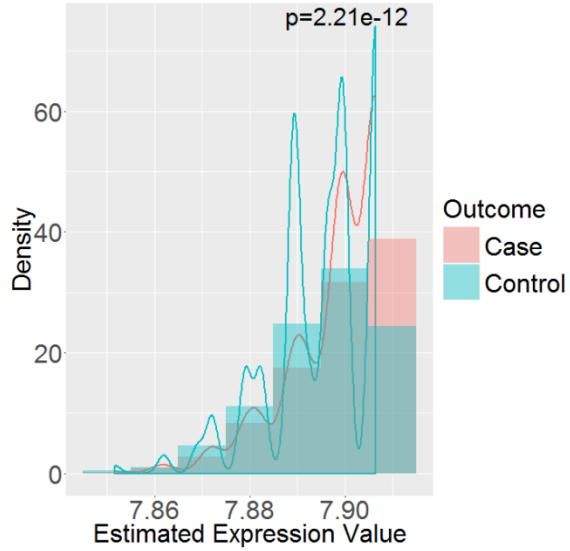
LIME1 in Glioma GWAS Data



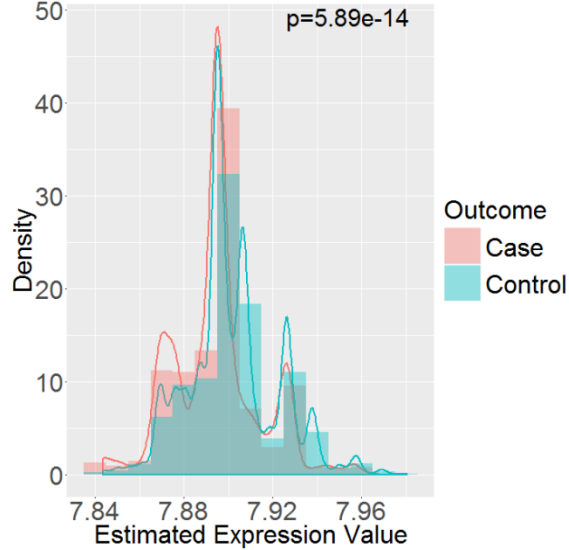
USP17L16P in Glioma GWAS Data



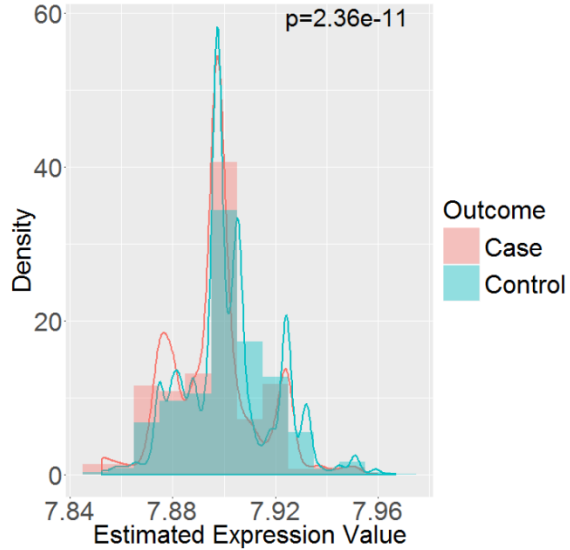
USP17L9P in Glioma GWAS Data



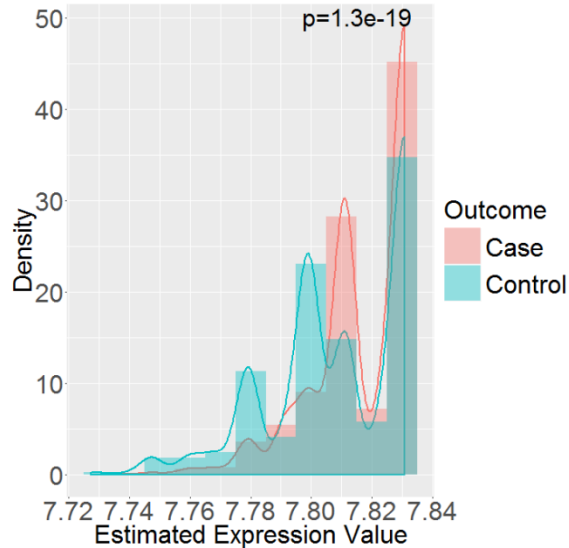
USP17L9P in Glioma GWAS Data



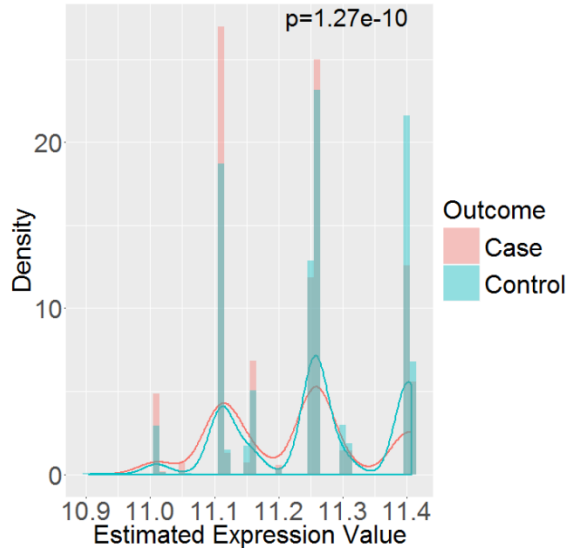
USP17L6P in Glioma GWAS Data

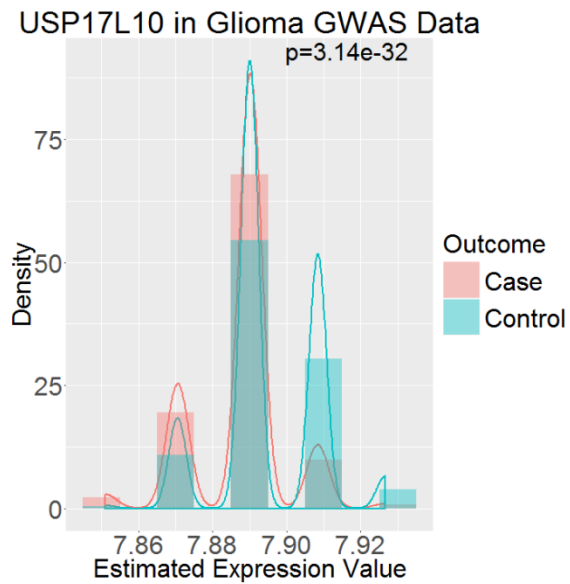
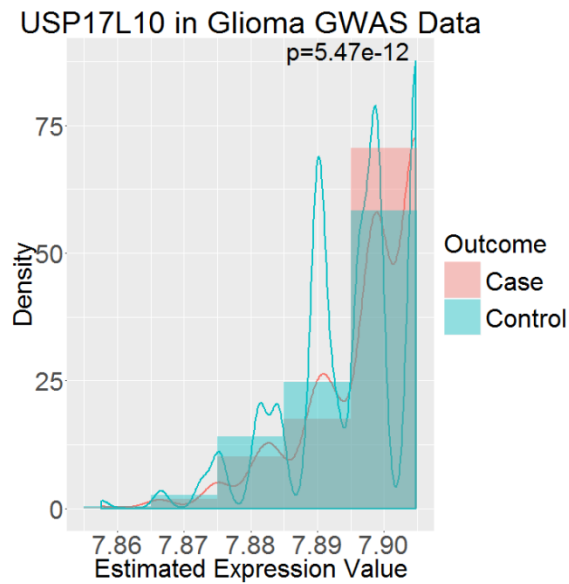
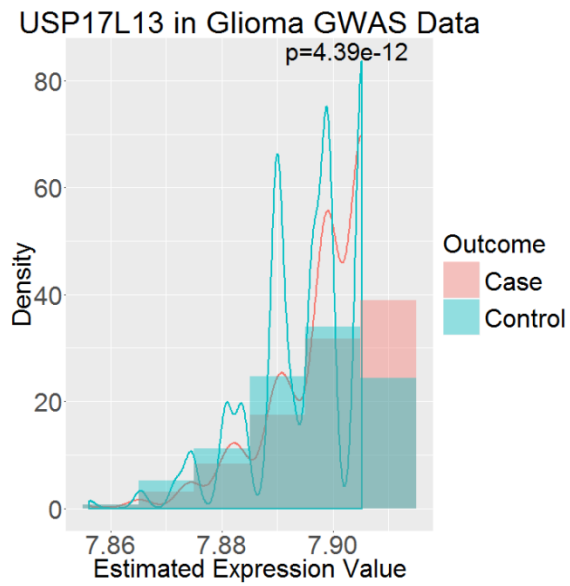
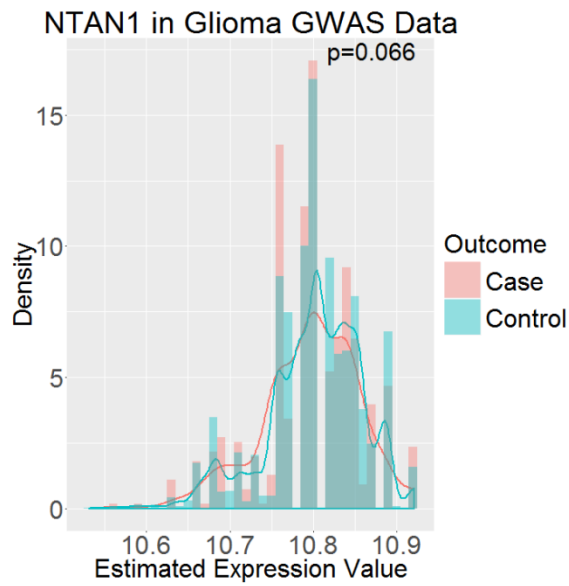
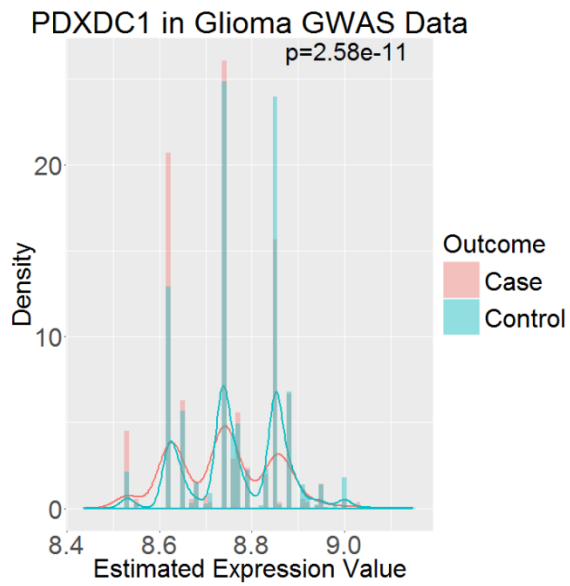
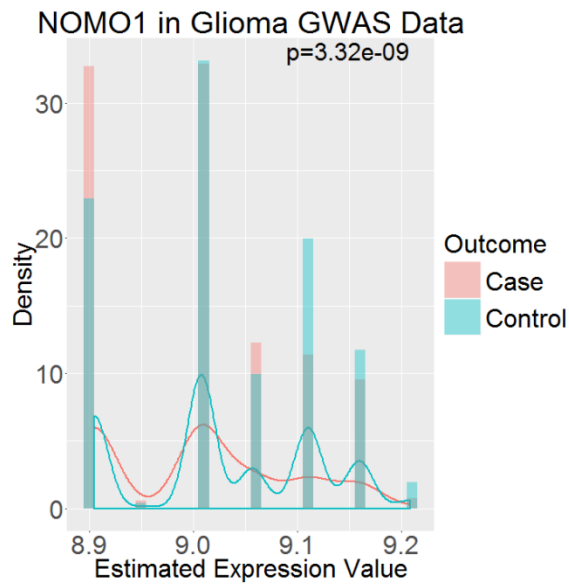


OR7E85P in Glioma GWAS Data

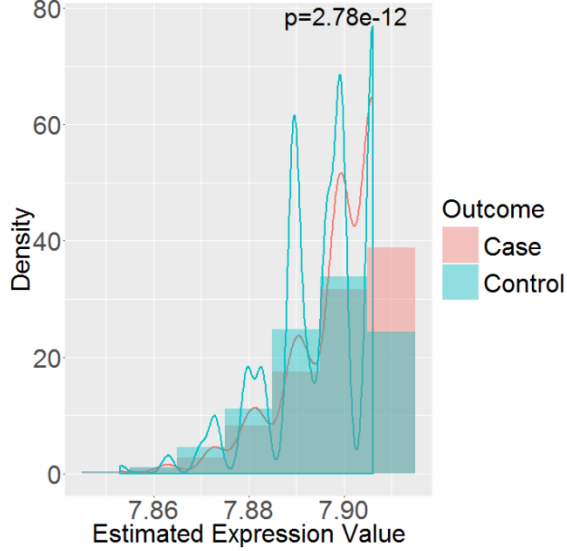


NOMO1 in Glioma GWAS Data

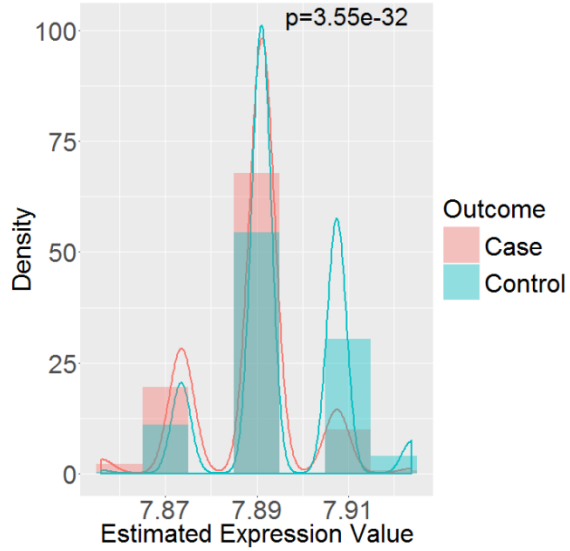




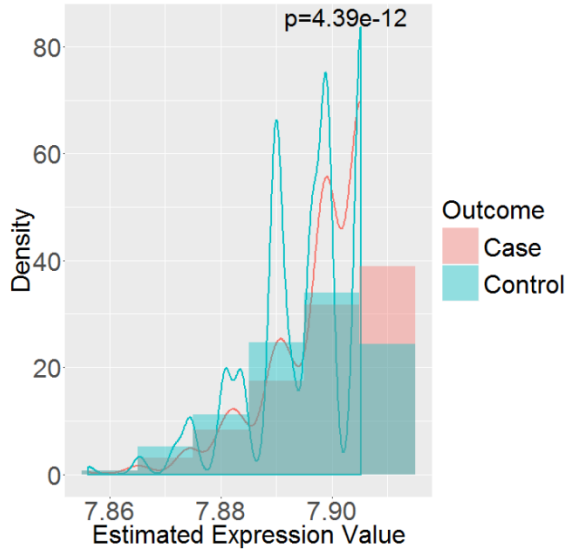
USP17L11 in Glioma GWAS Data



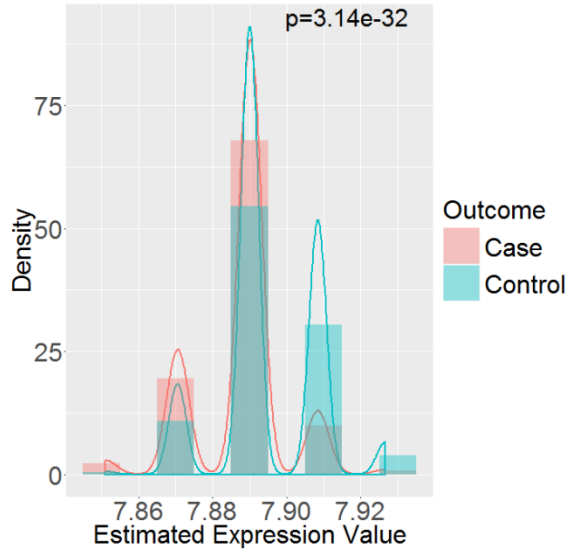
USP17L11 in Glioma GWAS Data



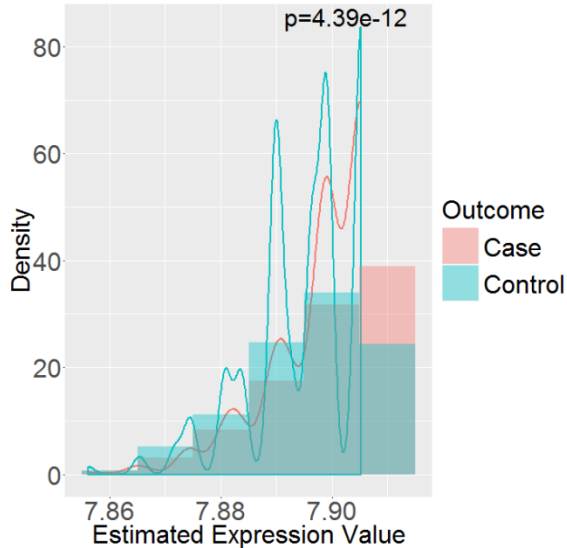
USP17L12 in Glioma GWAS Data



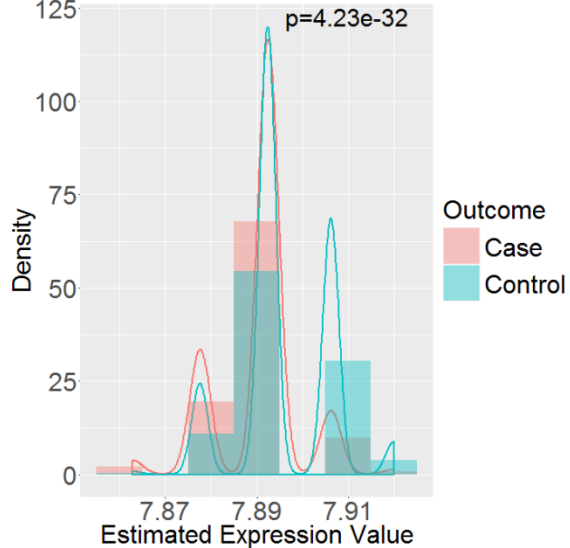
USP17L12 in Glioma GWAS Data



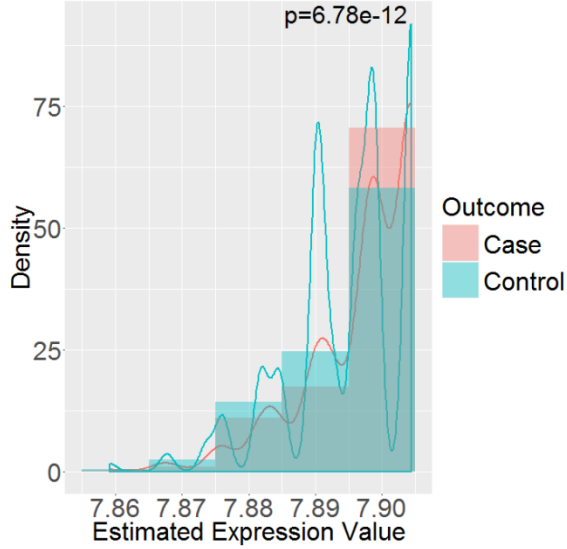
USP17L15 in Glioma GWAS Data



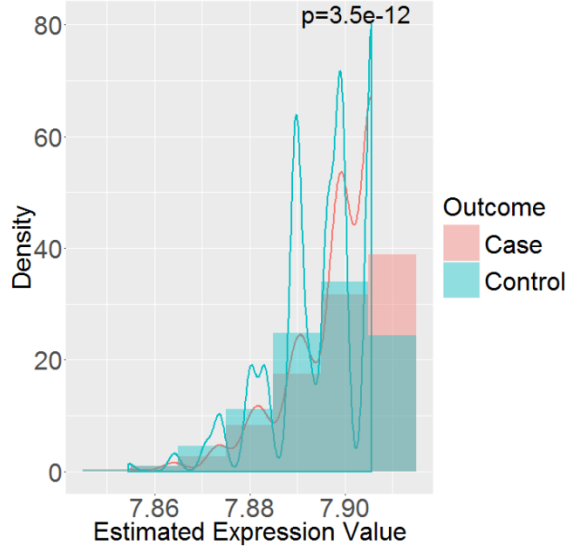
USP17L15 in Glioma GWAS Data



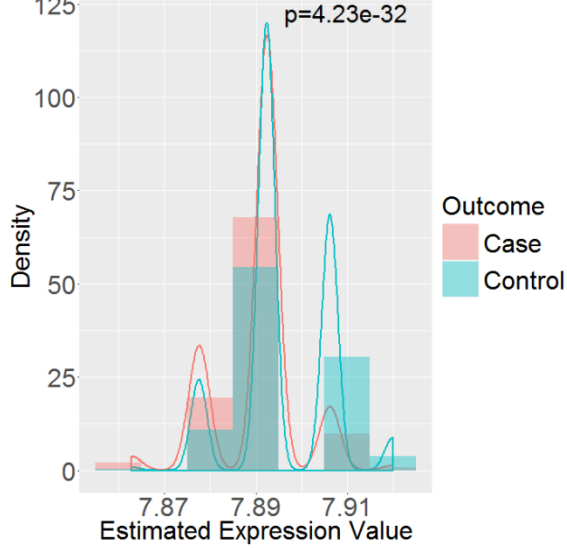
USP17L17 in Glioma GWAS Data



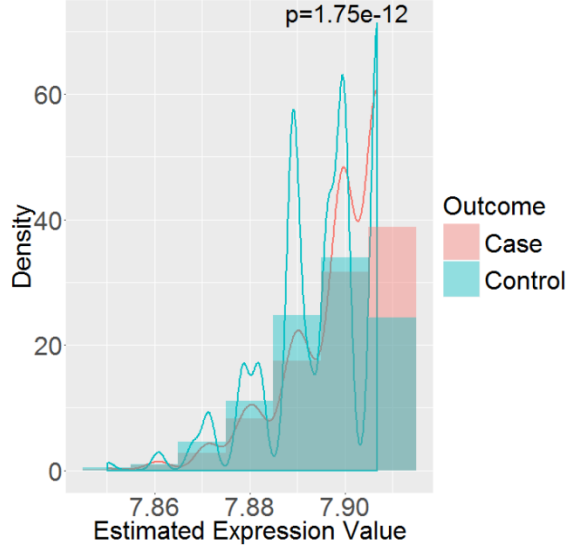
USP17L18 in Glioma GWAS Data



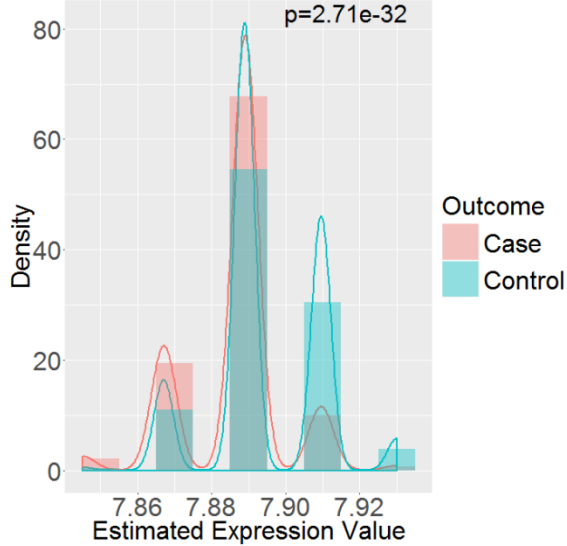
USP17L18 in Glioma GWAS Data



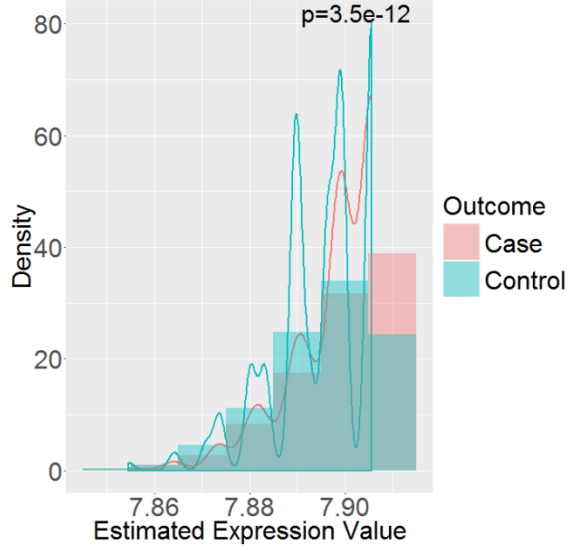
USP17L19 in Glioma GWAS Data



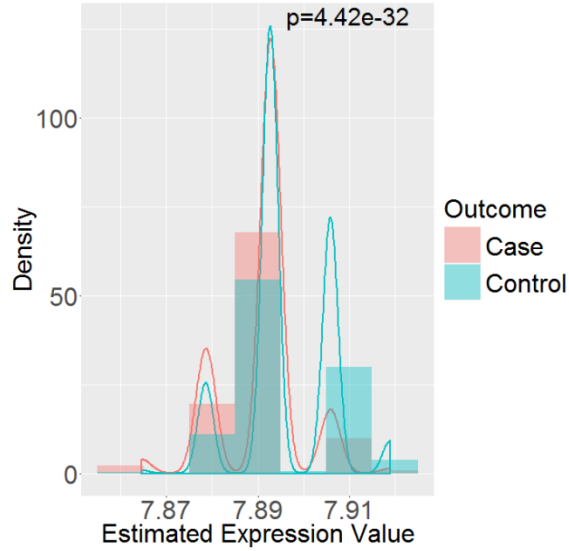
USP17L19 in Glioma GWAS Data



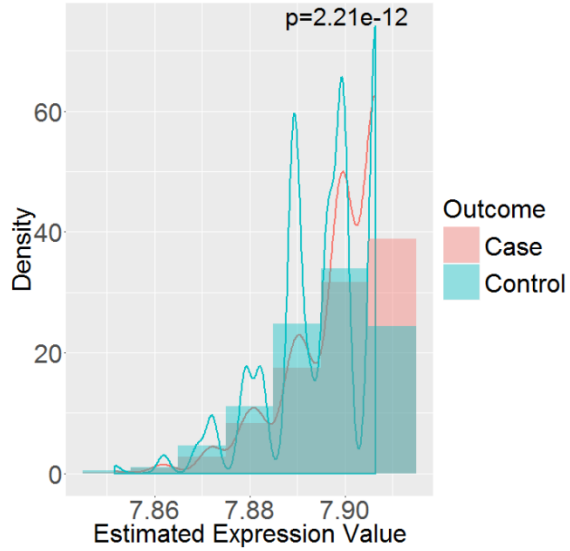
USP17L20 in Glioma GWAS Data



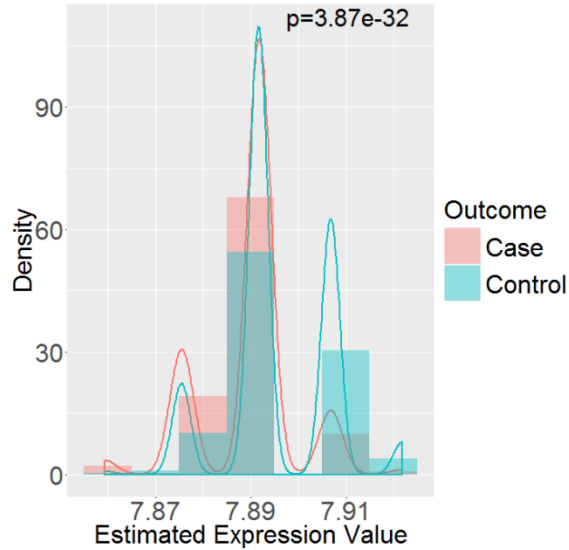
USP17L20 in Glioma GWAS Data



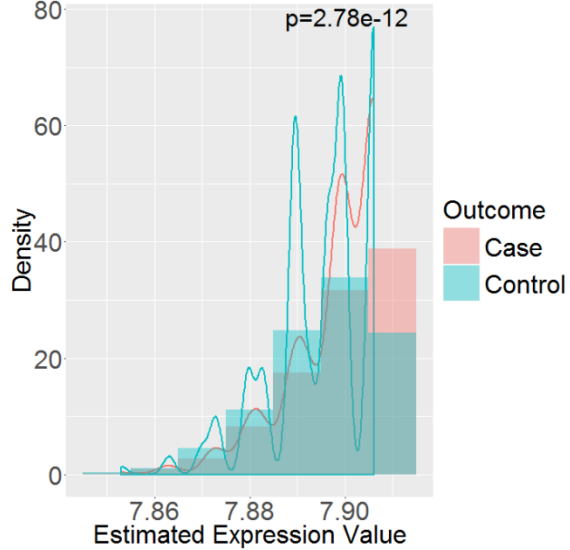
USP17L21 in Glioma GWAS Data



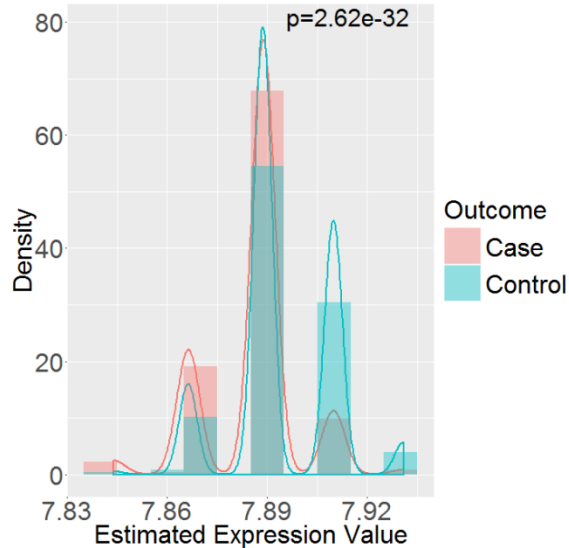
USP17L21 in Glioma GWAS Data



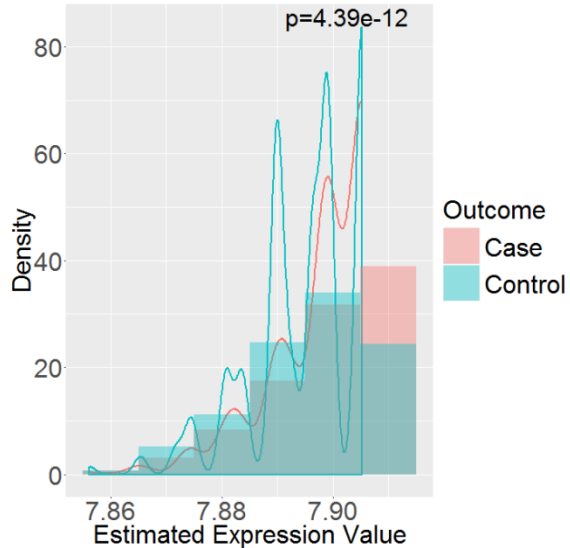
USP17L22 in Glioma GWAS Data



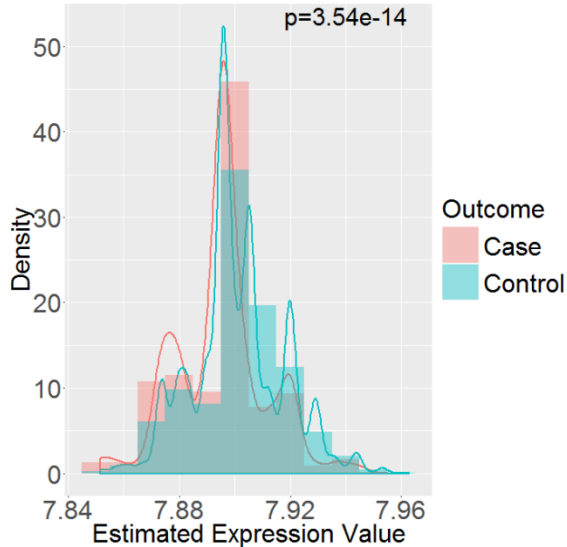
USP17L22 in Glioma GWAS Data



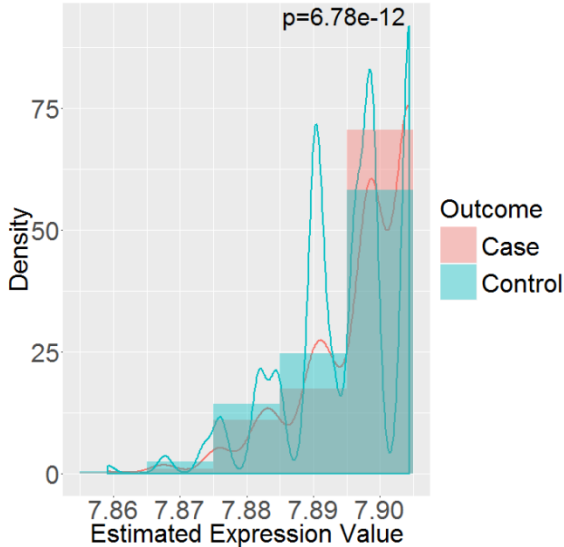
USP17L24 in Glioma GWAS Data



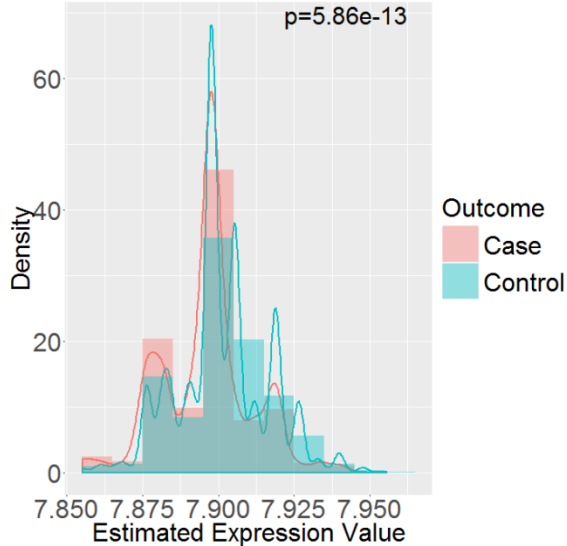
USP17L24 in Glioma GWAS Data



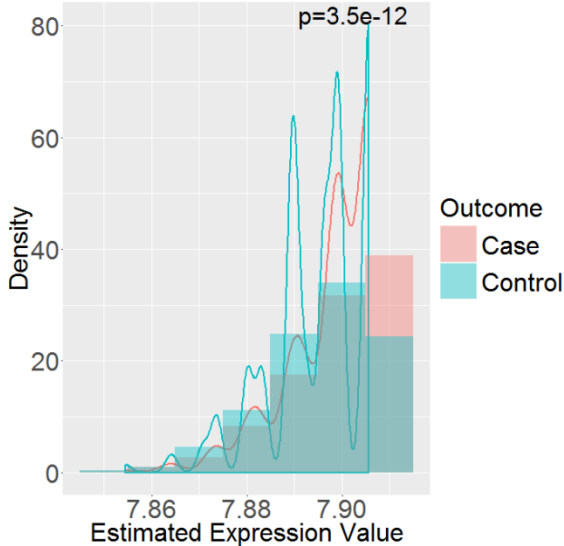
USP17L25 in Glioma GWAS Data



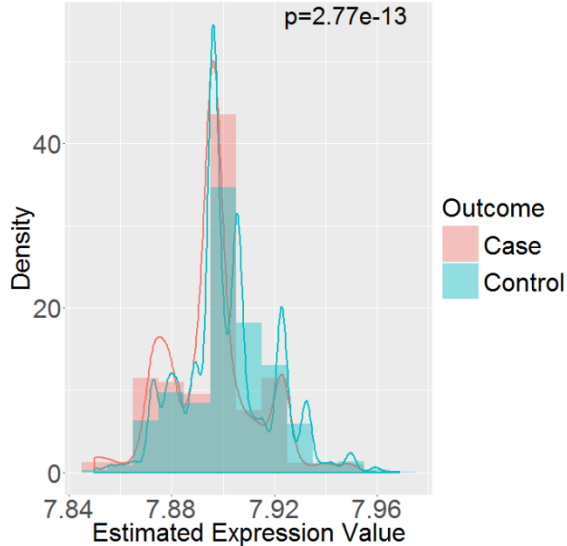
USP17L25 in Glioma GWAS Data



USP17L26 in Glioma GWAS Data



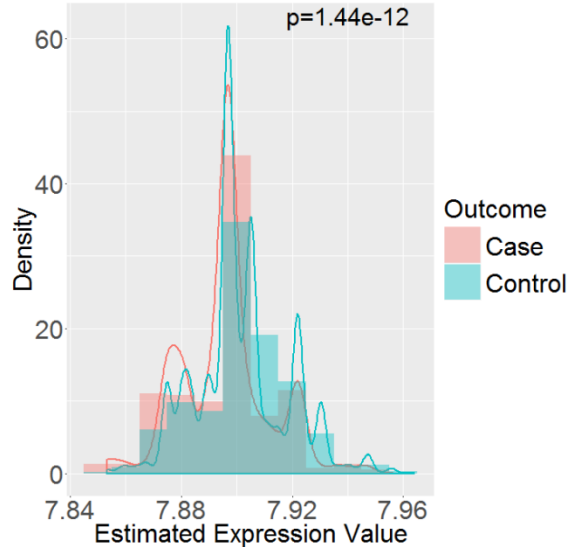
USP17L26 in Glioma GWAS Data



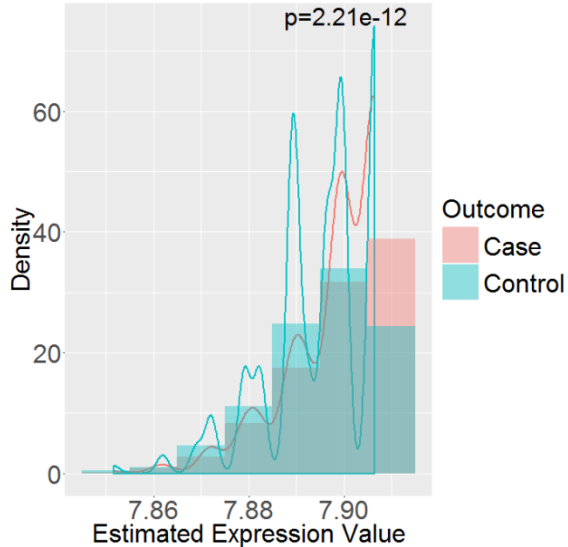
USP17L5 in Glioma GWAS Data



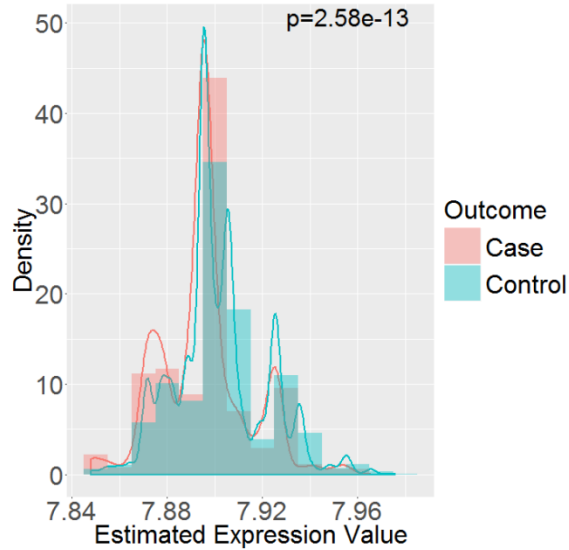
USP17L5 in Glioma GWAS Data



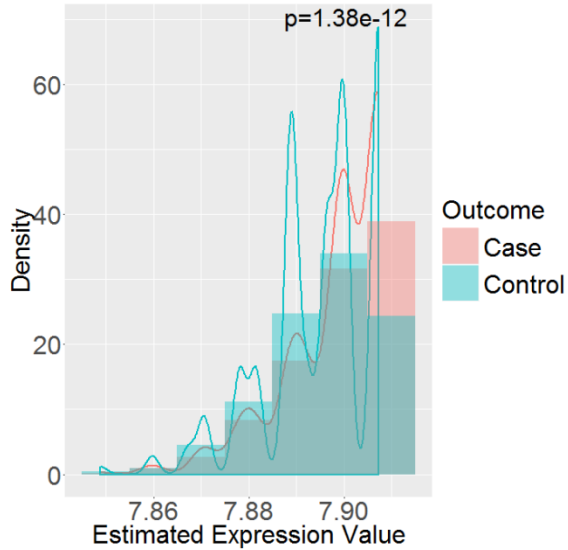
USP17L27 in Glioma GWAS Data



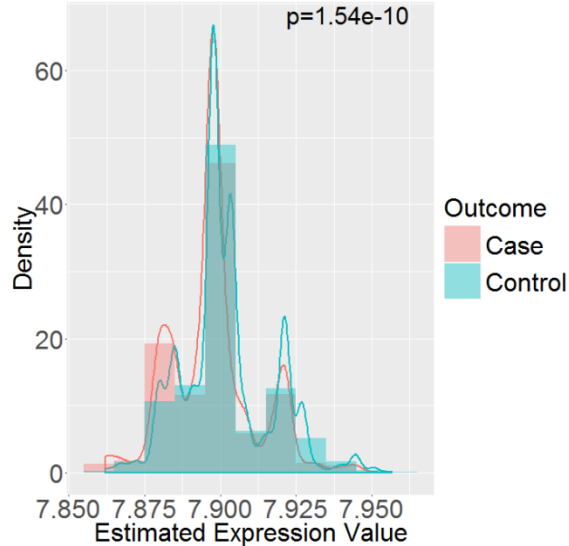
USP17L27 in Glioma GWAS Data



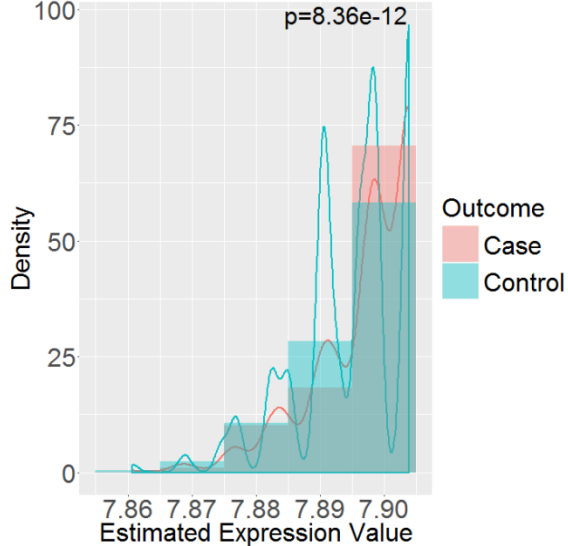
USP17L28 in Glioma GWAS Data



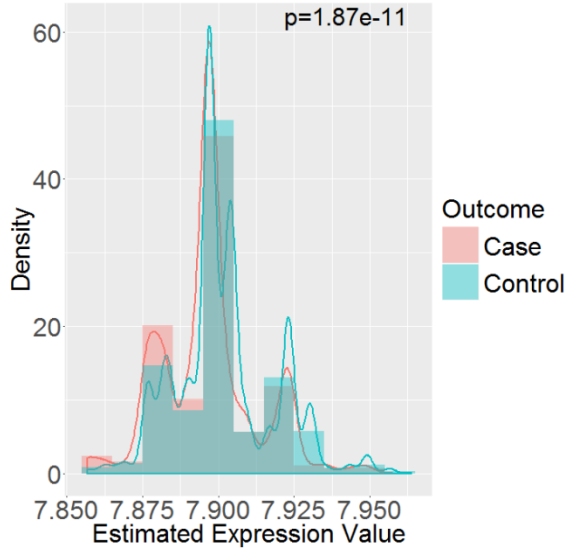
USP17L28 in Glioma GWAS Data



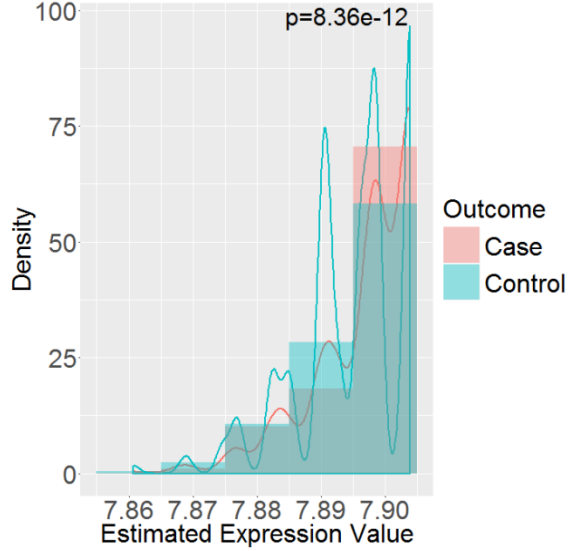
USP17L29 in Glioma GWAS Data



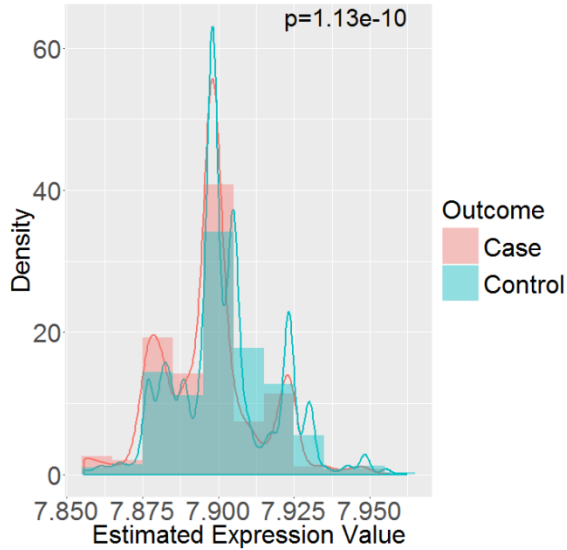
USP17L29 in Glioma GWAS Data



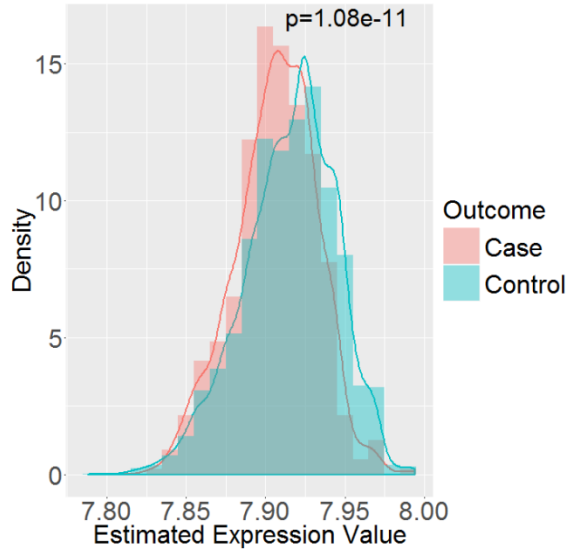
USP17L30 in Glioma GWAS Data



USP17L30 in Glioma GWAS Data



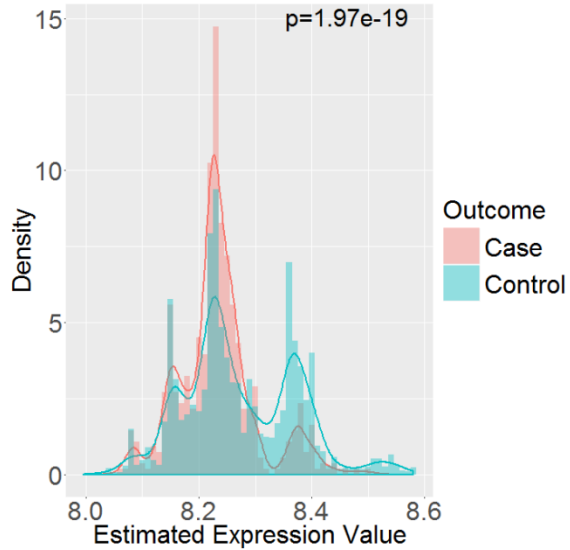
SLC2A9 in Glioma GWAS Data

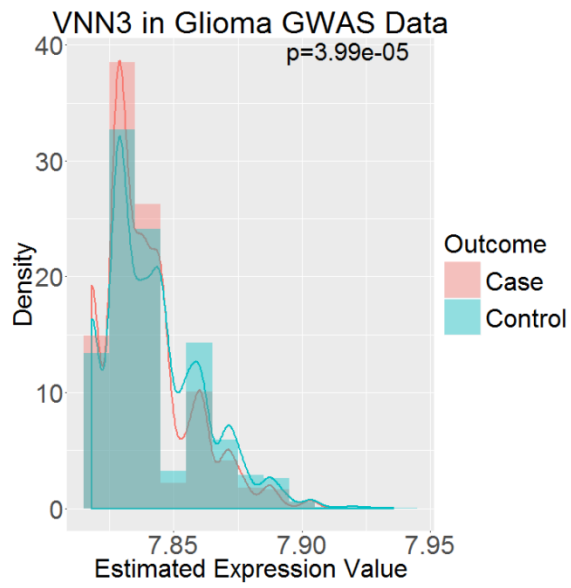
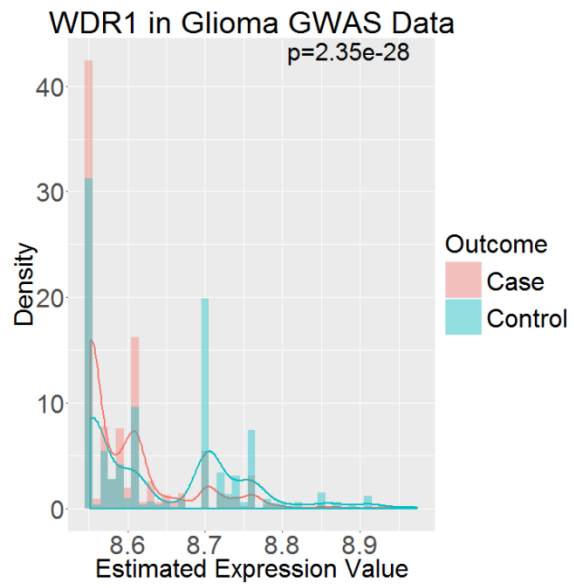
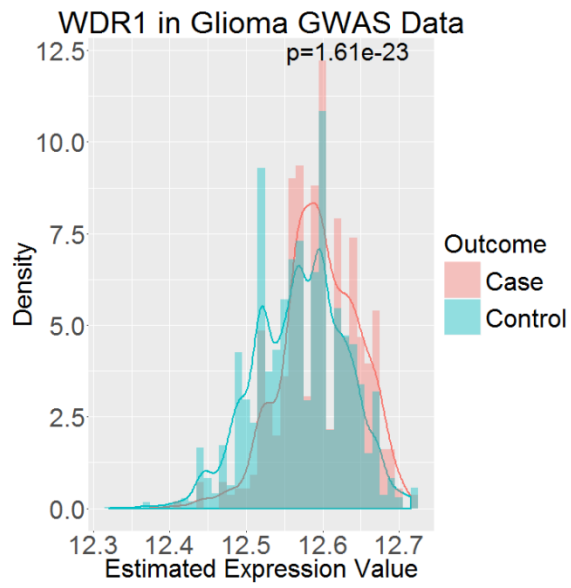


SLC2A9 in Glioma GWAS Data

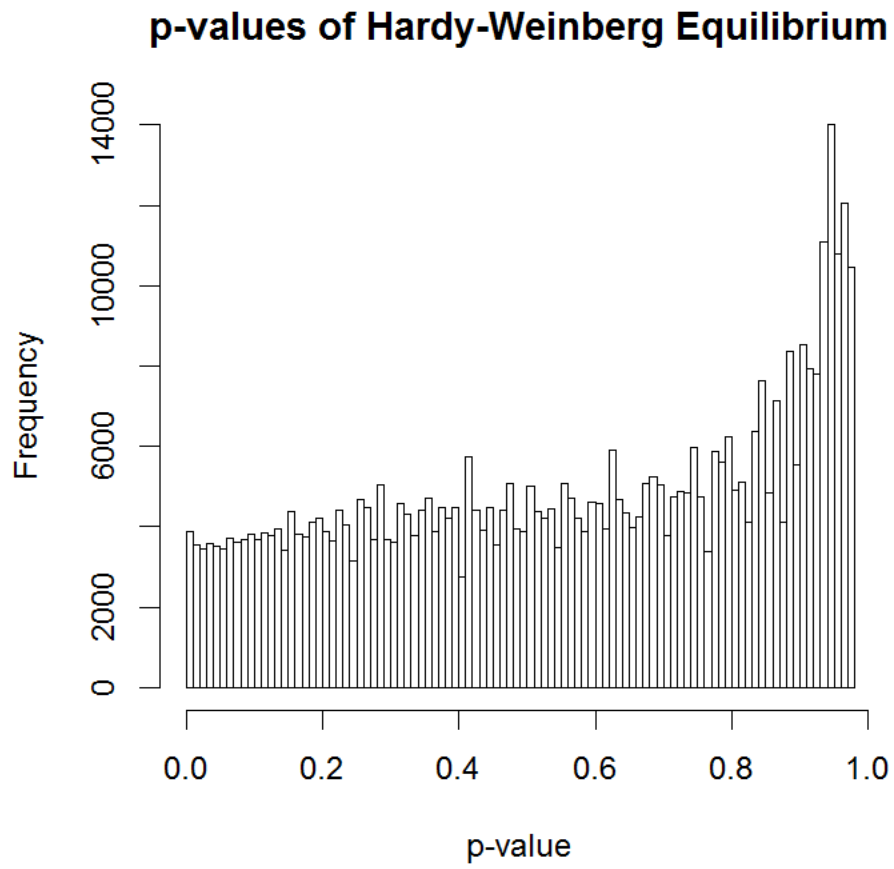


DRD5 in Glioma GWAS Data

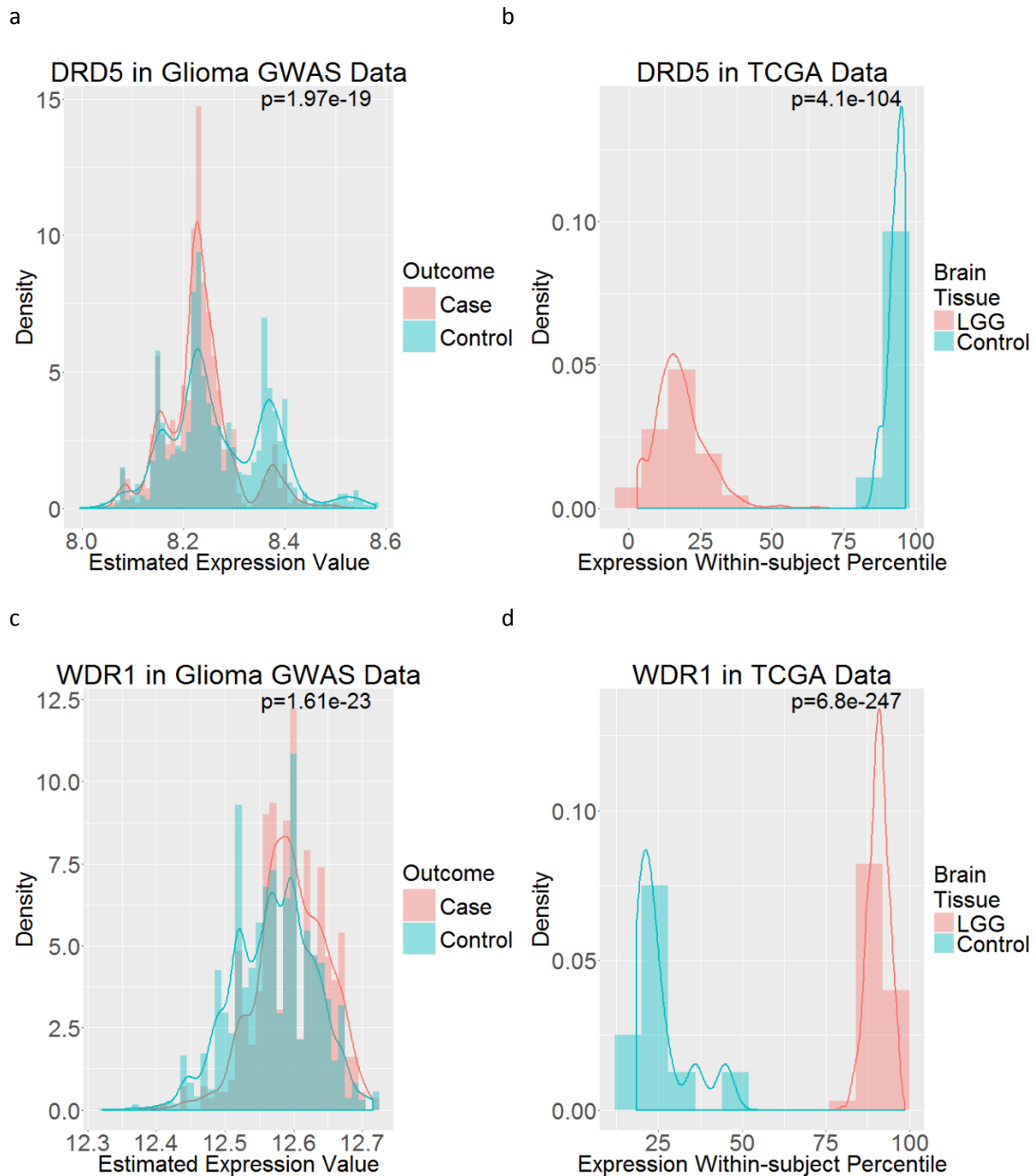




sFigure 9. Histogram of Hardy-Weinberg Equilibrium p-value.



sFigure 10. Gene expression in glioma GWAS data and TCGA LGG (low grade glioma) data. (a), The estimated gene expression level of *DRD5* estimated for glioma cases and controls in our glioma GWAS data ((a) *DRD5*, (c) *WDR1*). The relative gene expression level (measured as within subject percentile) of brain tissue from LGG patients and organ-specific controls from TCGA GBM project ((b) *DRD5*, (d) *WDR1*).



REFERENCE

1. van Leeuwen, E.M., Kanterakis, A., Deelen, P., Kattenberg, M.V., Genome of the Netherlands, C., Slagboom, P.E., de Bakker, P.I., Wijmenga, C., Swertz, M.A., Boomsma, D.I., et al. (2015). Population-specific genotype imputations using minimac or IMPUTE2. *Nat Protoc* 10, 1285-1296.
2. Genomes Project, C., Auton, A., Brooks, L.D., Durbin, R.M., Garrison, E.P., Kang, H.M., Korbel, J.O., Marchini, J.L., McCarthy, S., McVean, G.A., et al. (2015). A global reference for human genetic variation. *Nature* 526, 68-74.
3. Hinrichs, A.S., Karolchik, D., Baertsch, R., Barber, G.P., Bejerano, G., Clawson, H., Diekhans, M., Furey, T.S., Harte, R.A., Hsu, F., et al. (2006). The UCSC Genome Browser Database: update 2006. *Nucleic Acids Res* 34, D590-598.
4. Purcell, S., Neale, B., Todd-Brown, K., Thomas, L., Ferreira, M.A., Bender, D., Maller, J., Sklar, P., de Bakker, P.I., Daly, M.J., et al. (2007). PLINK: a tool set for whole-genome association and population-based linkage analyses. *Am J Hum Genet* 81, 559-575.
5. Delaneau, O., Marchini, J., and Zagury, J.F. (2012). A linear complexity phasing method for thousands of genomes. *Nat Methods* 9, 179-181.
6. Durinck, S., Spellman, P.T., Birney, E., and Huber, W. (2009). Mapping identifiers for the integration of genomic datasets with the R/Bioconductor package biomaRt. *Nat Protoc* 4, 1184-1191.
7. Demirkan, A., van Duijn, C.M., Ugocsai, P., Isaacs, A., Pramstaller, P.P., Liebisch, G., Wilson, J.F., Johansson, A., Rudan, I., Aulchenko, Y.S., et al. (2012). Genome-wide association study identifies novel loci associated with circulating phospho- and sphingolipid concentrations. *PLoS Genet* 8, e1002490.
8. Suhre, K., Shin, S.Y., Petersen, A.K., Mohny, R.P., Meredith, D., Wagele, B., Altmaier, E., CardioGram, Deloukas, P., Erdmann, J., et al. (2011). Human metabolic individuality in biomedical and pharmaceutical research. *Nature* 477, 54-60.
9. Global Lipids Genetics, C., Willer, C.J., Schmidt, E.M., Sengupta, S., Peloso, G.M., Gustafsson, S., Kanoni, S., Ganna, A., Chen, J., Buchkovich, M.L., et al. (2013). Discovery and refinement of loci associated with lipid levels. *Nat Genet* 45, 1274-1283.
10. Durinck, S., Stawiski, E.W., Pavia-Jimenez, A., Modrusan, Z., Kapur, P., Jaiswal, B.S., Zhang, N., Toffessi-Tcheuyap, V., Nguyen, T.T., Pahuja, K.B., et al. (2015). Spectrum of diverse genomic alterations define non-clear cell renal carcinoma subtypes. *Nat Genet* 47, 13-21.
11. Uhlen, M., Oksvold, P., Fagerberg, L., Lundberg, E., Jonasson, K., Forsberg, M., Zwahlen, M., Kampf, C., Wester, K., Hober, S., et al. (2010). Towards a knowledge-based Human Protein Atlas. *Nat Biotechnol* 28, 1248-1250.
12. Uhlen, M., Fagerberg, L., Hallstrom, B.M., Lindskog, C., Oksvold, P., Mardinoglu, A., Sivertsson, A., Kampf, C., Sjostedt, E., Asplund, A., et al. (2015). Proteomics. Tissue-based map of the human proteome. *Science* 347, 1260419.
13. Maglott, D., Ostell, J., Pruitt, K.D., and Tatusova, T. (2011). Entrez Gene: gene-centered information at NCBI. *Nucleic Acids Res* 39, D52-57.
14. Kim, D.H., Bae, J., Lee, J.W., Kim, S.Y., Kim, Y.H., Bae, J.Y., Yi, J.K., Yu, M.H., Noh, D.Y., and Lee, C. (2009). Proteomic analysis of breast cancer tissue reveals upregulation of actin-remodeling proteins and its relevance to cancer invasiveness. *Proteomics Clin Appl* 3, 30-40.
15. Izawa, S., Okamura, T., Matsuzawa, K., Ohkura, T., Ohkura, H., Ishiguro, K., Noh, J.Y., Kamijo, K., Yoshida, A., Shigemasa, C., et al. (2013). Autoantibody against WD repeat domain 1 is a novel serological biomarker for screening of thyroid neoplasia. *Clin Endocrinol (Oxf)* 79, 35-42.
16. Haslene-Hox, H., Oveland, E., Woie, K., Salvesen, H.B., Wiig, H., and Tenstad, O. (2013). Increased WD-repeat containing protein 1 in interstitial fluid from ovarian carcinomas shown by comparative proteomic analysis of malignant and healthy gynecological tissue. *Biochim Biophys Acta* 1834, 2347-2359.

